

BEN-GURION UNIVERSITY OF THE NEGEV
FACULTY OF ENGINEERING SCIENCES
DEPARTMENT OF INDUSTRIAL ENGINEERING AND MANAGEMENT

AUTOMATIC COW'S BODY CONDITION SCORING
THESIS SUBMITTED IN PARTIAL FULFILLMENT OF THE REQUIREMENTS FOR THE
M.Sc. DEGREE

By: AMOS BERCOVICH

BEN-GURION UNIVERSITY OF THE NEGEV
FACULTY OF ENGINEERING SCIENCES
DEPARTMENT OF INDUSTRIAL ENGINEERING AND MANAGEMENT

AUTOMATIC COW'S BODY CONDITION SCORING
THESIS SUBMITTED IN PARTIAL FULFILLMENT OF THE REQUIREMENTS FOR THE
M.Sc. DEGREE

By: AMOS BERCOVICH

Supervised by: Yael Edan and Ilan Halachmi

Author:.....

Date:.....

Supervisor:.....

Date:.....

Supervisor:.....

Date:.....

Chairman of Graduate Studies Committee:..... Date:.....

OCTOBER 2012

Acknowledgments

To:

Dr. Victor Alchanatis (A.R.O.), my image processing and modeling advisor.

Dr. Ephraim Maltz (A.R.O.), my experiments and cow BCS advisor.

Dr. Uzi Muallem (A.R.O.), for the manual, expertly cow scoring.

Mr. Aharon Antler (A.R.O.), for unique research facility building and the experiments running in the barn.

DVM Dr. Hen hana Honig (A.R.O.) for the priceless veterinary advice at early stage of the project.

Mr. Shamay Yakobi (A.R.O.) the research-farm manager for his valuable help in chasing the cows, always in a good-will mood.

Dr. Yisrael Parmet (BGU) for the statistical advice and support.

And finally my supervisors Dr. Ilan Halachmi (A.R.O.) and Prof. Yael Edan (BGU) for the support, patience and professional guidance.

Abstract

Body condition scoring (BCS) indicates energy reserves of dairy cows for estimating their fatness or thinness according to a 5-point scale. Despite several attempts to automate it, it is still handled manually. The goal of this study is to develop an automatic computer vision tool for evaluating BCS. Digital Images of 151 cows were collected in the Bet Dagan dairy farm (Israel) using a Nikon DSLR camera located at the entrance of the milking parlor. The cows were manually scored by an expert. Images for training and testing were manually selected. Cow's tail head area and its contour were segmented and extracted automatically using Matlab software. Two types of features of the tail head contour were extracted for BCS prediction: (1) Five anatomical points that were automatically detected by analyzing the sequence of the peaks and valleys of the tail head contour. The angles and distances between these five points were computed. (2) The cow's contour was presented as a one dimensional vector of the distances from each point in the contour to the object center. In order to eliminate influence of size and orientation each contour was interpolated to a fix number of points and scaled to a range between zero to one. Each contour was described by two forms: (1) selected number of latent variables produced by Partial least square (PLS) (2) the Fourier descriptors of the one dimensional contour vector. The prediction models were derived by backward regression and the features found as best for BCS prediction were the first ten Fourier descriptors of the one dimensional vector resulting in a R^2 of 0.77 and 0.64 for the training and testing set respectively.

Classification results between different classes of BCS indicate that it is possible to automatically extract and analyze BCS from digital images without involving any manual labeling procedure and without causing any interruption to the animal.

Table of Contents

1	INTRODUCTION.....	1
1.1	DESCRIPTION OF THE PROBLEM	1
1.2	OBJECTIVES.....	1
2	LITERATURE REVIEW.....	2
2.1	BODY CONDITION SCORING (BCS).....	2
2.2	AUTOMATION IN DAIRY FARMING	7
3	METHODS.....	20
3.1	GENERAL OVERVIEW	20
3.2	IMAGE ACQUISITION	21
3.3	DATABASE	22
3.4	IMAGE PROCESSING	23
3.5	IMAGE INTERPRETATION AND FEATURE EXTRACTION	24
3.6	REGRESSION MODELING	24
3.7	PERFORMANCE ANALYSIS	25
3.8	CLASSIFICATION MODELING	26
3.9	SENSITIVITY ANALYSES	26
4	ALGORITHMS	28
4.1	IMAGE PROCESSING	28
4.2	FEATURE EXTRACTION	37
5	RESULTS	46
5.1	BCS PREDICTION USING ANATOMICAL POINTS FEATURES	46
5.2	BCS PREDICTION USING AUTOMATICALLY EXTRACTED COW-CONTOUR	47
5.3	BCS PREDICTION USING BY FOURIER TRANSFORM OF THE CONTOUR	48
5.4	VALIDATION.....	51
5.5	MODEL PERFORMANCE	52
5.6	CLASSIFICATION MODEL.....	56
5.7	MODEL REPEATABILITY	58
5.8	SENSITIVITY ANALYSES	59
6	DISCUSSION, CONCLUSIONS AND FUTURE RESEARCH	63
7	REFERENCES	67
8	APPENDICES	74

List of Figures

FIGURE 1 – BODY ENERGY RESERVE	2
FIGURE 2 -BACKBONE, LOIN AND RUMP AREAS	3
FIGURE 3 –FERGUSON BCS FLOWCHART FROM 3.25 TO 4	5
FIGURE 4 –FERGUSON BCS FLOWCHART FROM 4 TO 5	5
FIGURE 5 –FERGUSON BCS FLOWCHART FROM 3 TO 2.5	6
FIGURE 6 –FERGUSON BCS FLOWCHART FROM 2.5 TO LESS THAN 2.....	6
FIGURE 7- TWENTY-THREE KEY ANATOMICAL POINTS.....	14
FIGURE 8- TWENTY-THREE KEY ANATOMICAL POINTS WITH X/Y VALUES.	14
FIGURE 9- IMAGE OF A THINAND A FAT COWS AND THIER PARABOLIC FIT	15
FIGURE 10- ANATOMICAL LANDMARKS IN A COW BODY SHAPE	16
FIGURE 11- RESEARCH MAIN STEPS	20
FIGURE 12- COWS ENTERING THE MILKING PARLOR. TWO SELECTED IMAGES AND TWO NOT-SELECTED IMAGES	21
FIGURE 13- BCS DISTRIBUTION IN TRAINING SET AND TESTING SET	23
FIGURE 14- EDGE DETECTION OPERATORS	28
FIGURE 15- BACKGROUND IMAGE PIXEL VALUE DISTREBUTION	31
FIGURE 16- THE SEGMENTATION PROCEDURE	32
FIGURE 17-RECONSTRUCION AND MORPHOLOGICAL PROCEDURE.....	34
FIGURE 18- EXAMPLE OF THE SEGMENTATION PROCEDURE	35
FIGURE 19- EXAMPLE OF THE RECONSTRUCTION AND MORPHOLOGICAL PROCESS.....	36
FIGURE 20- EXAMPLE OF MANUAL SEGMENTATION.....	37
FIGURE 21-CONTOUR EXTRACTION AND NORMALIZATION PROCEDURE	38
FIGURE 22- AUTOMATIC EXTRACTION OF TAIL HEAD PEAKS AND VALLEYS.....	40
FIGURE 23- EXAMPLE OF EXTRACTION OF THE PEAKS AND VALLEYS.	41
FIGURE 24-FEATURE EXTRACTION.....	41
FIGURE 25- 3 THIN COWS AND 3 FAT COWS SIGNATURE CURVE.....	42
FIGURE 26- COW SIGNATURES FOURIER DESCRIPTORS	44
FIGURE 27- 1000 FOURIER DESCRIPTORS AND THE FIRST 50 DESCRIPTORS AND THEIR VALUE	45
FIGURE 28- THE 2-10 FOURIER DESCRIPTORS OF 4 THIN COWS AND 4 FAT COWS	45
FIGURE 29-LATENT VARIABLE SELECTION BY ROOT MSE	48
FIGURE 30- CORRELATION IN TRAINING SET BETWEEN THE MODEL OUTPUT AND THE MANUALLY BCS.....	50
FIGURE 31- CORRELATION IN TESTING SET BETWEEN THE MODEL OUTPUT AND THE MANUALLY BCS	51
FIGURE 32- THE BCS COMPUTED FOR 5 DIFFERENT IMAGES OF 5 COWS TAKEN IN THE SAME DAY.....	58
FIGURE 33- RANDOMLY SEPRATION OF EQUAL DISTRBUTED TRAINING AND TESTING SETS	60
FIGURE 34- BLURRING EXAMPLES	62

List of Tables

TABLE 1- THE BACK BONE AREA FOR EACH BCS 1 TO 5	4
TABLE 2- EXAMPLES OF DAIRY FARMING SENSORS.....	8
TABLE 3- EXAMPLES OF COMPUTER VISION APPLICATIONS	9
TABLE 4- EXAMPLES OF COMPUTER VISION SYSTEMS IN AGRICULTURE	11
TABLE 5- LIVESTOCK APPLICATIONS USING COMPUTER VISION	12
TABLE 6- DETAILS OF TRAINING AND TESTING SETS.....	22
TABLE 7- BCS DISTRIBUTION IN TRAINING SET AND TESTING SET	22
TABLE 8- FEATURE EXTRACTED FROM TAIL HEAD CONTOUR.....	24
TABLE 9- THE COLOR SPACE TRANSFORMATION	30
TABLE 10- FEATURE EXTRACTION BY BW-MATRIX	33
TABLE 11- MULTI CORRELATION OF ANATOMICAL POINTS MEASUREMENTS	46
TABLE 12- LINEAR REGRESSION FOR ANATOMICAL POINTS FEATURES.....	47
TABLE 13- CROSS CORRELATION BETWEEN BCS AND THE FIRST TEN FOURIER DESCRIPTORS	48
TABLE 14- LINEAR REGRESSION FOR FOURIER DESCRIPTORS	49
TABLE 15- EVALUATION OF ERROR RATE ON TESTING SET	51
TABLE 16- TRAINING SET CLASSIFICATION RESULTS OF COWS ABOVE AND BELOW 3.....	53
TABLE 17- TESTING SET CLASSIFICATION RESULTS OF COWS ABOVE AND BELOW 3	53
TABLE 18- TESTING SET CLASSIFICATION RESULTS OF COWS BETWEEN GROUPS (2-3,3-4,4-5).....	54
TABLE 19- TESTING SET CLASSIFICATION RESULTS OF COWS BETWEEN GROUPS (1-2,2-3,3-4,4-5)	54
TABLE 20- TRAINING SET CLASSIFICATION RESULTS OF THIN-MEDIUM AND FAT COWS.....	55
TABLE 21- TESTING SET CLASSIFICATION RESULTS OF THIN-MEDIUM AND FAT COWS	55
TABLE 22- PARAMETER ESTIMATION OF ORDINAL REGRESSION.....	56
TABLE 23- TRAINING SET CLASSIFICATION RESULTS BY ORDINAL REGRESSION	57
TABLE 24- TESTING SET CLASSIFICATION RESULTS BY ORDINAL REGRESSION	57
TABLE 25- BCS REPEATABILITY FOR EACH COW AND ITS STANDARD DEVIATION.....	58
TABLE 26- VARIANCE WITHIN COWS AND BETWEEN COWS	58
TABLE 27- ESTIMATION OF INFLUENCE OF TRAINING DATA SIZE ON THE MODEL MODIFIED.....	59
TABLE 27- ESTIMATION OF INFLUENCE OF TRAINING DATA SIZE ON THE MODEL MODIFIED.....	60
TABLE 28- INFLUENCE OF DIFFERENT RESOLUTIONS ON MODEL OUTPUT	61
TABLE 29- INFLUENCE OF BLURRING ON MODEL OUTPUT.....	61

1 Introduction

Description of the problem

Body condition scoring (BCS) estimates energy reserves of cows and their fatness or thinness according to a 5-point manual scale (Hady et al., 1994). Evaluation of BCS is a management tool associated with risk factors for health problems, feed intake and optimal insemination time (Rodenburg, 2004). Currently, BCS is measured manually: this is a time consuming process, it requires training, and its scores are subjective and may be influenced by the previous cow examined (Halachmi et al., 2008, Schröder and Staufenbiel, 2006). The lack of automation in this process is obvious. Despite several attempts to automate BCS of dairy cows (Coffey et al., 2003, Ferguson et al., 2006, Bewley et al., 2008, Halachmi et al., 2008, Azzaro et al., 2009) -it is still handled manually with no commercial applications and all state-of-the-art models involve a manual labeling procedure (Bewley et al., 2008, Halachmi et al., 2008, Azzaro et al., 2009) . Roche et al., 2009 suggested that “Ongoing research into the automation of body condition scoring are likely candidate to be incorporated into decision support systems in the near future to aid producers in making operational and tactical decisions”. Computer vision is used today in a wide variety of real-world industrial applications and can be applicable to BCS. The present study aims to develop an efficient and objective automatic computer vision tool to evaluate the cow's body condition. It differs from state-of-the-art models since it does not involve any manual labeling in neither the segmentation nor feature extraction process.

Objectives

The main objective of this study was to develop an automatic computer vision tool for evaluating body condition score including:

- 1) **Image acquisition:** design and implementation of a mechanical system for automatic capturing of images.
- 2) **Image processing and analysis:** development of image processing algorithms to extract the cow object from its natural background in the farm.
- 3) **Image interpretation:** statistically identification and selection of cow shape features that are correlated with body condition.
- 4) **Modeling:** development of a prediction and classification model of body condition.

The system was validated on a research dairy farm.

2 Literature review

Body Condition Scoring (BCS)

Body condition reflects body fat reserves of dairy cows (Hady et al., 1994). These reserves can be used by the cow in periods when she is unable to eat enough to satisfy her energy needs. In high producing cows, this normally happens during early lactation, but it may also happen when the cows get sick, or are fed poor quality feeds, or feed intake is restricted (Rodenburg, 2004). After a period of weight loss, cows should be fed more than their requirements to restore their normal body condition (Ferguson et al., 1994). Evaluation of body condition using a body condition score (BCS) is a useful management tool (Wildman et al., 1982). Excessive body condition has been recognized as a risk factor for health problems in dairy cows (Markusfeld et al., 1988, Gillund et al., 2001, Gearhart et al., 1990) and as a factor influencing feed intake (Gransworthy 1988), milk production (Domeq et al., 1997) and insemination time (Ruegg and Milton 1995, Syriyasathaporn et al., 1998). Excessive loss of body condition has been associated with lowered reproductive performance (Koenen and Veerkamp, 1998; Burke et al., 1996), and reduced milk production (Waltner et al., 1993). Thus, BCS has received considerable attention as a tool to aid in the management of nutritional programs in dairy herds. Cows should be scored regularly to reflect changes in fat reserves in each stage of lactation (Ferguson et al., 1994). Figure 1 shows the connection between body energy reserves and milk production, and also shows the optimal insemination time which is the maximum point of the energy reserve curve.

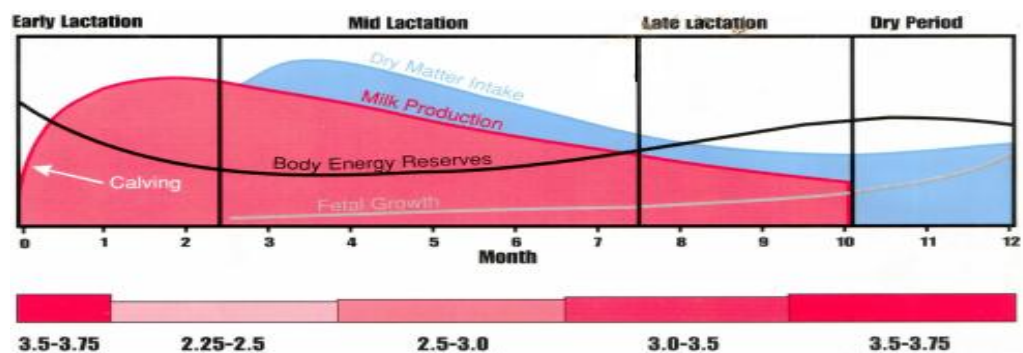


Figure 1 – Body energy reserve (black curve) and its connections with calving, milk production, and the optimum point before dry period which associated with optimal insemination time (Ferguson et al., 1994)

2.1.1 Body Condition Scoring techniques

There are many different scoring scales 0 to 5 (Lowman et al., 1976, Pedron et al., 1993), 1 to 10 (Morris et al., 2002), and 1 to 9 (Earle 1976). The most common system applied for BCS in the U.S.A. is the 1 to 5 scale (Ferguson et al., 1994), with 1 being emaciated, 2 thin, 3 average, 4 fat and 5 obese. It is common to divide the scale into 0.25 point increments (Ferguson et al., 1994).

The scoring technique includes looking at the cow and handling the pin bone, hip bone, the top of the backbone and ends of the short ribs, which all together combine the tail head area. The tail head area do not have muscle tissue covering, therefore any covering you see or feel is the combination of skin and fat deposits. As shown in Figure 2, only skin and fat cover the tail head area, making these ideal locations to assess body condition (Rodenburg, 2004).

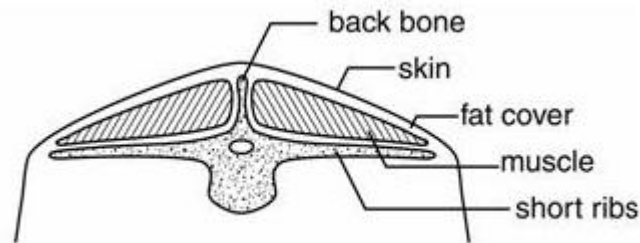






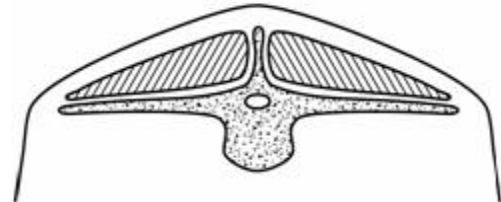

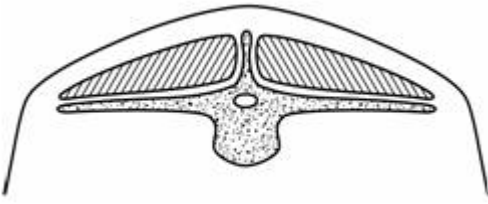



Figure 2 -Backbone, loin and rump areas (Rodenburg , 2004)

Table 1 shows the difference in the tail head area according to each body score from 1 to 5.

Ferguson et al., (1997) developed an organized flow chart for scoring body condition with a 5 point scale and accuracy of 0.25, when information needed for BCS is taken from the back side of the body. The flowchart scoring: Scores from 3.25 to 4 (Figure 3), from 4 to 5 (Figure 4), 3 to 2.5 (Figure 5) and, 2.5 to less than 2 (Figure 6).

Table 1- The back bone area for each BCS 1 to 5 (Rodenburg, 2004)

Condition score	Tail head area	
1 Emaciated cow		
2 A thin cow		
3 An average cow		
4 A fat cow		
5 Obese cow		

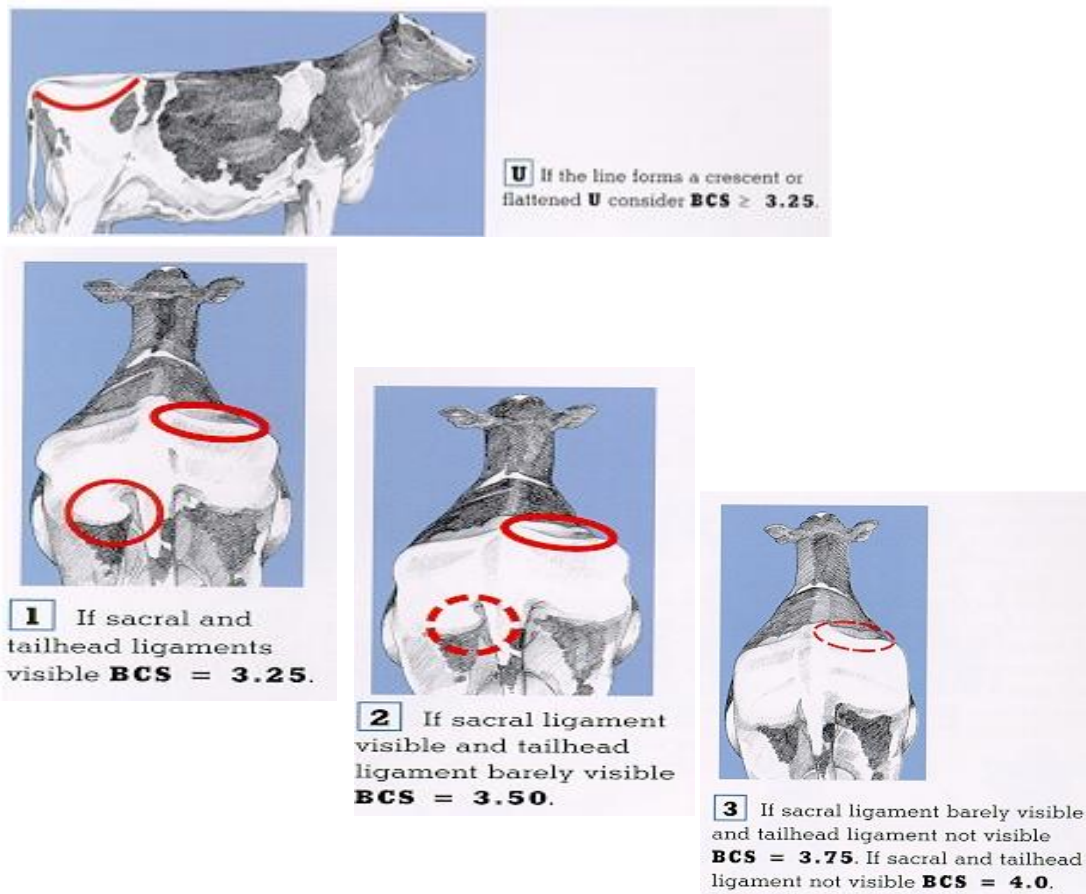


Figure 3 –Ferguson BCS flowchart from 3.25 to 4 (Ferguson et al., 1997)

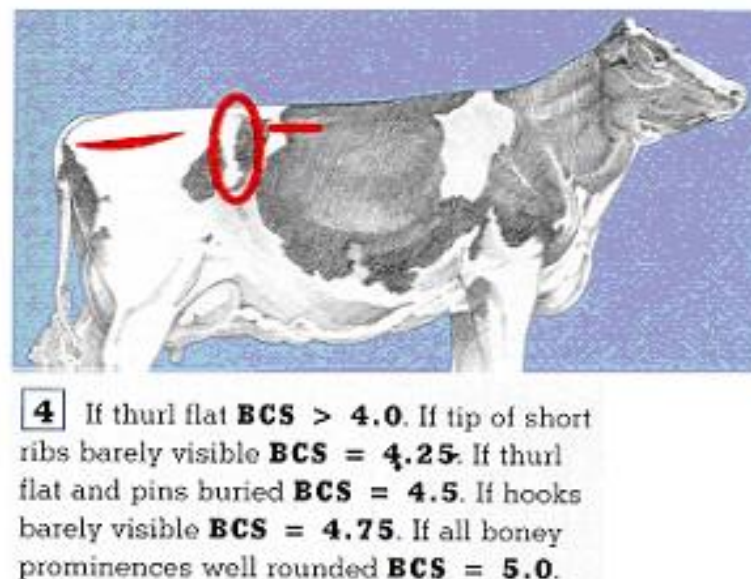


Figure 4 –Ferguson BCS flowchart from 4 to 5 (Ferguson et al., 1997)

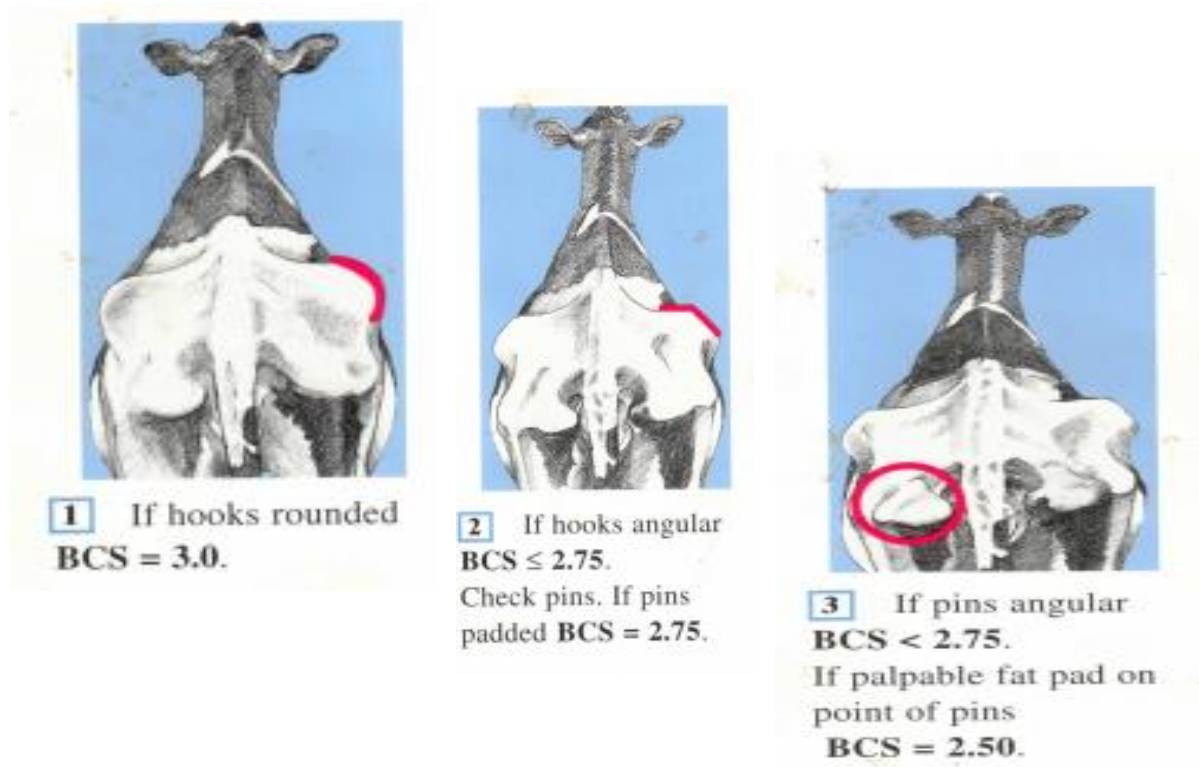
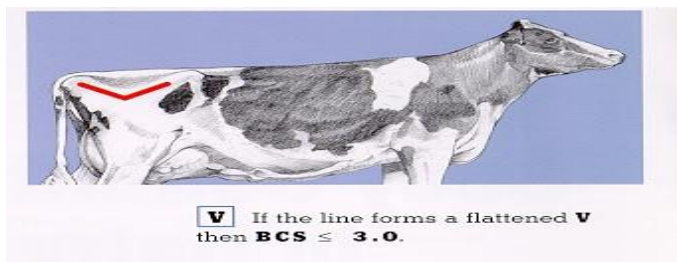


Figure 5 –Ferguson BCS flowchart from 3 to 2.5 (Ferguson et al., 1997)

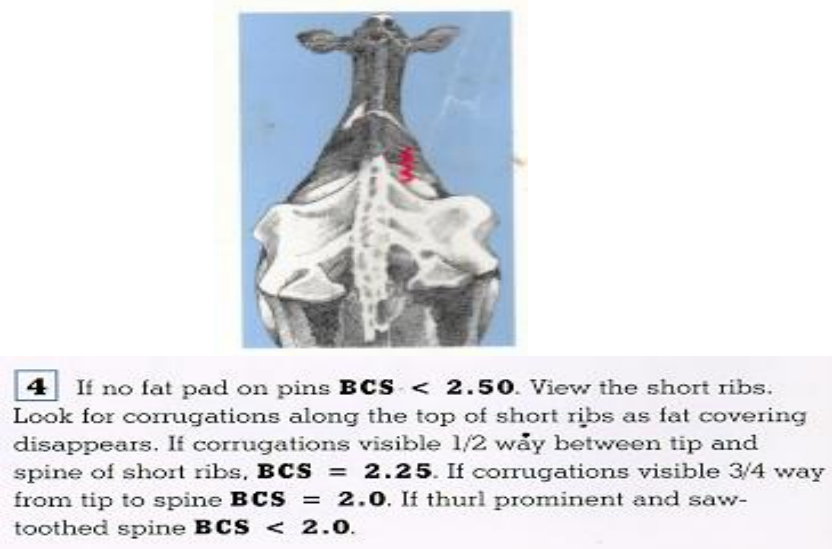


Figure 6 –Ferguson BCS flowchart from 2.5 to less than 2 (Ferguson et al., 1997)

Automation in dairy farming

Modern dairy farming is characterized by automation and information systems that support decision making. The data is usually collected by a variety of sensors (Table 2). However, the current method of measuring BCS in modern dairy farms is still manual. Manual BCS is time consuming in large farms and requires trained labor (Halachmi et al., 2008). Another problem associated with the manual scoring is the subjectivity of the process, the score depends on the person who performs the measurement, and the score of the specific cow can be influenced by the previous cow examined (Schröder and Staufienbiel, 2006). “Despite the general consensus of dairy producers and herd managers, on the benefits of the BCS evaluation, less than 5% of U.S. dairy farms have adopted this practice in the production chain” (Azzaro et al. 2011). The main reasons that discourage the use of BCS evaluation techniques are the lack of computerized reports, its subjectivity and time consumption of on-farm training of technicians. Furthermore, the measurements must be conducted frequently for each cow, expanding the costs for the farmers (Azzaro et.al., 2009). Bewley et al (2008) suggested that an automatic BCS requires less time, is less stressful on the animal, more objective and consistent, and possibly be more cost effective. Therefore, the development of an automatic device based on digital images for monitoring BCS is of economic interest (Halachmi et al., 2008).

Table 2- Examples of dairy farming sensors

Domain	Technology	Description	Source
Detection	Radio Frequency Identification (RFID) sensor	Detect the specific cow by using a unique serial number	Senger, 1994, Pendell et al., 2010
Weight	Weigh scale	Weigh cows during their movement out of the milking parlor.	Peiper et al., 1993 Passtel et al., 2005
Milk meters	Metering device controls the flow of milk	Alert when milk flowing is about to end in order to prevent over milking.	Flochini, 1980 Hogeveen et al., 2001
Milk quality	Near-infrared (NIR) sensor	predicting three major milk constituents (fat, protein and lactose)	Kawamura et al., 2007 Tsenkova et al., 2000
Mastitis detection	Measuring electrical conductivity	Measure the level of conductivity of each quarter separately.	Gotien, 2006, Neiln et al., 1992
Lameness detection	Force–plate system	Alert for Hoof care, by generating signatures of ground reaction	Rajkondawar et al., 2002
Estrous detection	Pedometer pressure sensors	Alert for estrous and optimal insemination time.	Maatje et al., 1997 Senger 1994
Behavioral evaluation	Pedometer Plus	Measures cow's comforts by counting steps, lying time and lying frequency.	Maltz et al., 2007
Rumination behavior	Sound sensor	Monitoring changes in time of rumination reflecting the cows comfort	Bar-Shalom, 2008

Computer vision

Computer vision can extract more information than a specific sensor (Chen et al., 2002). This is due to its ability to draw on a far richer blend of image components (including visible light, X-rays, ultrasound, and nuclear magnetic resonance), coupled with its flexibility as a tool for filtering and extracting the information that are the most relevant (Van der Stuyft et.al., 1991). Computer vision is used today in a wide variety of real-world industry applications such as shown in Table 3.

Table 3- Examples of computer vision applications (Szeliski, 2008)

Domain	Applications	Sensor
Quality Control	Machine inspection: rapid parts inspection for quality assurance measure. Retail: object recognition for automated checkout lanes	Stereo vision X-ray vision NIR Digital Camera
Industrial sorting & Food quality.	Meat \ Fruit \ Vegetables \ Fish \ Grain quality evaluation and ingredients.	Microscopic Video camera, Digital Camera, Ultrasound, X-ray, NIR.
Medical	Real-time vision to detect pose of markers during surgical, Registering pre-operative and intra-operative imagery, Detecting tumors.	Stereo vision X-ray vision
Vehicle guidance	Detecting pedestrians, or obstacles on the road.	Video Camera
Law enforcement and surveillance	Advanced video surveillance, Post event analysis, Shoplifting, Suspect tracking and investigation.	Digital Camera Video Camera
Biometrics	Using face recognition algorithms for: Drivers' licenses, Voter registration	Digital Camera Thermal Infra-red
Information security	Personal device logon, Desktop logon Database security, Intranet security.	Digital Camera Video Camera

Agriculture computer vision applications

Computer vision holds potential for the agriculture industry because of its simplicity, noninvasive sensing ability and low cost (Chen et al., 2002). It has been used to define characteristics of fruits, vegetables, meat and fishes with color, size, shape and texture features that can be drawn from images (Ram, 2009).

Gross et al., (2001) showed that the most progressive face recognition algorithms find difficulties dealing with wide range of variation including different viewing angle of the person face, illumination, occlusion, time delay between acquisition of gallery and probe images, and individual differences between different persons. Agriculture is characterized by large variation in both the environment and the objects:

- Illumination, caused by different times along the day or different weather conditions (e.g., clouds, fog)
- Different viewing angles caused by different poses of the object (fruit, or animal).
- Time delay between images, animals and fruits change their appearance during time, due to randomness (wind, animal motion).
- Individual differences between objects (fruit, or animal) due to their biological nature.

Table 4 shows several examples of uses of computer vision in agriculture and the different size, shape, texture and color of the features extracted.

Computer vision in livestock

Nowadays, computer vision has been developed to a stage that it could possibly help a stockman by automating some of his routine tasks. Twenty two years ago, a review by DeShazer et al. (1990) identified over 90 potential applications for vision systems in livestock production simply by considering the tasks a stockman performs using his eyes. Table 5 shows examples of computer vision in livestock application. Those applications mainly aim to monitor the wealth of the animals and to reduce the stress causing by the traditional invasive examinations. The majority of applications regarding poultry and pigs brought in Table 5 are commercial while the lameness detection and BCS prediction for dairy cattle are not commercial yet.

Table 4- Examples of computer vision systems in agriculture

Application	Sensor	Extracted features	Source
Pickling cucumbers classification	NIR spectrometer	Intensity reflectance of wavelength in range of 950- 1650 nm	Ariana et al., 2006
Olive classification	Digital camera	Size , Shape, Texture, Color, Defects	Laykin et al.,2008
Tomatoes classification	Digital camera	Color, color homogeneity, defects, shape	Laykin et al.,2002
Potato classification	Digital camera and multispectral sensor	intensity reflectance of wavelength in range of 450- 870 nm	Noordam et al., 2005
Ripened bananas sorting	Digital camera	brown area percentage, number of brown spots per cm ² , homogeneity, entropy	Mendoza & Aguilera, 2004
Pomegranate sorting	2 Digital camera	Color	Blasco et al., 2009
Citrus sorting	2 Digital camera & Illumination system	3D Shape, size	Blasco et al., 2009
Grape Grading	Digital camera	homogeneity of surface	Vazquez-Fernandez et al., 2009
Measurement of Grains	Scanner	Shape, Boundary identification	Igathinathane et al., 2009
Watermelons quality determination	NIR spectrometer	Weight, Height, Internal defects, Sugar content, soluble solid contents	Lee et al.,2008
Disease detection in Greenhouse	Scanner	Color, texture, shape and size.	Boissard et al., 2008
Finding the optimal harvesting time of olive grove	Digital camera Low Resolution-Nuclear Magnetic Resonance (LR-NMR)	Size, shape, color and texture	Ram, 2009

Table 5- Livestock applications using computer vision

Application	Sensor	description	source
Fish sorting	Digital camera	The contour lines and the body's geometry characteristic were extracted in order to detect the fish type between three different classes	Zion et al., 2006
Social behavior of poultry	Video Camera	Motion tracking used for tracking the route taken to feed by focal birds.	Collins, 2008 Dawkins et al., 2009
poultry thermal comfort	Thermal camera	Motion tracking used for classifying specific behaviors in different temperatures.	Nääs et al., 2009
Monitoring pigs thermal comfort	Video Camera	Motion tracking used to detect resting behavioral patterns.	Shao & Xin, 2008
Tracking piglets	Video Camera	Motion tracking used for detecting long period between piglets being born, or piglets being unable to find the sow's teats.	McFarlane & Schofield, 1995, Navarro et al., 2009
Predicting pigs weight	Video Camera	The plan view area measured from images used to predict pig weight with an accuracy of 5 %.	Schofield, et.al., 2005 Schofield at al., 1999
Describing pigs growth	Digital Camera	11 size Measurements of shape and size.	Doeschl-Wilson Et.al., 2004
Distinguishing between pig types and sexes	Video Camera	Measuring the plan view area.	White et al., 2004
Finding relationship between body weight and body measures in three different breeds of beef cattle	Digital Camera	6 size Measurements of shape and size	Ozkaya & Bozkurt, 2008

Application	Sensor	description	source
Dairy cattle lameness detection	Video Camera	Measuring the distance between hoofs using edge detection	Song et al., 2008
Dairy cattle lameness detection	Video Camera	Fitting a circle to the back posture while walking.	Poursaberi et al., 2010
Assessing energy requirements for cattle on pasture	Thermal Camera	Modeling the cattle heat losses and gains using a 3D model of the animal	Keren & Olson, 2007
Pigs body condition scoring	Stereo imaging system with six high-resolution and three flash units.	Capturing 3D shapes in order to evaluate their body score from the images.	Wu et.al.,2004
Cow's body condition	Digital camera Line laser	Capturing 3D shape of the cows surface and extracting the body contour	Pompe et al., 2005
Cow's body condition	Ultrasound	distinguish between skin, sub dermal fat and muscle	Mizrach et al., 1999
Cow's body condition	Digital camera	19 points were manually identified for describing the cow contour from the back side of the cow.	Leroy et al., 2005
Cow's body condition	Digital camera Laser light	Manually extraction of cow shape by spotting the laser light in the digital image	Coffey et al., 2003
Cow's body condition	Digital camera	Manually identification of 23 anatomical points describing the cows contour and computing the angles between those points	Bewley et al., 2008
Cow's body condition	Thermal camera	Cow parabolic shape factor	Halachmi et al.,2008
Cow's body condition	Digital camera	Manually identification of 23 anatomical points, and computing their principal components	Azzaro et al., 2011

Computer vision in BCS

2.1.2 Manually BCS from images

Coffey et al., (2003) evaluated the possibility of scoring the cow's body condition by using digital images and a red laser light that created light lines across the tail head area of the cow. The light lines in the image allowed extracting manually a curve that represented the fat tissue around the tail head area of the animal. Results indicated that it is feasible to extract the shape of the hooks and the tail head area and to use this information in order to score the cows from those digital images and that those scores are correlated to BCS taken apart. Ferguson et al., (2006) evaluated the correlation between regular BCS and BCS taking from images of the rear of the cow at 0 to 20 degrees angle, similar to the photos in Table 1. Four observers scored cows both on live visit in the farm and from images. The mean of live BCS did not differ from the mean photo BCS. Correlation coefficients between BCS assigned live and from photos were 0.84, 0.82, 0.82, and 0.90 for observers 1 to 4, respectively and therefore it was concluded that body condition can be assessed by observers from images taken on the farm without visiting the farm. Bewley et al., (2008) identified 23 anatomical points representing the cow shape as shown in figure 7. The images were acquired automatically above the weighing station. The points were derived manually from images and transformed to an x/y coordinate system as shown in Figure 8. From the coordinates the angles of both sides of hooks and pins were calculated (overall 15 angles were calculated), and then two types of linear mixed models considering the effect of the angles and interaction between the angles were evaluated for BSC prediction. Results showed strong relationship between calculated angles and the BCS determined by experts.

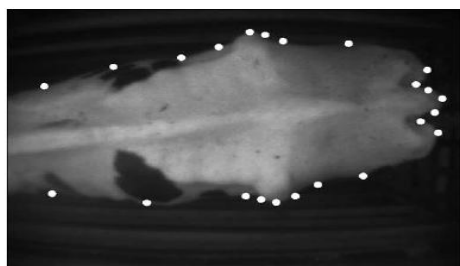


Figure 7- Twenty-three key anatomical points identified (Bewley et al., 2008).

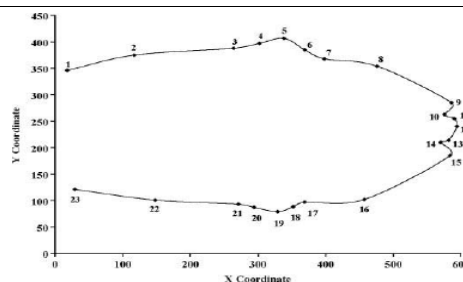


Figure 8- Twenty-three key anatomical points with x/y values (Bewley et al., 2008).

2.1.3 Automatic BCS from images

Fitting cow's body shape to a parabolic curve using a thermal camera (Halachmi et al., 2008):

Images were taken automatically from above the cows at a weighing station with a thermal camera. The hypothesis of the research was that fat cow's have a round contour similar to parabolic, and so for each cow it is possible to fit a polynomial and to calculate the mean absolute error (MAE) from her own contour. The thinner the cow, the larger the MAE will be as shown in Figure 9. The scoring model presented as: $BCS = 5 \times 9 \times (1/MAE)$ where 9 is the best fit in the specific herd, 5 is the factor that normalize the score to a 1-5 scale. Matlab software was used for taking the images and fitting them with a polynomial, calculating the MAE and then providing a score on a 1-5 scale, advancing this process one more step toward full automation.

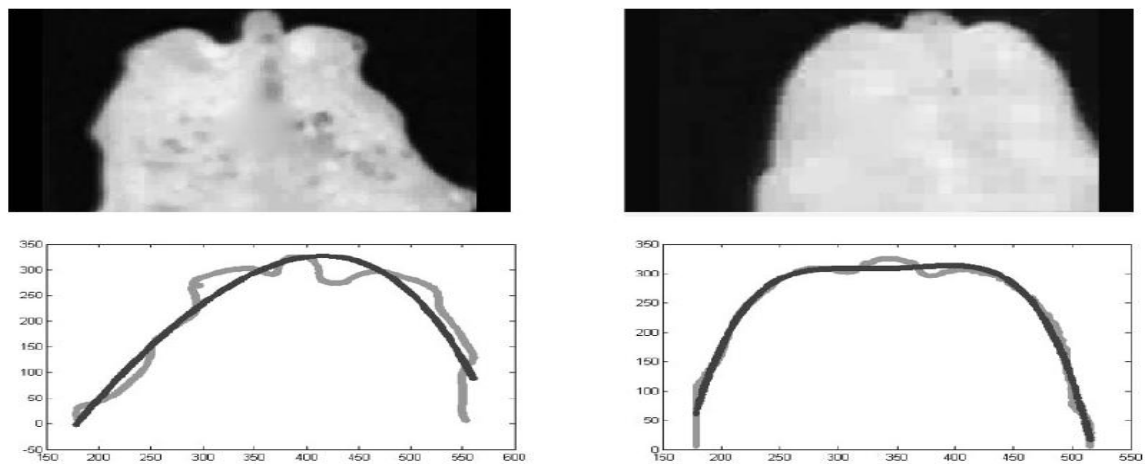


Figure 9- On the left side an image of a thin cow and her parabolic fit and on the right side an image of a fat cow (Halachmi et al., 2008).

A 0.89 correlation found between the scores of the model and scores taken manually and by ultrasound (Halacmi et. al, 2009). The results indicate that it is feasible to fully automate the BCS process.

This M.Sc. study aims to build upon Halachmi (2008, 2009)'s results using digital camera instead of a thermal camera which is less expensive and hence more attractive to industry.

Estimating BCS from digital images (Azzaro et al., 2011):

The images were taken from above by a low cost digital camera. The researchers obtained a consistent shape representation by aligning the corresponding anatomical landmarks. The landmarks were selected according to Bewley et al., (2008) 23 anatomical points. The alignment of shapes was carried out by establishing a coordinate reference to which all shapes must be referred as shown in figure 10(a). First, shapes are translated to the origin (Figure 10b). Shapes are then rotated such that the left hook and the right hook have the same horizontal coordinate (Figure 10c). To perform translation and rotation of shapes, the middle point between the left hook and the right hook was taken into account. Finally, shapes are scaled to fit in a unit square (Figure 10d)". After alignment, all the shapes referred to the same coordinate system centered into the origin.

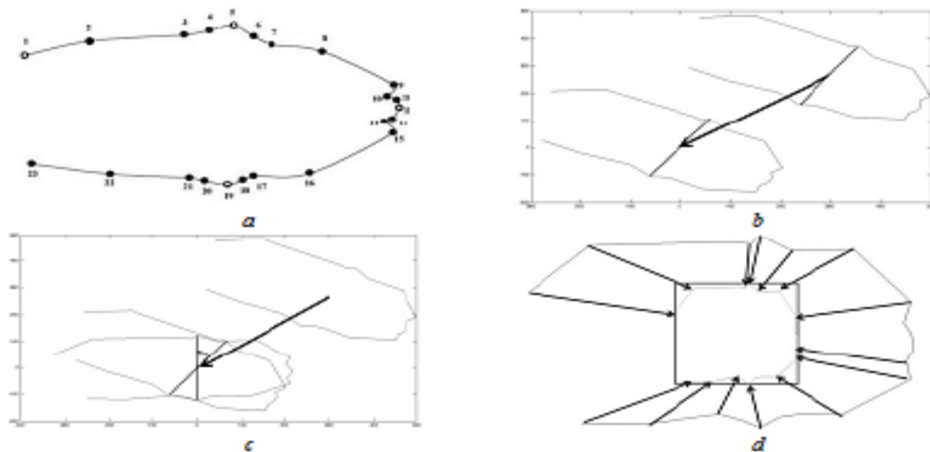


Figure 10- Anatomical landmarks in a cow body shape (a), shape translation (b), shape rotation (c), and shape scaling (d) (Azzaro et al., 2009).

The researchers used this system in order to evaluate state-of-the-art BCS models such as the Bewley linear model, Halachmi parabolic model, and a model based on Principal Component Analysis (PCA).

Results indicated that the Bewley model and the PCA models achieved lower mean error (0.3289 and 0.3059 respectively) than the parabolic model regarding the manual BCS. The results indicated that further research is needed in order to build a fully automatic system for BCS evaluation in which the shape of a cow will be automatically extracted through segmentation

procedure from digital images acquired with a low cost camera, and further research is needed for better estimation of BCS.

Steps in computer vision

Groover (2001) describes the operation of machine vision as a three step operation including acquisition and digitization of the image, image processing and analysis and finally interpretation of the image.

Image acquisition: is accomplished by dividing the viewing area into a discrete matrix of the picture elements call pixels. This operation is conduct by the digital camera itself and a data acquisition card (Groover, 2001).

Image processing and analysis: Before image processing some Pre-processing is needed for clarification of the image and noise removal. Techniques such as High-Pass and Low-pass filters, median filters and morphological operations are productive (Sonka et al, 2007). After producing the new image, the image can be segmented. Segmentation techniques are aided to define and separate regions of interest in the image. Two of the most common segmentation techniques are Tresholding and Edge detection (Groover, 2001). Thresholding involves transforming the intensity values of the pixels to binary values according to a value determent according to the object of interest and the image characteristics (Sonka et al, 2007). The image values are naturally given from the camera in the RGB space, but they also can be transformed according to image characteristics to other types of three dimensional spaces such as HSV, HSI and Lab spaces (Zheng et al., 2006).It is possible to transform the image, in any color space, to a one-dimensional image by using relative values that emphasize the difference between the three dimensions (Bakker et al., 2008).

Edge detection is a method for determining the boundaries and location of an object within his background. It is usually used following the threshold operation however; it can also include the threshold operation (Groover, 2001). Edge detection drastically reduces the amount of data to be processed while preserving useful structural information about the objet boundaries (Canny, 1986).The edges are defined as the set of points which after a smooth operation (Low-Pass filter) the norm of the gradient reach to local maximum(Catte et al., 1992). There are many edge operators in literature, the

most common ones use the first directional derivative such as Sobel (Cherry & Karim, 1984), Roberts (Robert, 1984) and Prewitt (Cherry & Karim, 1984) and operators that use the second derivative such as Laplacian and Gaussian operators such as canny (Canny, 1986).

Following segmentation usually comes feature extraction procedures. The feature extraction procedures (such as Blob analysis) characterize the object in means of area, length, width, diameter, perimeter, orientation and center of gravity by using simple geometry on the binary image (Groover, 2001). For tracking piglets McFarlane & Schofield, 1995 (Table 5) used the fact that the piglet's skin is brighter than their background in order to reduce two sequential images and then threshold the background that had low intensity values. In order to monitor their movement they used Laplacian edge detector to track the movement of the piglet's edges instead of the whole object and finally to remove noises they used Blob analysis to extract only the features that resembled the geometry form of ellipse. For tracking lameness Song et al., 2008 (Table 5) reduced two sequential images in order to segment the cows hoof and blob analysis was applied on the binary image in order to find the area and the center point of the hoofs. Zion et al., 2006 (Table 5) segmented fish from their background by threshold each band separately and applying the AND operator on the three binary images. By blob analysis the area of the fish, perimeter, orientation and the foremost pixel were extracted.

Image interpretation (Zhang and Lu, 2003): There are mainly two approaches to shape representation, the region-based approach and the contour-based approach. Region-based techniques often use moment descriptors to describe shapes but, in many applications the internal shape is not as important as its contour. Contour-based techniques tend to be more efficient for handling shapes that are describable by their object boundary (Zhang and Lu, 2003). These techniques use a shape signature function which aims to create one dimension vector representing a two dimension shape.

The most common shape signatures are: radial distances from the object centroid (Zhang et al., 2003), angular functions representing the changes in the directions of the contour (Zhan et al., 1972), and polar coordinate representations which combine the radial distances and the polar angle (Kunttu et al., 2007). Zion et al., 2006 (Table 5) used the fish contour signature of polar

coordinates followed by Partial Least Square regression in order to compute the latent variable describing the variances between the contours and to classify their type. Zhang and Lu, 2003 suggested the discrete Fourier transform as a powerful tool for reducing noise sensitivity, for shape analysis of the chosen signature and in order to make the transformation of the shape invariant to the starting point (absolute values must be used).

3 Methods

General overview

Figure 11 illustrates the data collection, image processing and model development main steps. All methods are detailed in chapter 3.2-3.7 and all algorithms are detailed in chapter 4. The selected algorithms in final model are marked in red. The motivation for selecting each algorithm is also detailed in chapter 4.

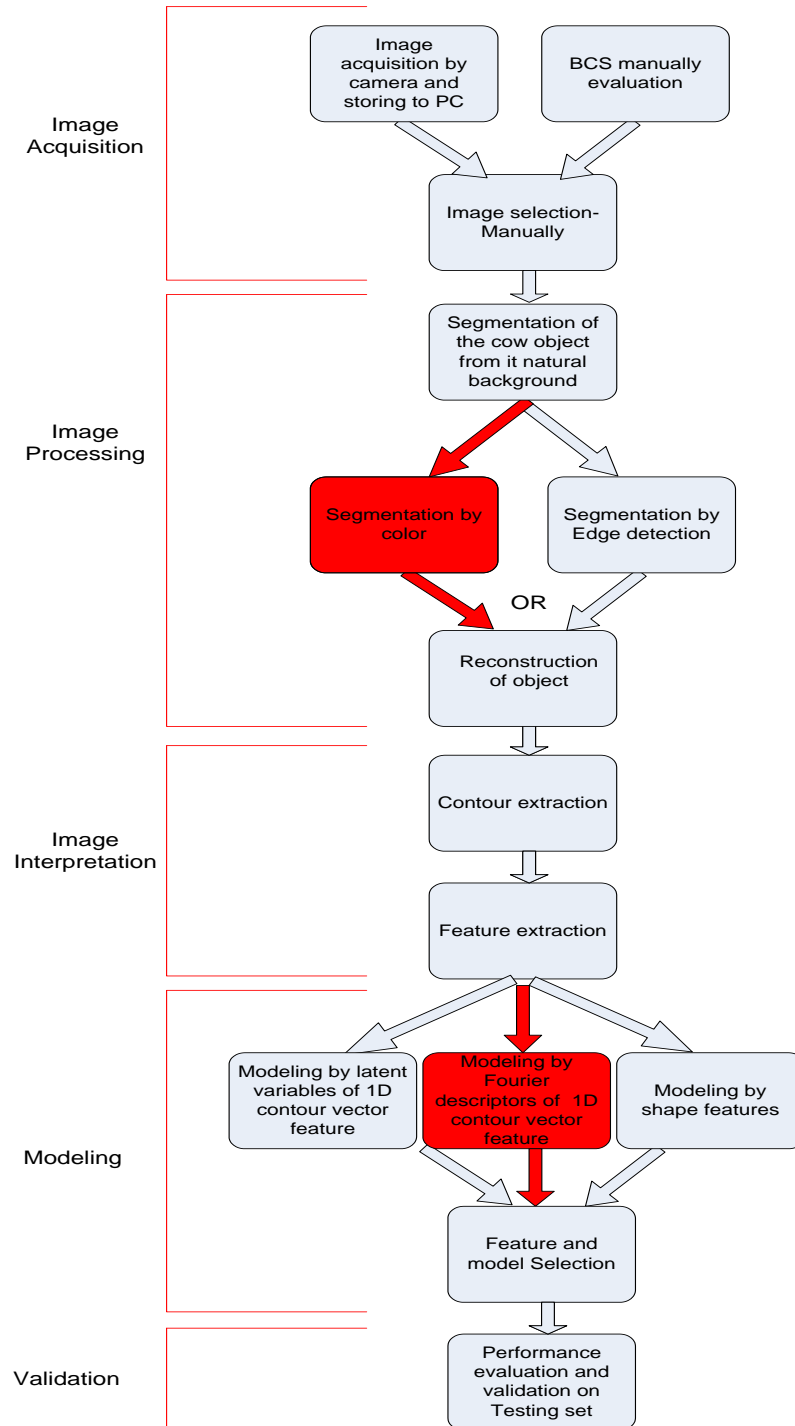


Figure 11- Research main steps

Image acquisition

The images were collected in the ARO research farm at Bet Dagan, Israel between October 2011 and February, 2012. A Nikon D 7000 DSLR camera was located at the entrance of the milking parlor at 2.5 meter height. All images were taken at the noon milking. The camera was activated manually from a PC via a USB cable by Nikon Camera Control pro 2 software (Nikon Corporation, USA, Appendix A. image acquisition software). Each time a cow entered through the parlor gate the camera was activated, and acquired six consecutive images in resolution of 1632X2464. All images were downloaded to the PC (Appendix B .cow digital images) and processed off-line. The images for processing were selected manually by the following criteria: (1) the entire tail head area of the cow was above the red floor of the milking parlor entrance. (2) The tail head area was not connected to forging objects including other cows. (3) The tail and legs were straightened. Figure 12 demonstrate two selected images (on the top) and two images that weren't selected (bottom).



Figure 12- Cows entering the milking parlor. Two selected images (top) and two not-selected images (bottom)

Database

Two sets of data were collected by the same procedure mentioned above. A training data set was collected between October and December 2011 and was used for the development of the prediction model. A testing data set was collected in February 2012 (Appendix B .cow digital images). The cows were photographed at eight different days in both the training set and testing set. The details of the two data sets are shown in Table 6 and all cows were manually scored by an expert (Appendix C. manual BCS).

Table 6- Details of training and testing sets

Data base	No. of images	No. of cows	Collection date	Expert scoring dates
Training set	87	71	10.10.2011	10.10.2011
			21.11.2011	21.11.2011
			18-20.12.2011	20.12.2011
Test set	64	41	21-23.2.2012	22.2.2012

Training set: The training set contains eighty seven Images of fifty nine different cows. The data (scores and images) were collected at three different dates (Table 6) and their scores distribution is given in Table 7 and Figure 13 (left). The majority of the scores are between 2-3, there are no extremely thin cows (below 2) and there is a small amount of very fat cows (around 4.5).

Testing set: The testing data set included sixty four images of forty one different cows. The distribution of scores in the testing set is given in Table 7 and Figure 13 (right). The majority of the scores are between 2-3 and between 3.5-4. Unlike in the training set, there are no very high scores (above 4.5) and there are two scores below 2. As discussed in chapter 2.2, the manual scoring include some natural error which may limit the classification results. According to Ferguson et al., 2006 the natural human error for fat and very thin cows ($BCS > 3.5$ and $BCS < 2.5$) is 0.5 while for medium cows ($2.5 < BCS < 3.5$) the natural error is 0.25.

Table 7- BCS distribution in training set and testing set

BCS	Data set	1-2	2-2.5	2.5-3	3-3.5	3.5-4	4-4.5	4.5-5	Total
Amount	Training	0	32	26	13	5	6	5	87
Percentage in data set	Training	0.00%	37%	30%	15%	5.5%	7%	5.5%	100.00%
Amount	Testing	2	20	17	7	14	4	0	64
Percentage in data set	Testing	3%	31%	27%	11%	22%	6 %	0%	100%

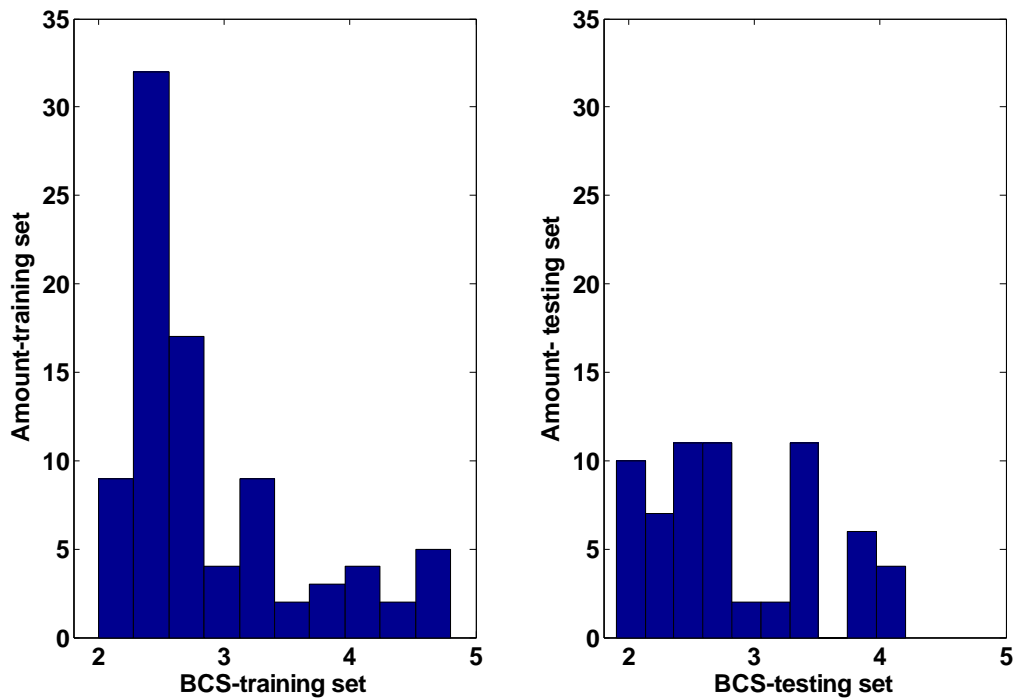


Figure 13- BCS distribution in training set (left) and testing set (right)

Image processing

3.1.1 Segmentation

Two different methods were tested for segmentation: (1) edge detection using common operators (Sobel, Roberts, Prewit and Canny) and (2) a second method which included three steps, the first step is transformation to different color masks, followed by applying the Otsu method (Otsu, 1979) for automatic selection of threshold from gray level histogram and subtraction of the proper background image (detailed in chapter 4.1.3). The best color mask was selected by univariate analysis of the threshold effectiveness followed by LSD post hoc testing.

3.1.2 Image reconstruction

The morphological operations in this stage were performed with Matlab's image processing functions: (1) 'bwlabel'- for objects labeling. (2)'regionprops'-for extraction of shape features of binary object (BW matrix) such as area, orientation, etc. (3) erosion and dilation - for removal of small objects and smoothing of the object. (4) 'bwboundaries'- for labeling holes inside the object (detailed in chapter 4.1.4).

Image interpretation and feature extraction

The information for BCS classification is contained in the object shape. Therefore, the contour of the tail head area was extracted, and the features for BCS classification were extracted directly and automatically from each contour (Table 8). The algorithms for extracting the features are detailed in chapter 4.

Table 8- Feature extracted from tail head contour

Feature name	Description	Source
X, Y coordinates	5 points given in X and Y coordinates representing the peaks and valleys of the Tail head area	Bewley et al., 2008
X Distances	5 distances between the points in X coordinate	
Y Distances	5 distances between the points in Y coordinate	
Angles	The angle of the triangles assembled from the 5 points	Bewley et al., 2008
1000 Distances Vector	The radial distance was computed from each point in the cow's contour to the center of the object	Zhang and Lu , 2003

Bewley et al., 2008 and Halachmi et al., 2008 suggested the hypothesis that rounder shape of the tail head area indicates higher BCS. Therefore, a wide angle between the peaks and valleys in the contour indicate a rounder contour implying a fatter cow with a higher score. On the other hand, high distance between the peaks and valleys in the cow contour indicate a thin cow and hence, the score is lower.

In general, in this study we applied state-of-the-art methods with some differences caused by the automated process and by different approaches as detailed in the following: (1) only 5 anatomical points from Bewley's 23 anatomical points were extracted due to the fact that Bewley et al., 2008 did not use all points in his final model and since the hook area was difficult to extract automatically while the cow was walking. (2) the curvature of the tail head contour was computed with the 1000 distances vector instead of the polynomial fit of Halachmi et al., 2008.

Regression modeling

Prediction of BCS was achieved by developing a linear regression model. Two different types of features were taken for the development of the regression models: the first model used the anatomical points extracted from the contour. The second

model used the vector of distances from the center object to each point in the contour. The distances were described by two forms: the first form is by producing a small number of latent variables that describe the majority of the variance data in the contour. The latent variables were derived using Partial Least squares Regression (PLSR). The second form of describing the contour used the Fourier descriptors of the curve. The Fourier transform was conducted using Fast Fourier Transform (FFT). The most important Fourier descriptors were selected using Stepwise Regression.

Features were selected by analyzing the correlation matrix of the different predictors with BCS and the model goodness of fit was examined by: R^2 , R^2_{adjusted} , Akaike information criterion (AIC) and the Bayesian information criterion (BIC). Cross-validation was implemented using the ‘*Leave One Out*’ procedure (Stone, 1974).

Performance Analysis

The model's performance was tested and validated on the observations taken from the testing data base which was collected between the 21th and the 23th of February. The model was also analyzed by its capability of distinguishing between BCS classes. Confusion matrices were calculated for the different classes. Due to (1) the inherent subjectivity of the golden reference (2) possibility large variations in the expert's golden reference, and (3) vague borders between classes; it was decided to assign artificially classes of scores. In practice, the main interest is in the BCS class and trend the absolute numerical value is meaningless. For example, it is important to know if the cow is thin, very thin, fat cow, etc and not if it has a specific BCS of 2.4, 2.5, and 2.6. Ferguson et al., 2006 recommended that in general, cows with BCS lower than 2.5 are too thin and cows with BCS higher than 3.5 are too fat. Therefore, actual classification results were derived for different class combinations including different borders between the classes.

Comparing with state-of-the-art methods: Azzaro et al., (2011) compared the performance of state-of-the-art methods for BCS predictions (Bewley et al., 2008, Halacmi et al., 2008, Azzaro et al., 2011). The comparison was based on calculating the average error between the models outputs and the manual BCS by:

$$BCS_error = \frac{1}{N} \sum_{i=1}^N |ModelBCS_i - ManualBCS_i|$$

In order to compare the current model results with the state-of-the-art results the BCS error was calculated also as a performance measure.

The repeatability of the model results was examined by calculating the standard deviation of five measurements of five cows measured on the same day.

Classification modeling

Instead of computing linear regression followed by classification (by creating the borders between BCS) in this model the BCS will be labeled as classes and then a classification model will be computed by Ordinal regression. The Ordinal regression was conducted using the cumulative Logit link function:

$$\ln\left(\frac{\text{prob}(\text{group}_i)}{1 - \text{prob}(\text{group}_i)}\right) = \beta_0 + \beta_1 X$$

group_i is the class that the BCS belongs, $\text{prob}(\text{group}_i)$ is the probability of belonging to the group and, $\ln\left(\frac{\text{prob}(\text{group}_i)}{1 - \text{prob}(\text{group}_i)}\right)$ is the link function.

The selected classes were: thin cows (below 2.5, labeled as 1) medium-thin, (2.5-3, labeled as 2) medium-fat, (3-3.5, labeled as 3) and fat (above 3.5, labeled as 4). The model performance was evaluated by the error rate of the classification table.

Sensitivity analyses

The following sensitivity analyses were performed:

- Different sizes of training data set: both the training set and testing set were combined to one data set which contains 151 images and then new, randomly, calibration and validation sets were created.
- Distribution of training set: The BCS were divided to new, theoretical 1 to 7 classes (1.5-2, 2-2.5, 2.5-3, 3-3.5, 3.5-4, 4-4.5, 4.5-5). Then, the 151 images data set was equally randomly, divided to two separate sets so the proportion of each category was identical in both the training and the testing sets.
- Estimation of the sensitivity of the model to the imaging properties conducted by evaluating the difference in the model output under different: (1) image resolution -conducted with Matlab function 'imresize'. The input of this

function is the original image and the new resolution desired. (2) blurred image- conducted by creating a “motion” filter by Matlab’s function ‘fspecial’ and then convolving it on the image. The direction of the filter was set to zero (to visualize the motion of cow going straight). Different sizes of the filter were evaluated.

4 Algorithms

Image processing

4.1.1 Edge detection

Several common edge detection methods were applied (Sobel, Prewitt and Roberts, Figure 14). Qualitative analyses of results indicate that these methods have difficulties in finding the back-bone contour due to the many lines that appear in the images. It is very hard to distinguish between lines that represent the contour and lines that represent black & white stains. It seems that in order to solve this problem a color transformation is needed in order to eliminate the black and white stains of the cow.

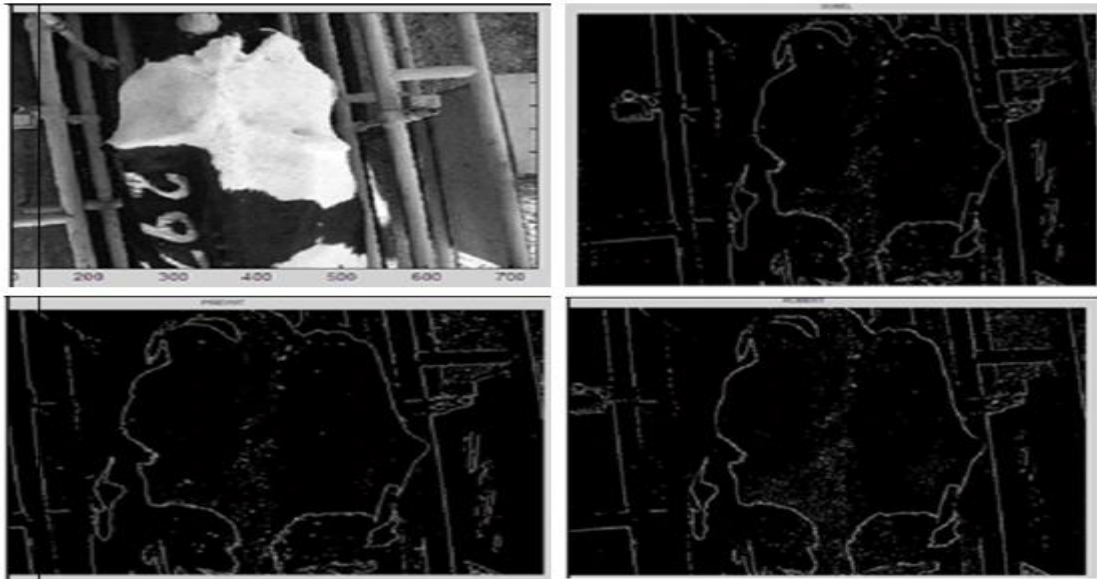


Figure 14- Edge detection operators: gray scale image (upper left), Sobel operator (upper right), Prewitt operator (bottom left) and Robert operator (bottom right)

4.1.2 Color masks determination

To automatically determine the threshold, the Otsu method (Otsu, 1979) was applied. This method looks for a separation between two groups that their centers are as far as possible and the variance inside the group is as small as possible. Therefore, it is needed to construct from the RGB image a gray-level image with a bimodal histogram. The aim is to find a suitable color space that separates between the floor and the rest of the picture. Twenty five different color masks (Table 9) were tested to derive an image with bimodal distribution of the pixel values. By looking at the images in Appendix D (color masks images) it is possible to see that in all

transformations that involve the H space the floor color is not homogeneous; hence, transformations 10, 13-18 were not considered. The Otsu method was applied with the Matlab function- Gray Thresh. This function returns the threshold value and the effectiveness of this threshold. Univariate analysis of variance was tested on sixty three images with the effectiveness of the threshold tested on the eighteen different color masks. The results (Appendix E. color masks effectiveness statistic results) show that the difference in the threshold effectiveness between the color mask is significant. According to The LSD post hoc analysis (Appendix E. color masks effectiveness statistic results) the selected mask will be transformation 19 (C1) which is significantly different from the rest of the masks and has the highest mean effectiveness in the specific barn.

4.1.3 Segmentation procedure

The segmentation procedure involves the background image and the cow image. Each image is transformed to the R-G space and then transformed to gray level (values between zero and one) by the `mat2gray` function (Matlab) and followed by increase of the image contrast (`Imadjust`, Matlab). From these images the threshold is computed using Matlab's Gray thresh function. Figure 15 shows the original background image (upper left) and its gray level distribution (upper right). The pixel distribution is obviously not bimodal. On the other hand, it is possible to see that for the transformed background image (R-G transform, middle left). The pixel values distribution is bimodal (middle right). The high values around 70 are the values of the pixels representing the red floor. On the bottom left the values of the transformed pixels are presented in gray level and in the bottom right the pixel values are presented after increasing the contrast in the image. In this stage the threshold is computed. The Otsu threshold for the specific image was computed as 0.4. The result of the threshold operation is a binary background image. Figure 16 illustrates the segmentation process which involves the subtraction of the two binary images (cow and background images). Figure 18 demonstrates an example of the segmentation procedure. The outcome of this procedure is a binary image containing two objects: the cow object and noise. Following segmentation, the image was reconstructed using morphological operations.

Table 9- The color space transformation

Space Num	Name	Transformation
	RGB	RGB(1,2,3)
1	R	RGB(:, :, 1)
2	G	RGB(:, :, 2)
3	B	RGB(:, :, 3)
4	R	$R/(R+G+B)$
5	G	$G/(R+G+B)$
6	B	$B/(R+G+B)$
7	deltaR	$(R-G)+(R-B)$
8	deltaG	$(G-R)+(G-B)$
9	deltaB	$(B-G)+(B-R)$
10	H	hsv(:, :, 1)
11	S	hsv(:, :, 2)
12	V	hsv(:, :, 3)
13	H	$H/(H+S+V)$
14	S	$S/(H+S+V)$
15	V	$V/(H+S+V)$
16	deltaH	$(H-S)+(S-V)$
17	deltaS	$(S-H)+(S-V)$
18	deltaV	$(V-S)+(V-H)$
19	C1	R-G
20	C2	R-B
21	C3	G-B
22	C4	2G-R-B
23	NDI1	$(R-G)/(R+G)$
24	NDI2	$(G-R)/(R+B)$
25	NDI3	$(R-B)/(R+B)$

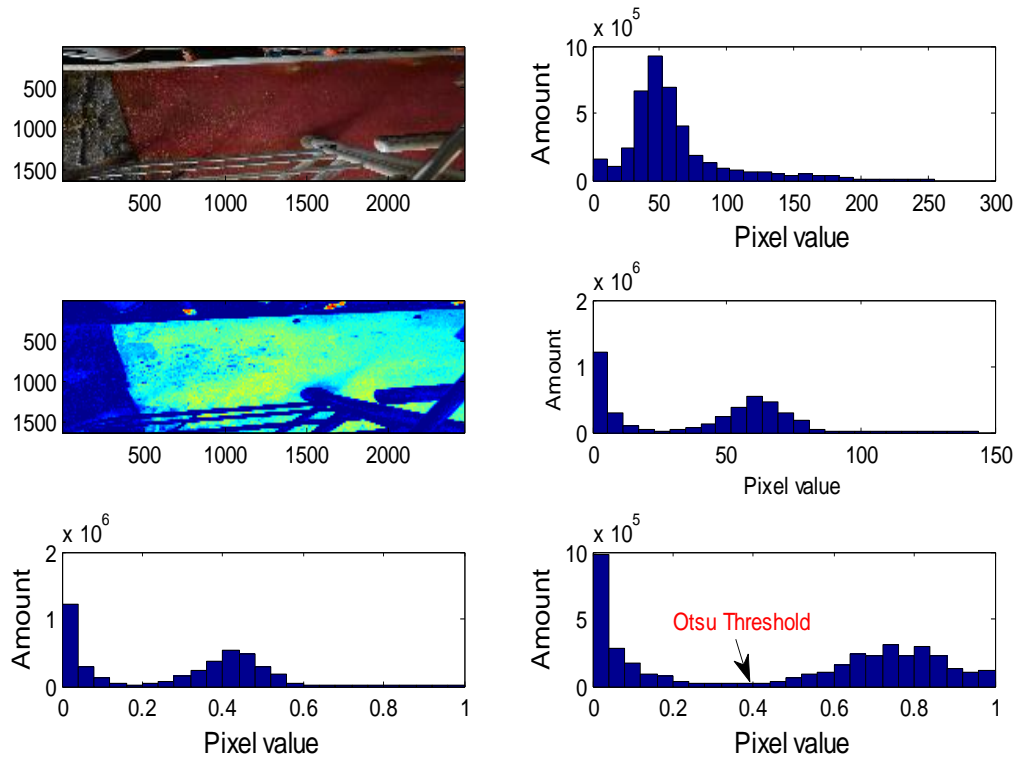


Figure 15- Background image in RGB space (upper left) and its gray level pixel distribution (upper right). Background image of R-G transform (middle left), R-G pixel values distribution (middle right), pixel value distribution in gray level (bottom left), pixel values distribution after increasing of contrast and threshold computation (bottom right).

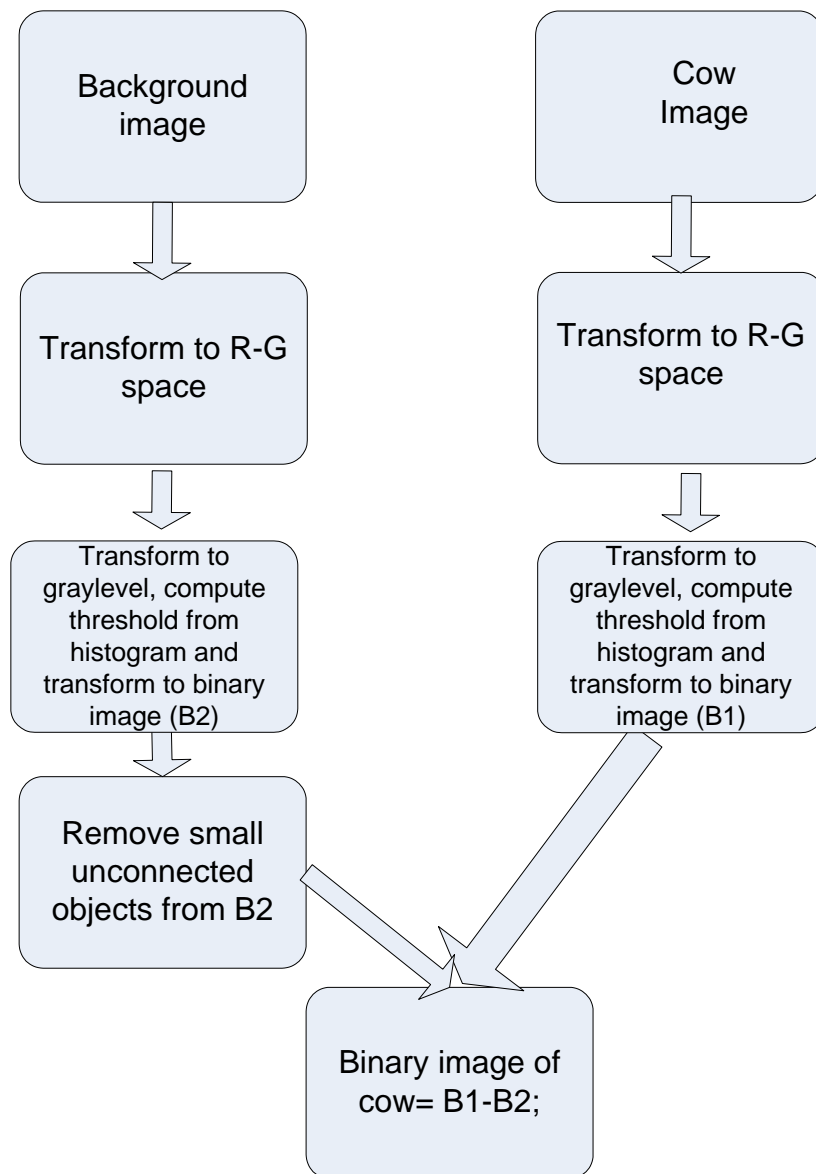


Figure 16- The segmentation procedure

4.1.4 Reconstruction and Morphological operations

After obtaining the cow's binary image the next step was to derive the body contour defined as the region of interest in the cow. In order to reach the body contour a blob analysis was conducted by using Matlab's BW matrix and the following features were extracted (Table 10). The procedure pseudo code is provided in Figure 17 and is conducted by three stages. First, noise was removed by selecting the biggest object in the image and then erosion and dilation were applied to reach a smooth binary cow (Figure 17 rows 1-7). In this stage, noise can appear due to many reasons such as secondary objects in the image caused by parts of another cow entered the frame, by another object in the background or on the cow's body

such as mud “connected” to the cow object. The aim of the second stage (Figure 17 rows 8-15) is to provide an image containing only the region of interest of the cow object and to eliminate orientation influence. Therefore, the object was rotated to 90 degrees (rows 8, 9,15) and only the upper third part of the object was saved (rows 10-14) in order to eliminate artificial cuts created in the segmentation by the background objects. The last stage (rows 16-19) involved removal of small objects and “holes” elimination (by labeling them by bwboundaries function row 18) in the cow’s body that may resulted from the segmentation procedure and previous operations. Figure 19 demonstrates the reconstruction and morphological process. The noises in the cow object (holes and connected objects) are marked by yellow circles. The result of this process is the tail head area of the binary cow.

A comparison between the automatic segmentation and manual segmentation was applied with Matlab’s function impoly. Figure 20 illustrates an example of the manual labeling (upper left) and its result (upper right). Visual analysis of the automated segmentation (Figure 20, bottom) indicated that it provides a smoother and more natural contour than the manual segmentation.

Table 10- Feature extraction by BW-Matrix

Feature	Description
Area	Number of relevant pixels
Orientation	The angle between the x-axis and the major axis of the ellipse that has the same second-moments as the Object
Pixel list	The coordinates of the pixels in the object
Bounding Box	The smallest rectangle containing the region. The bounding Box contains the length and width of the rectangle.
X min	Represent the coordinate of the edge of the tail head. Minimum point of x-axis pixel list

Reconstruction and morphological operations procedure:

```

1. Create b2 an image of Labels of all objects in binary image b1; % Bwlabel function (MATLAB)
   % cleaning other objects by the area criterion
2. Assign L1 as the label of the object with the largest area in b2; % finding all objects areas with regionprops (MATLAB)
3. Extract pixel coordinates of L1; % regionprops (MATLAB)
4. Create new image, b3 in the size of b1 ;
5. Assign 1 in all pixels coordinates of L1 in b3; %b3 contain only binary cow
6. Create disk1 size of 10, create disk2 size of 7; % the erosion and dilation operators
7. Perform erosion on b3 with disk1; Perform dilation on b3 with disk; Perform erosion on b3 with disk2; % perform opening and closing of object
8. Compute orientation of b3; % regionprops (MATLAB)
9. Rotate b3 by (-orientation); % rotate by the opposite angle to bring object to be horizontal
10. Extract pixel coordinates list for y and x, and BoundingBox of b3 ;% regionprops (MATLAB)
11. Compute Xmin= the minimum coordinate in x from pixel list;
12. Create new image, b4 of zeros in the size of b3;
13. Compute Xrange=the range from Xmin to (length of BoundingBox)/3;
14. Assign 1 in b4 in all coordinates that are in Xrange and in y list;
15. Rotate b4 by (-90) degrees;
16. Label b4; % Bwlabel function (MATLAB)
17. If find b4>1 % if new objects were created in the previous morphological operations
    Run again cleaning of objects by the area criterion
    End
18. Label all holes in b4 % bwboundaries (MATLAB)

19. If find b4>1
    Assign all labels in b4 to 1 % eliminate all holes in the cow object
    End

End % end procedure

```

Figure 17-Reconstrucion and morphological procedure

4.1.5 Demonstration of image processing procedures

Segmentation

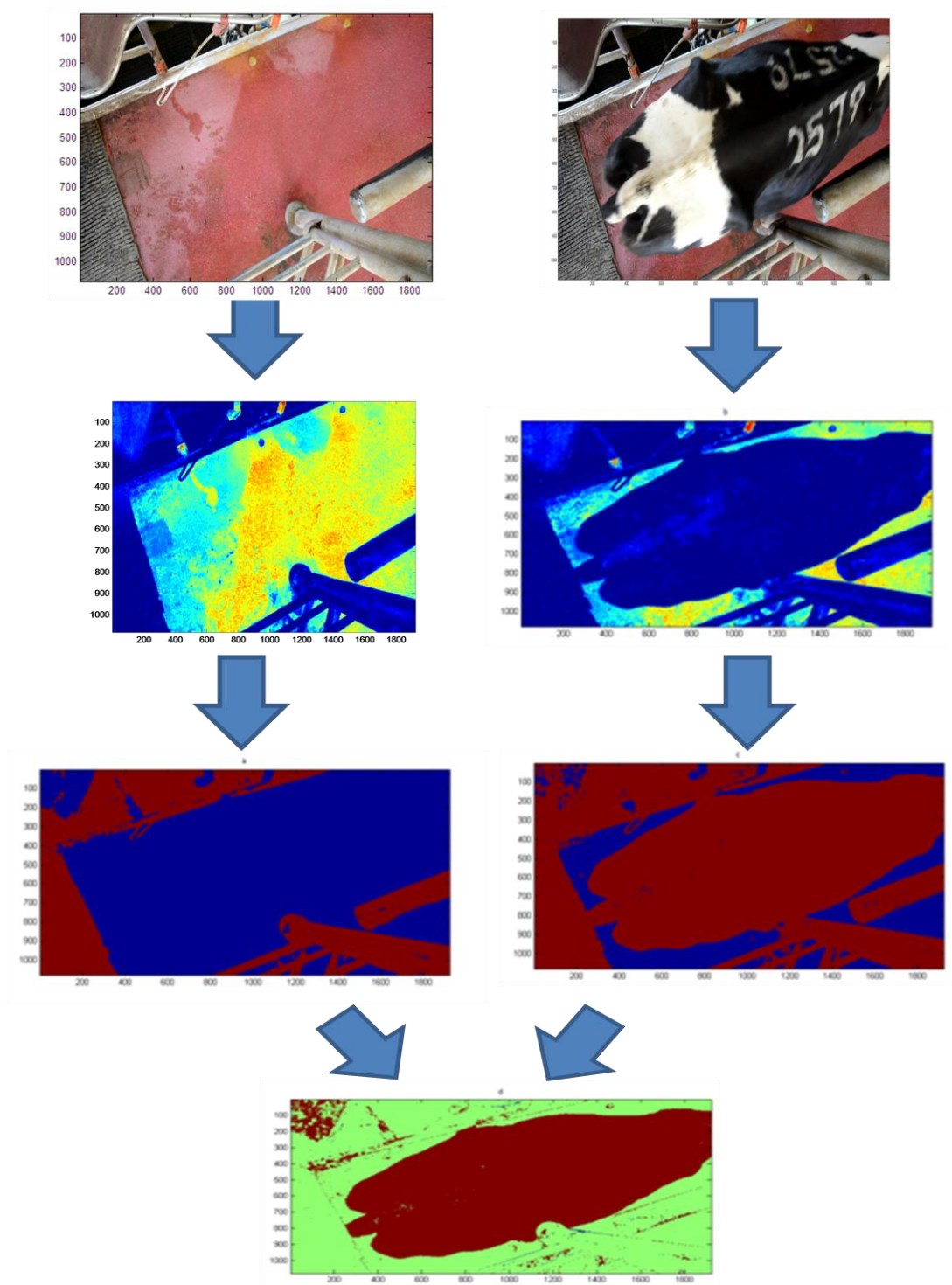


Figure 18- Example of the segmentation procedure

Reconstruction and Morphological process

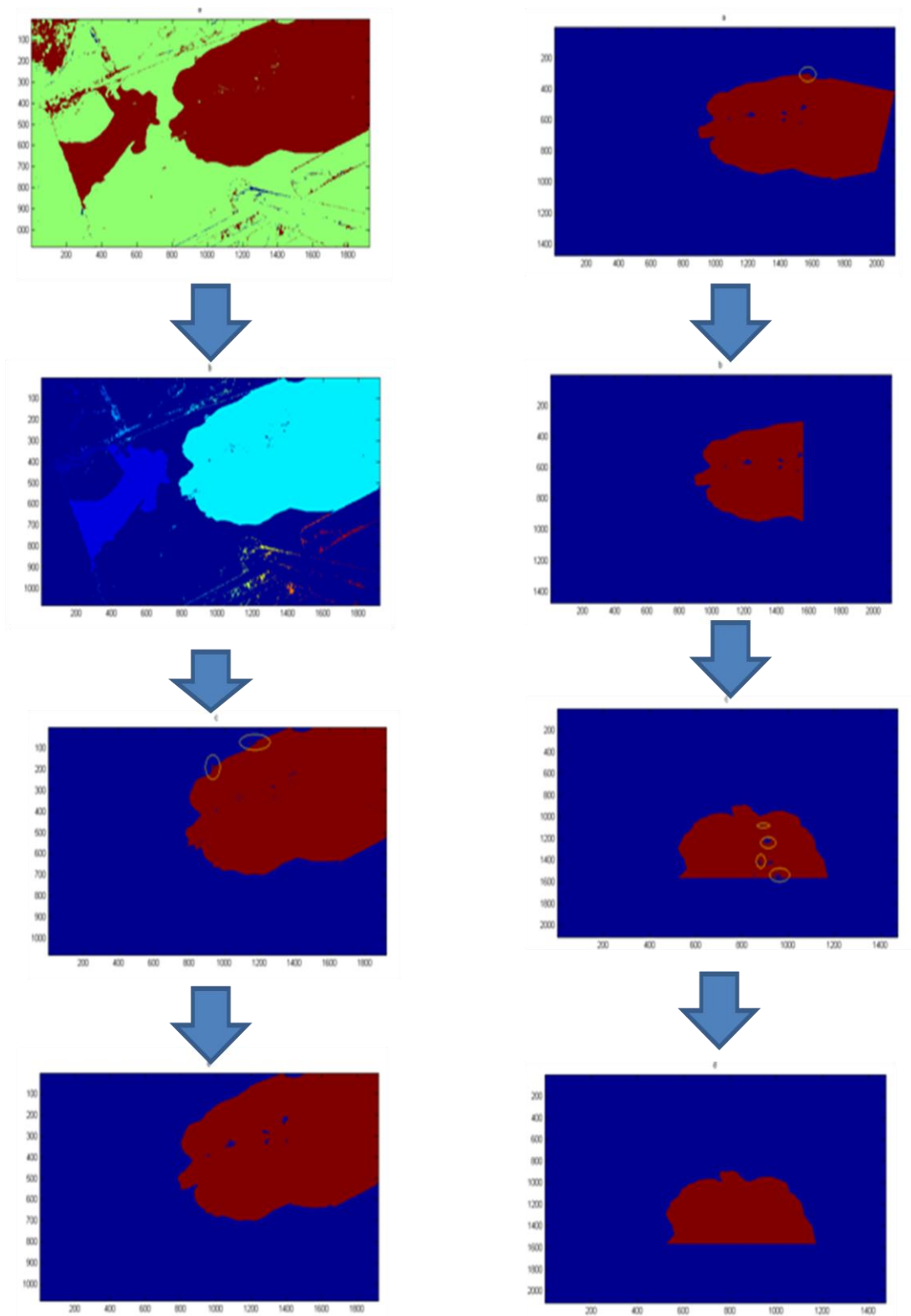


Figure 19- Example of the reconstruction and morphological process

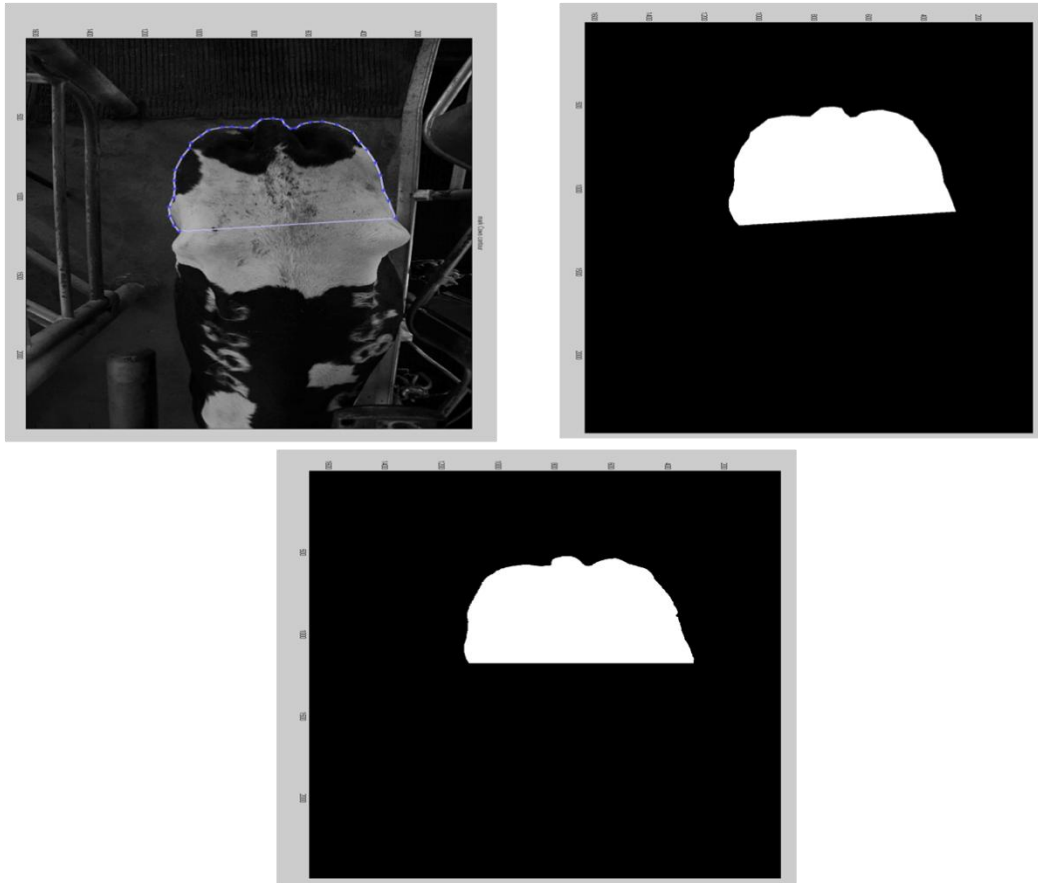


Figure 20- Example of manual segmentation (impoly function) and the automate result. Upper left- the manual labeling, upper right- manual segmentation result, bottom- the automate process result.

Feature extraction

4.1.6 Extracting the contour of the tail head area of the cow:

In order to eliminate the influence of size on image features, the contour was normalized to a given number of points by sorting the y coordinates and selecting the highest 1500 points, followed by interpolation to 1000 points and scaling them to a 0-1 range that will represent the new cow curve. The procedure is given in Figure 21 starting from the extraction of the curve coordinates. The outcome of this procedure is the cow tail head area curve (Figure 21 row 11). Another feature extracted is a one dimensional vector representing the tail head area contour. This vector is extracted by assigning the center point as (0.5,0.5) and all distances on the normalized contour line are presented by the radial distance from the center.

Curve extracting procedure

```
1. Extract contour coordinates Xj, Yj % imcontour (MATLAB)
2. maxY=max(Yj);
3. Yj =maxY- Yj; % rotate the axis so the highest point in the image will have the
   highest coordinate
4. NumberOfpoints=1500;
5. If length(Yj)<numOfpoints
       numOfpoints=length(Yj);
   end
6. Sort Yj by descending order;
7. Assign Yj and Xj with the highest numOfpoints;
8. Interpolate Yj and Xj to 1000 points; % interp (MATLAB)
9. Calculate max and min of Yj and Xj;
   %Scale Xj and Yj to 0...1 range:
10. for i=1:length(Xj)
       xj(i)=((xj(i)-xMin)/(xMax-xMin));
       yj(i)=((yj(i)-yMin)/(yMax-yMin));
   End
11. Provide tail bone area curve (xj,yj);
End % end of procedure
```

Figure 21-Contour extraction and normalization procedure

4.1.7 Distances and angles of the tail head anatomical points:

For each contour, the extreme points are computed by the following algorithm (Figure 22) first by smoothing the curve using the Savitsky-Golay algorithm (PLS toolbox, Eigenvectors Inc.) This algorithm receives the size of the window (in this case defined as 25 points) and the degree of the fitted polynomial (in this case 1). The smoothing allows easy selection of peaks and valleys. Due to noise that still may appear in the signal, the extreme points are selected in the surroundings of 100 points. When more than 5 points were found, the algorithm uses the information on the order of points: Max point, Min Point, Max point, Min Point, Max point. For this, the algorithm sorts the peaks and valleys by their X coordinate and removes minimum points from the edges, if still there are more than two minimum points and three maximum points the algorithm seeks consecutive points of the same type and selects the maximum or minimum point correspondingly. The vertical and horizontal distances between those points are computed. In order to compute the five angles

representing the tail head area two more points are added by constructing a horizontal line from the valleys points to the contour line. If the algorithm cannot reduce the amount of points to 5 or finds less than 5 points, then the features are not extracted. Figure 22 shows an example of the sequence filtering. It is possible to see that from the three consecutive minimum points in the middle (marked in green, Figure 22 a) the selected point is the minimum point (Figure 22 b). Figure 22 c holds an example of a situation where five points cannot be extracted due to the tail orientation and therefore this image is not suitable for BCS extraction with this method.

Figure 24 shows the outcome of applying the three procedures on the original cow image (Figure 24 a). Figure 24 (b) illustrate the outcome of the segmentation and morphological procedures. The peaks and valleys are marked in Figure 24 (c) in red and green respectively, and the points marked in pink are the points added for computing the angles. The distances and angles are shown in Figure 24 (e and f) and the 1D vector is shown in Figure 24 d.

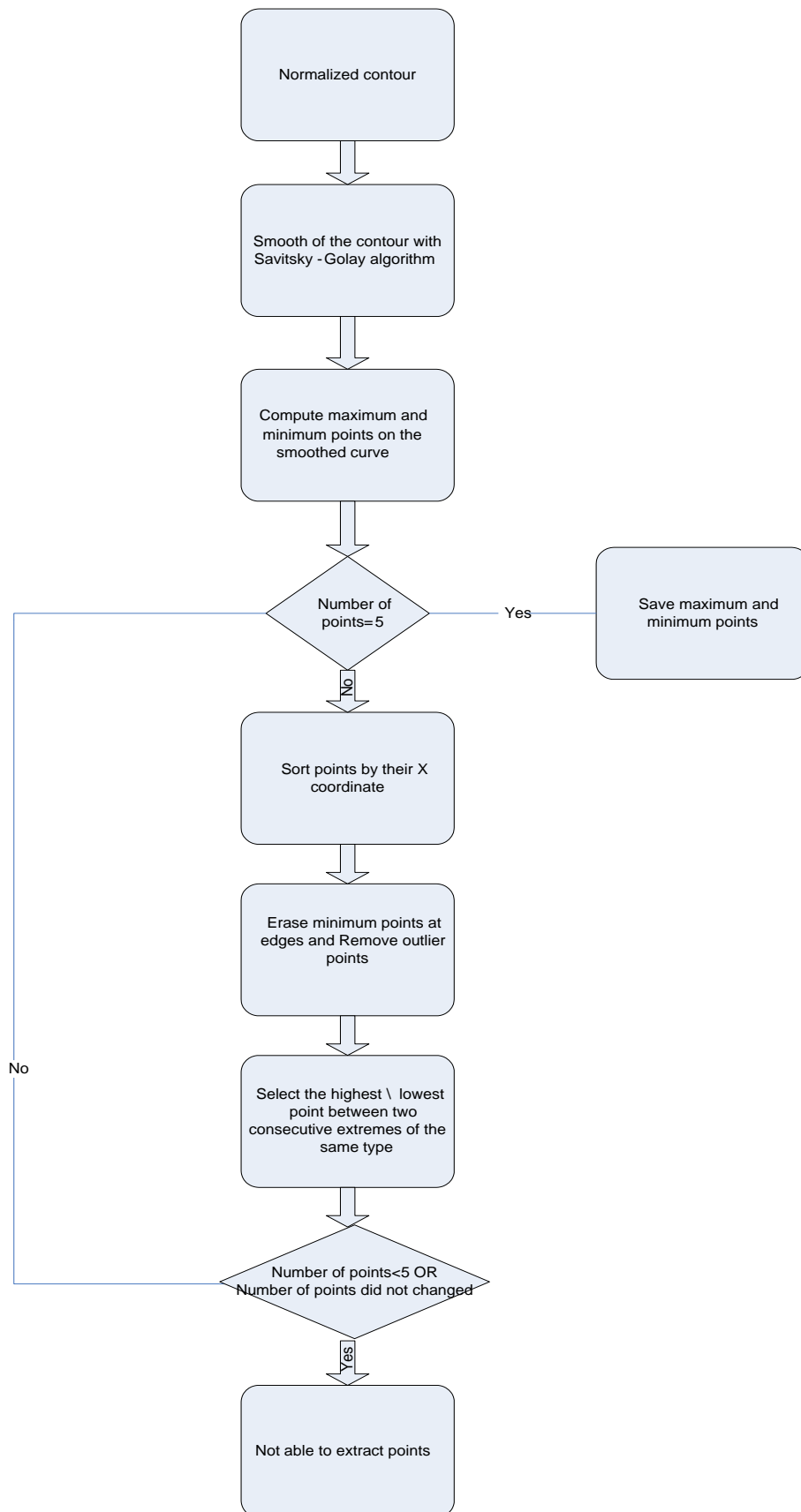


Figure 22- Automatic extraction of tail head peaks and valleys

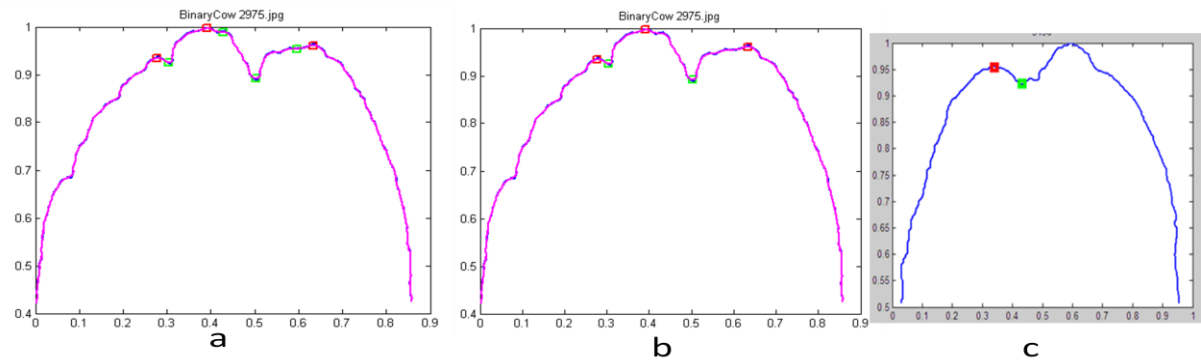


Figure 23- Example of extraction of the peaks and valleys. 7 points automatically extracted (a), 5 remaining points after the sequence filtering (b), example of contour that points cannot be extracted due to bad tail orientation (c)

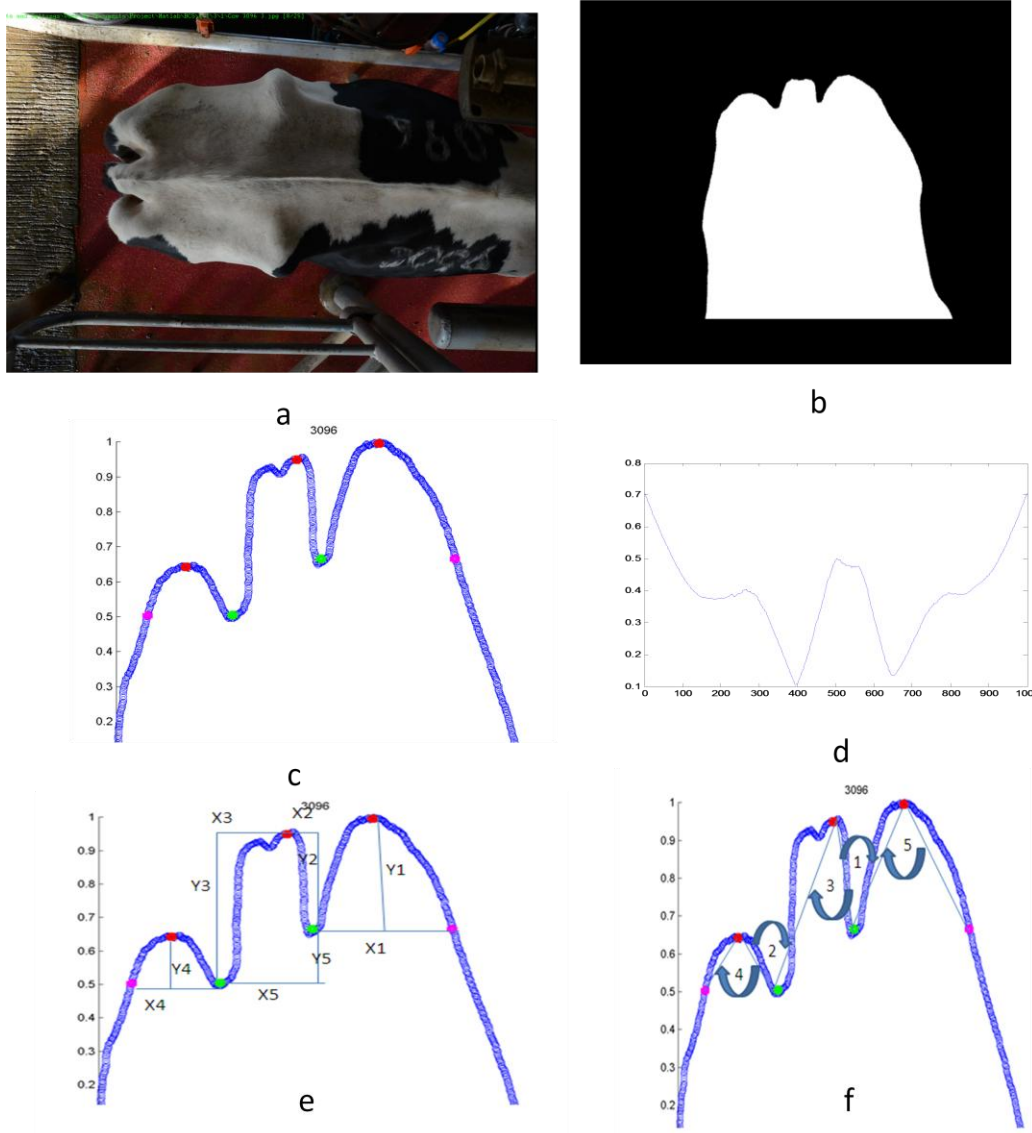


Figure 24-Original image (a) the segmentation outcome (b) the cows normalized curve (c) 1 dimension cows curve signature (d) vertical and horizontal distances (e) angles (f) between peaks and valleys.

4.1.1 Describing the distance vector by latent variables:

The contour vector size is 1X1000 for each cow. Partial Least Square Regression (PLS toolbox, Eigenvectors Inc.) was applied to reduce the problem dimensions. The latent variables were selected using the “Leave-One-Out” method (Stone, 1974) in order to avoid over fitting of the variables selected to the data. The number of latent variables was selected by the number that brings the root MSE of the validation (“Leave-One-Out”) to minimum.

4.1.2 Describing the distance vector Fourier transform:

Figure 25 shows the one dimension contour vector of three thin (blue) and three fat (red) cows. It is possible to distinguish the low valleys of the blue curves, but it is also possible to distinguish the variance in their location, causing difficulty for identification. To overcome this problem we propose to use the Fourier descriptors of each curve. The Fourier transform was applied by using Matlab’s Fast Fourier Transform command. The Fourier transform allows to reduce the dimension of the problem by examining the descriptors that can reconstruct the cow contour.

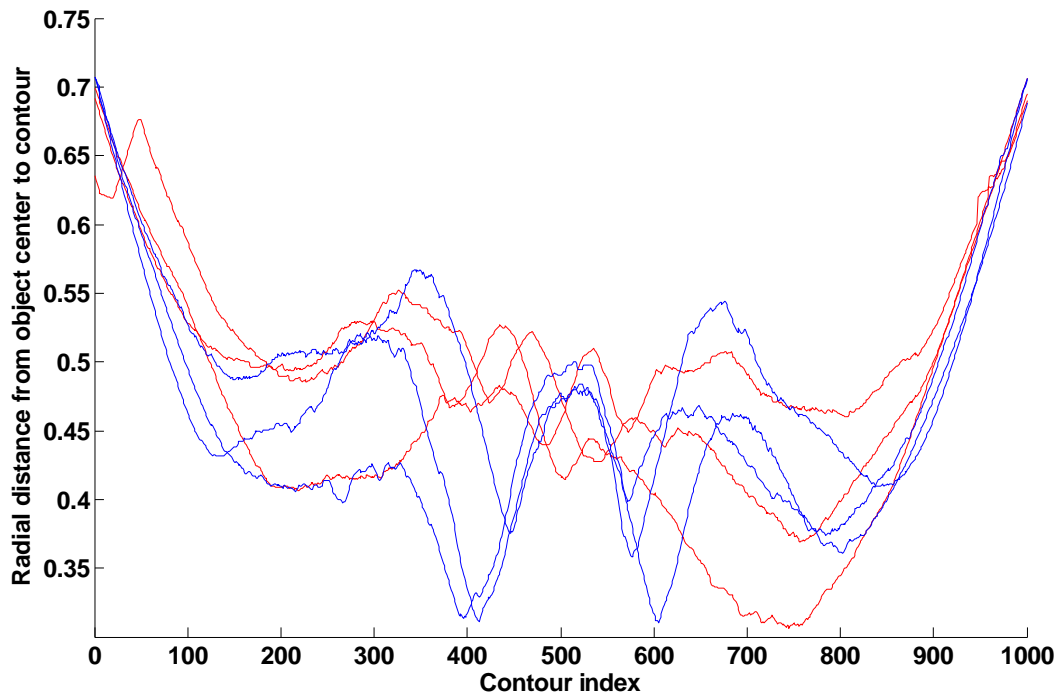


Figure 25- 3 thin cows (blue) and 3 fat cows (red) signature curve

Figure 26 suggests that by using only fifty Fourier descriptors it could be enough to reconstruct the cows curve. Ten descriptors are also sufficient to show the trend and

the curve is much smoother. The reconstruction was applied by the inverse fast Fourier transform. Before applying the transform a Low-Pass filter of moving average with a window of size of five was used in order to reduce noise in the data. Figure 27 holds an example of the absolute values of the Fourier descriptors derived from a cows curve. On the left side all 1000 descriptors are shown and for the majority of descriptors the value is around zero, except for the descriptors in the edges (the values in the edges are similar due to the symmetric of the Fourier transform) which are marked in red circle. The right side of Figure 27 shows, by zooming on the first 50 descriptors, that from the 10th descriptor the values drop almost to zero. This indicates that probably the first ten descriptors hold the majority of variance between fat and thin cows and therefore they will be taken in to consideration. Figure 28 shows the advantage in using the Fourier transform, by looking at the second to the tenth Fourier descriptors of four thin cows (BCS lower than 2.5, marked in blue dots) and four fat cows (BCS above 4, marked in red dots) the variance within the red group and the blue group and the variance between the group is much more obvious.

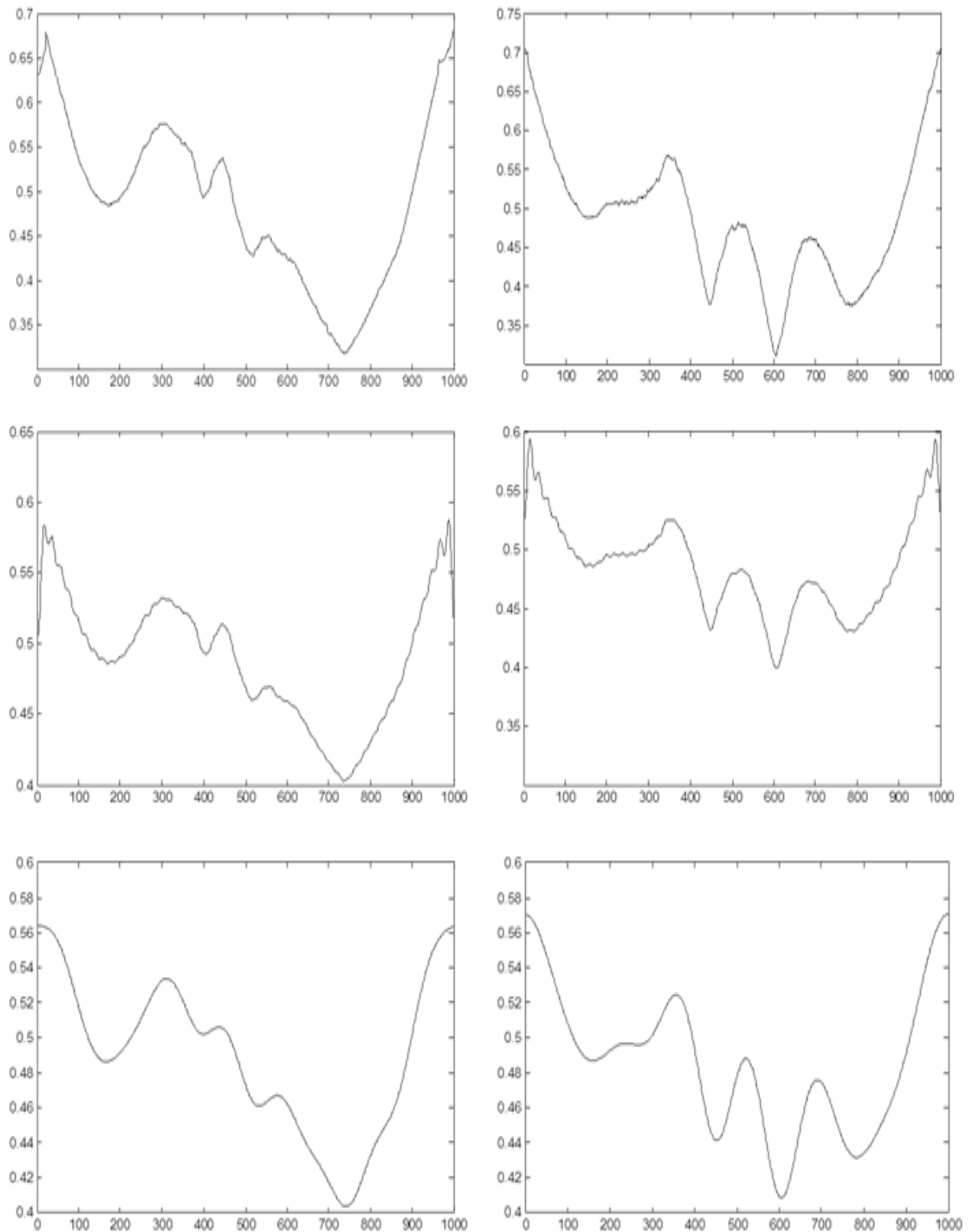


Figure 26- On the left side: a fat cow original 1D vector of distances from center (upper image) , and its reconstruction by 50 descriptors (in the middle) and 10 descriptors (bottom), in the right side: the same example for a thin cow. In all plots the X axis represents the index of the point in the contour. The Y axis represents the distance of that point .

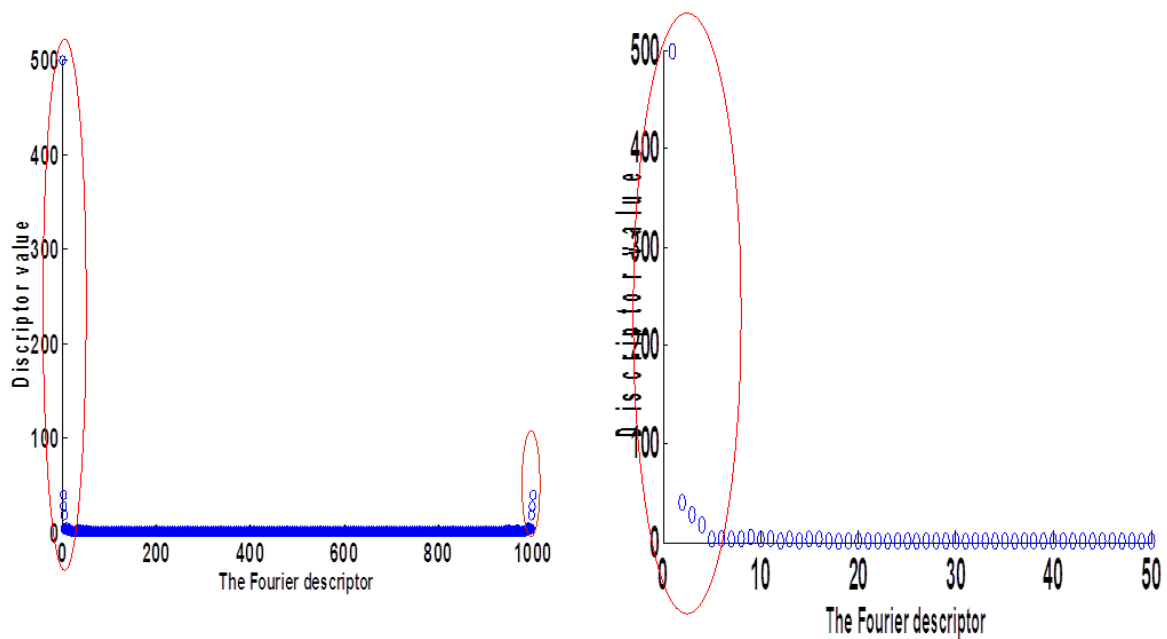


Figure 27- Left side: All 1000 Fourier descriptors (X axis) and it absolute value (Y axis). Right side: Zoom in on the first 50 descriptors and their value

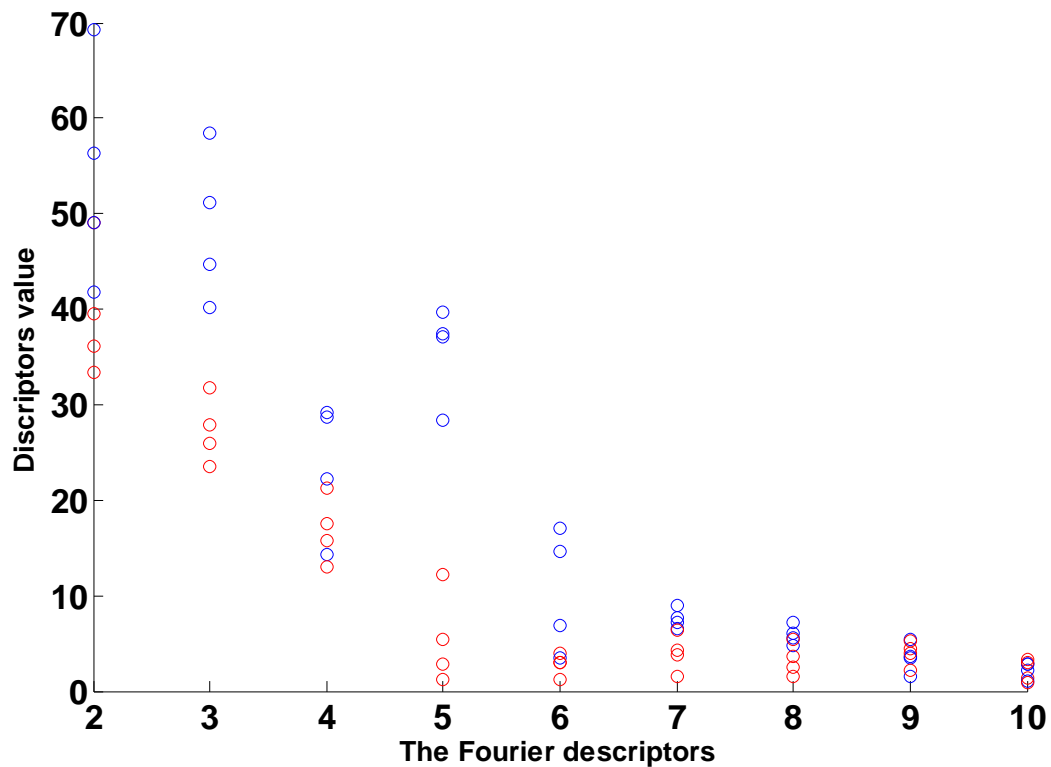


Figure 28- the 2-10 Fourier descriptors of 4 thin cows (blue) and 4 fat cows (red).

5 Results

BCS prediction using anatomical points features

Correlation analysis: The linear correlations between the anatomical point's features (ten distances and angles, Figure 24 e-f) and the BCS are shown in Table 11. The Y1, Y4, and Angle1-5 features were correlated with BCS (correlation higher than 0.5 are marked in red). The X1-X5, Y1-Y5, and Angle1-5 features were inter-correlated (high correlations are marked in red). This is due to the fact that the obtained angles are based on the distances between the peaks and valleys and vice versa.

Table 11- Multi correlation of anatomical points measurements

	X1	X2	X3	X4	X5	Y1	Y2	Y3	Y4	Y5	Angle1	Angle2	Angle3	Angle4	Angle5	BCS
X1	1	0.2	-0.09	0.38	0.07	0.82	0.58	0.55	0.48	0.07	-0.65	-0.58	-0.62	-0.56	-0.76	-0.42
X2		1	-0.34	0.11	0.48	0.28	0.41	0.32	0.1	0.12	-0.14	-0.2	-0.23	-0.11	-0.2	-0.2
X3			1	-0.07	0.67	-0.07	0.11	0.26	-0.06	0.22	-0.15	-0.17	0.01	0.01	0	0.01
X4				1	0.02	0.51	0.44	0.51	0.82	0.26	-0.54	-0.5	-0.65	-0.73	-0.52	-0.38
X5					1	0.15	0.43	0.5	0.03	0.3	-0.25	-0.32	-0.18	-0.08	-0.16	-0.15
Y1						1	0.73	0.73	0.65	0.28	-0.81	-0.69	-0.74	-0.71	-0.86	-0.52
Y2							1	0.91	0.51	0.21	-0.81	-0.88	-0.71	-0.54	-0.67	-0.49
Y3								1	0.54	0.45	-0.77	-0.86	-0.72	-0.57	-0.63	-0.44
Y4									1	0.22	-0.65	-0.56	-0.81	-0.89	-0.69	-0.53
Y5										1	-0.27	-0.26	-0.28	-0.27	-0.2	-0.19
Angle1											1	0.92	0.88	0.8	0.92	0.7
Angle2												1	0.86	0.68	0.74	0.63
Angle3													1	0.93	0.85	0.75
Angle4														1	0.83	0.72
Angle5															1	0.69

Modeling: The prediction model using linear regression (Table 12 and Appendix F. anatomical points results) suggests that: (a) The difference between model 2 ($R^2=0.56$, the outcome of the Forward or Stepwise methods) and model 1 ($R^2=0.65$ the Backward method) is minor (the R^2 adjusted and AIC are better in model 1 and BIC is better in model 2). In both cases the results are poor and can be explained by the strong correlation between the features. (b) The coefficients estimates (Appendix F. anatomical

points results) indicate that as the distance increases, the score decreases, and the angles have opposite influence on the scores. These results fit the research assumption. Model 3: Although the cow contour supposes to be symmetric the anatomical point's locations do not always indicate this. Therefore, another model that uses the average distance and angles from both sides of the tail head was tested. The results of this model do not show BCS prediction improvement. The AIC and BIC show improvement from model 2 (lower values) but, the R^2 adjusted is lower.

Table 12- Linear Regression for anatomical points features

Model no.	Features	Method	Variables in Model	R^2	R^2_{adj}	AIC ¹	BIC ²	P.Value
1	5 Angles and 10 distances	Backward	X2, Y3, Angle2, Angle4	0.65	0.62	104	118.3	<0.01
2	5 Angles and 10 distances	Forward\ Stepwise	Angle3	0.56	0.55	108	116	<0.01
3	Average Angles and distances	Forward\ Stepwise\ Backward	Average AngleIn (1,3), Average AngleOut (4,5) Average height(Y1,Y4)	0.61	0.6	101	113.5	<0.01

1 Akaike information criterion

2 Bayesian information criterion

BCS prediction using automatically extracted cow-contour

Figure 29 shows that when selecting more variables, the error on the calibration set (calculated by root MSE) reduces monotonically (green line), the error of the validation (the leave one-out method) reaches a minimum value (around 0.5) in three variables and then the error increases dramatically. Therefore, the number of variables selected for the model was three. The results of the Linear Regression of the three variables did not indicate improvement in predicting BCS. The R^2 on the calibration set was 0.6 and with “Leave-One-Out” method the R^2 value drops to 0.486 (Appendix G. PLS results). Pre-processing methods available by PLS toolbox such as smoothing, scaling and derivative of the contour did not improve the model results.

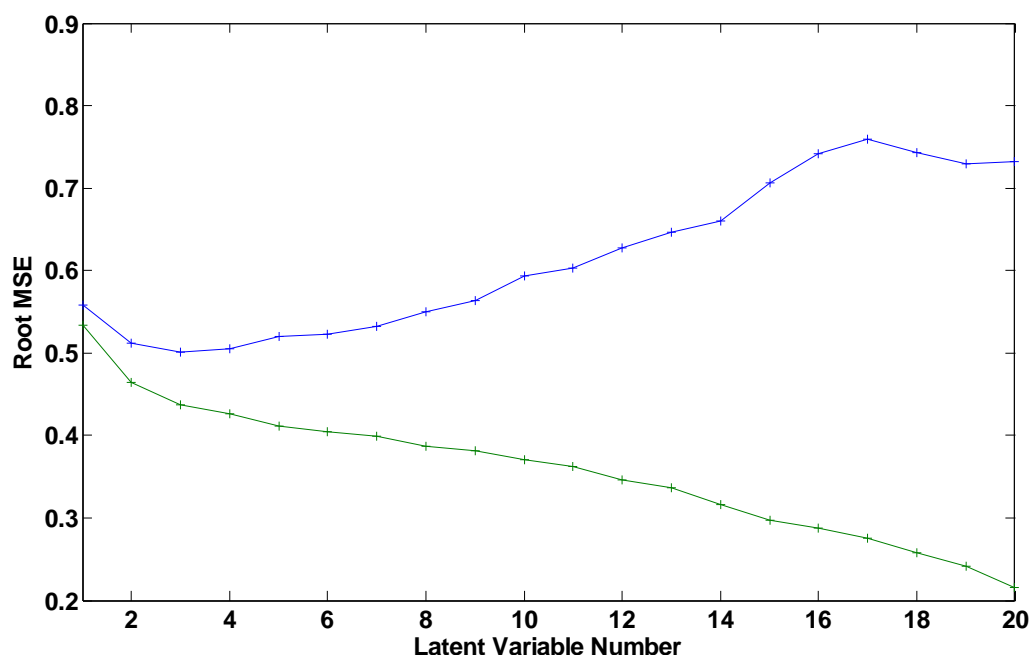


Figure 29-Latent Variable selection by Root MSE on calibration (green line) and Leave one out method (blue line)

BCS prediction using by Fourier Transform of the contour

Correlation analysis: A Pearson correlation matrix (Table 13) between BCS and the Fourier descriptors (F1...F10) indicates that nine descriptors (except F1) have negative connection with BCS. In general, there are no descriptors with high correlation (the highest correlation is achieved by the fifth and six descriptors) with BCS. On the other hand, there is no high cross correlation within the Fourier descriptors indicating that a linear combination between them can be useful.

Table 13- Cross correlation between BCS and the first ten Fourier descriptors

	BCS	F1	F2	F3	F4	F5	F6	F7	F8	F9	F10
BCS	1.00	0.47	-0.15	-0.09	-0.39	-0.52	-0.59	-0.35	-0.30	-0.11	-0.02
F1		1.00	-0.77	-0.79	-0.19	-0.81	-0.13	0.39	-0.06	-0.10	-0.10
F2			1.00	0.65	0.16	0.60	-0.01	-0.49	-0.08	0.05	0.07
F3				1.00	-0.03	0.36	-0.35	-0.59	0.08	0.05	0.01
F4					1.00	0.15	0.06	-0.01	0.39	0.05	-0.28
F5						1.00	0.47	-0.21	-0.03	0.12	0.26
F6							1.00	0.38	-0.15	0.09	0.21
F7								1.00	0.04	-0.27	-0.14
F8									1.00	0.24	-0.21
F9										1.00	0.25
F10											1.00

Modeling: A linear model of the absolute value of the first ten descriptors by using forward, backward and stepwise regression was performed in SPSS. Table 14 (and Appendix H. Fourier transform model results) suggests that the two models modified are similar with a very small advantage for model 1 (higher R^2 , and the lower AIC and BIC).

The backward model (Eq .1):

$$BCS = 6.405 - 0.027F3 - 0.024F4 - 0.011F5 - 0.081F6 - 0.087F7 - 0.072F8$$

The stepwise model (Eq .2):

$$BCS = 3.654 + 0.005F1 - 0.018F3 - 0.022F4 - 0.083F6 - 0.081F7 - 0.074F8$$

Table 14- Linear Regression for Fourier descriptors

Model	Method	Variables in Model	R^2	R^2_{adj}	R^2 (Leave-One-Out)	AIC ¹	BIC ²	P.Value
1	Backward Regression	F3-F8	0.77	0.75	0.732	79	98	<0.01
2	Stepwise \ Forward Regression	F1,F3,F4,F6, F7, F8	0.76	0.75	0.732	80	99	<0.01

1 Akaike information criterion

2 Bayesian information criterion

Figure 30 demonstrates the correlation between the BCS observed manually by the expert and the model output (Eq.1). The Pearson correlation is 0.77. 53% of scores were classified correctly within the range of 0.25, 82% were classified within the range of 0.5, 98% within the range of 0.75 and 100% were within the range of 1.

Model assumption: By examining the residuals distribution and the residuals scattering of model 1 (Appendix H) the model assumptions can be satisfied. The residuals do not show any trend and are normally distributed, indicating that a linear model is suitable for the problem.

Model meaning: It is possible to see in model 1 that for a cow with a straight line (zero frequency) the score will be 6.4. Although this score, and a constant curve are impossible, implying that any addition of curvature (frequency) to the cows contour will directly reduce BCS. These results confirm the research assumption. In model 2

the constant is lower (3.6) due to the fact that the only variable with positive connection to BCS (F1, Table 13) has entered the model.

Feature selection: The best feature for BCS prediction seems to be the cow's tail head area contour presented as the radial distances from its center. The best form to describe the vector is by Fourier descriptors which are uninfluenced by the peaks and valleys locations. Finally, it seems that the first ten descriptors hold the majority of information in the curve, meaning that they are the most important features for BCS prediction. Combining the anatomical points features together with the Fourier descriptors into one model did not change the results since the anatomical points features (in backwards, stepwise or forward methods) always excluded out of the model (Appendix I. combined Fourier descriptors and anatomical points model results).

Both models were evaluated on the testing set. The performance analysis was conducted on model 1- The model that achieved higher scores on the testing set (chapter 4.5). The PLS method was also applied on the entire set of Fourier descriptors. The results (Appendix J. PLS of Fourier descriptors model results) were not different (R^2 : 0.77 and by R^2 of Leave-One-Out: 0.73 by using 5 Latent variables) suggesting that due to simplicity of the model the PLS method in addition to the Fourier descriptors is not necessary in this case.

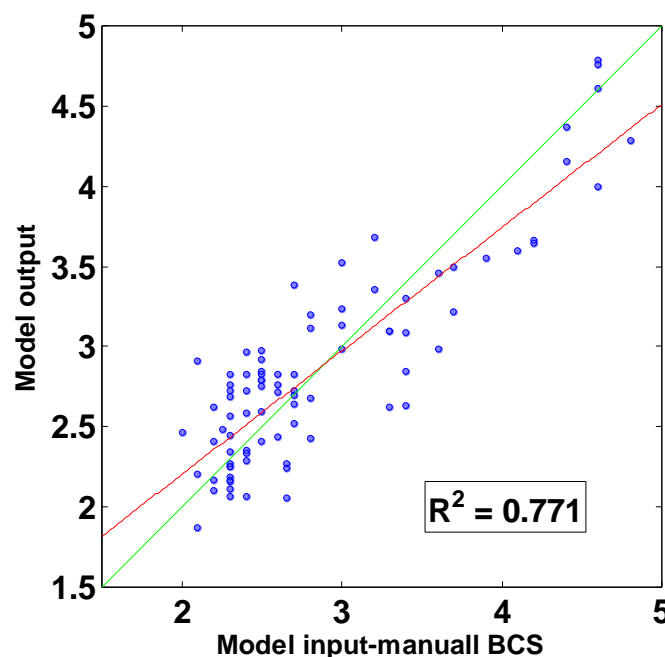


Figure 30- Correlation in training set between the model output (model 1, Y axis) and the manually BCS (X axis). The red line is the linear fit line and the green line is 1:1.

Validation

The R^2 between the expert results and BCS computed by model 1 is 0.643 and 0.6 for models 1 and 2 respectively (Figure 31, Appendix K. Testing results). The focus from now on will be on model 1 only, since it yields higher performance for both sets. The correlation is of course lower than in the training data set (calibration), but the difference is not large (0.643 vs. 0.77). Table 15 shows evaluation of the model errors: in more than half of the observations the error rate is bigger than 0.25, which represents one digression in Ferguson scale. For two and three digressions (0.5 and 0.75) the classification percentage climbs to 72% and 94% respectively. None of the cows were scored with an error rate bigger than 1.

Table 15- Evaluation of error rate on testing set

Error range	0-0.25	0-0.5	0-0.75	0-1
Amount	37	18	4	0
Classified percentage	43%	72 %	94%	100%

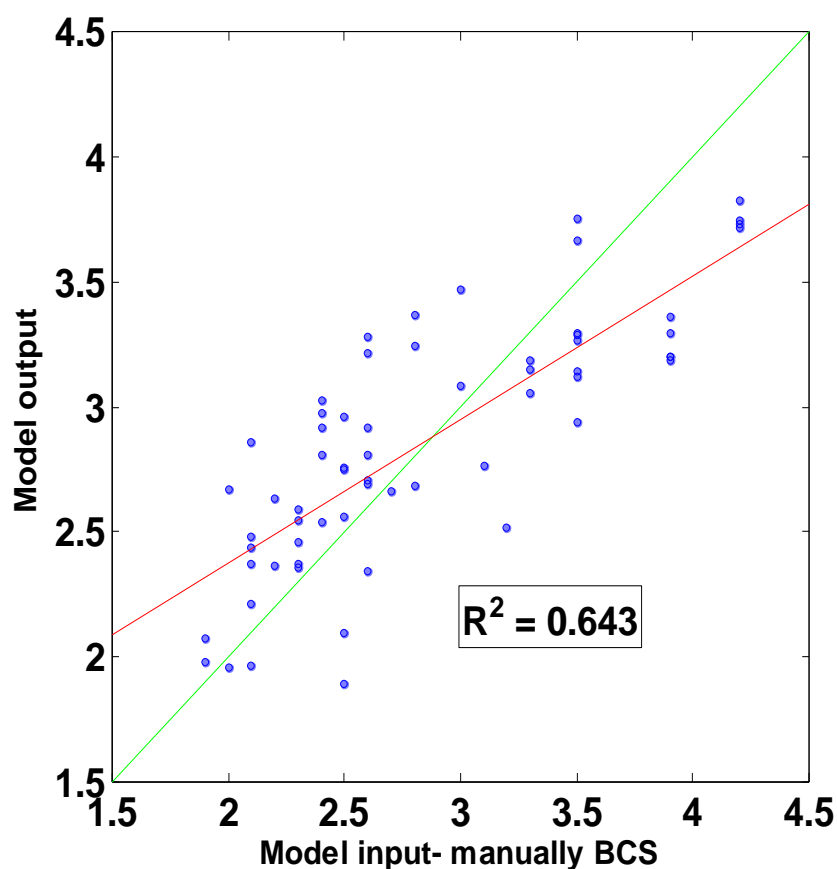


Figure 31- Correlation in testing set between the model output (model 1, Y axis) and the manually BCS (X axis). The red line is the linear fit line and the green line is 1:1.

Model performance

The results of the different borders are shown in Tables 16-21 and Appendix L (classification tables). From Table 16 and 17 we can derive that the model has high ability to distinguish between cows with BCS higher than 3 and lower than 3. This ability stays similar for both the training and testing sets. The model classified correctly almost 95% of cows below the score of 3 and 83% of cows that were above the score 3 for the training set and respectively 90% and 84% for the test set.

In Tables 18 and 19 the borders were constructed for gaps of one (1-2,2-3,3-4,4-5). Table 18 shows that in the training set, the majority of cows were classified correctly and that the distances of errors were not more than one category (none of the cows in category 4-5 were classified as 2-3 and vice versa). Table 19 indicates similar performances on the testing set: the majority of cows were classified correctly and that the distance of errors were not more than one category (for example, none of the cows in category 3-4 were classified as 1-2 and vice versa) but, all of the cows between 4-5 were classified as 3-4.

In Tables 20 and 21 four classes are presented: thin cows (below 2.5) medium-thin (2.5-3) medium-fat (3-3.5) and fat (above 3.5). In the training set (Table 20) one cow was miss-classified by more than one category (classified as 2.5-3 instead of 3.5-5) and in the testing set (Table 21) two cows were misclassified by more than one class (classified as 1-2.5 instead of 3-3.5 and classified as 2.5-3 instead of 3.5-5). However, the weakness of the model performance can be noticed in the model's output of class 2.5-3, where the cow's actual class according to manual classification comes from all four classes (48% and 52% of cows who were classified as 2.5-3 in the training and testing respectively, were actually miss-classified. see column 2 in Tables 20-21). In addition, in the testing set (Table 21) the problem of classifying fat cows is more obvious, where the majority of fat cows (above 3.5) were classified as 3-3.5. If we take, for instance, the eleven cows that were miss-classified as 2.5-3 (instead of 2-2.5 in the training set, Table 20) six of them were actually very close to their real class (less than 0.25 from the class border) with three out of six with a distance of approximately 0.1 from their real class. This implies that prediction ability is high despite the errors in exact class assignment which is problematic as discussed before since the borders between classes are not really well defined and the manual classification is also limited by its natural errors.

In Appendix L (classification tables) we present a classification table with a gap of 0.5 and 0.25 between classes. On the 0.5 gap, it is possible to notice that in both the training and testing sets only two cows were miss-classified with a distance of two classes; on the other hand, in the testing set, cows that were classified as 2.5-3 were originally from scores between 2- 4, and the majority of cows that were classified as 3-3.5 were actually manually scored as 3.5-5. When classes are set with very fine resolution (0.25, Appendix L), the classification rate drops (the majority of predictions are not in the diagonal of the table), especially in the high scores where the variance of errors is bigger. Misclassification by more than one class (which implies a prediction error of 0.50) is 25% and 45% in training and testing set respectively implying that larger data set is needed for improvement in the accuracy of predicting small resolution BSC.

Table 16- Training set classification results of cows above and below 3

Manual BCS category observed by expert	Model output category		Total
	1-3	3-5	
1-3 Count	55	3	58
% within BCS category	94.8%	5.2%	100.0%
% within Model output category	91.7%	11.1%	66.7%
3-5 Count	5	24	29
% within BCS category	17.2%	82.8%	100.0%
% within Model output category	8.3%	88.9%	33.3%

Table 17- Testing set classification results of cows above and below 3

Manual BCS category observed by expert	Model output category		Total
	1-3	3-5	
1-3 Count	35	4	39
% within BCS category	89.7%	10.3%	100%
% within Model output category	89.7%	16.0%	60.9%
3-5 Count	4	21	25
% within BCS category	16.0%	84%	100%
% within Model output category	10.3%	84%	39.1%

Table 18- Testing set classification results of cows between groups (2-3,3-4,4-5)

Manual BCS category observed by expert		Model output category			Total
		2-3	3-4	4-5	
2-3	Count	55	3	0	58
	% within BCS category	94.8%	5.2%	0.0%	100.0%
	% within Model output category	91.7%	14.3%	0.0%	66.7%
3-4	Count	5	13	0	18
	% within BCS category	27.8%	72.2%	0.0%	100.0%
	% within Model output category	8.3%	61.9%	0.0%	20.7%
4-5	Count	0	5	6	11
	% within BCS category	0.0%	45.5%	54.5%	100.0%
	% within Model output category	0.0%	23.8%	100.0%	12.6%

Table 19- Testing set classification results of cows between groups (1-2,2-3,3-4,4-5)

Manual BCS category observed by expert		Model output category				Total
		1-2	2-3	3-4	4-5	
1-2	Count	1	1	0	0	2
	% within BCS category	50.0%	50.0%	0%	0%	100.0%
	% within Model output category	25.0%	2.9%	0%	0%	3.1%
2-3	Count	3	30	4	0	37
	% within BCS category	8.1%	81.1%	10.8%	0%	100.0%
	% within Model output category	75.0%	85.7%	16.0%	0%	57.8%
3-4	Count	0	4	17	0	21
	% within BCS category	0%	19.0%	81.0%	0%	100.0%
	% within Model output category	0%	11.4%	68.0%	0%	32.8%
4-5	Count	0	0	4	0	4
	% within BCS category	0%	0%	100.0%	0%	100.0%
	% within Model output category	0%	0%	16.0%	0%	6.3%

Table 20- Training set classification results of thin-medium and fat cows

Manual BCS category observed by expert		Model output category				Total
		2-2.5	2.5-3	3-3.5	3.5-5	
2-2.5	Count	21	11	0	0	32
	% within BCS category	65.6%	34.4%	0.0%	0.0%	100.0%
	% within Model output category	77.8%	33.3%	0.0%	0.0%	36.8%
2.5-3	Count	6	17	3	0	26
	% within BCS category	23.1%	65.4%	11.5%	0.0%	100.0%
	% within Model output category	22.2%	51.5%	23.1%	0.0%	29.9%
3-3.5	Count	0	4	7	2	13
	% within BCS category	0.0%	30.8%	53.8%	15.4%	100.0%
	% within Model output category	0.0%	12.1%	53.8%	14.3%	14.9%
3.5-5	Count	0	1	3	12	16
	% within BCS category	0.0%	6.3%	18.8%	75.0%	0.0%
	% within Model output category	0.0%	3.0%	23.1%	85.7%	0.0%

Table 21- Testing set classification results of thin-medium and fat cows

Manual BCS category observed by expert		Model output category				Total
		1-2.5	2.5-3	3-3.5	3.5-5	
1-2.5	Count	14	8	0	0	22
	% within BCS category	63.6%	36.4%	0%	0%	100.0%
	% within Model output category	77.8%	38.1%	0%	0%	34.4%
2.5-3	Count	3	10	4	0	17
	% within BCS category	17.6%	58.8%	23.5%	0%	100.0%
	% within Model output category	16.7%	47.6%	21.1%	0%	26.6%
3-3.5	Count	1	2	4	0	7
	% within BCS category	14.3%	28.6%	57.1%	0%	100.0%
	% within Model output category	5.6%	9.5%	21.1%	0%	10.9%
3.5-5	Count	0	1	11	6	18
	% within BCS category	0%	5.6%	61.1%	33.3%	100.0%
	% within Model output category	0%	4.8%	57.9%	100%	28.1%

BCS error (Azzaro et al., 2011): The average of the absolute error between the model output and the manual BCS in the training and testing sets were 0.285 and 0.34 respectively with a combined average error of 0.31.

Classification model

The BCS classes were: thin cows (below 2.5, labeled as 1); medium-thin (2.5-3, labeled as 2); medium-fat (3-3.5, labeled as 3) and fat (above 3.5, labeled as 4).

The model was modified by backward regression in SPSS software by using the training set and was validated by the testing set. From the parameter estimation table (Table 22) it is possible to see that the variables entered to the model are F3, F4, F6, and F7 the three equations can be presented as:

$$Prob(Group_1) = \frac{1}{1+e^{-(-20.866-(-0.188F3-0.184F4-0.494F6-0.526F7))}}$$

$$Prob(Group_2 \text{ OR } Group_1) = \frac{1}{1+e^{-(-18.229-(-0.188F3-0.184F4-0.494F6-0.526F7))}}$$

$$Prob(Group_2 \text{ OR } Group_1 \text{ OR } Group_3) = \frac{1}{1+e^{-(-16.049-(-0.188F3-0.184F4-0.494F6-0.526F7))}}$$

$$Prob(Group_4 \text{ OR } Group_3 \text{ OR } Group_2 \text{ OR } Group_1) = 1$$

The probability for each group can be computed by:

$$Prob(Group_2) = Prob(Group_2 \text{ OR } Group_1) - Prob(Group_1)$$

$$Prob(Group_3) = Prob(Group_2 \text{ OR } Group_1 \text{ OR } Group_3) - Prob(Group_2 \text{ OR } Group_1)$$

$$Prob(Group_4) = 1 - Prob(Group_2 \text{ OR } Group_1 \text{ OR } Group_3)$$

Table 22- Parameter estimation of ordinal regression

Parameter	B	Std. Error	95% Wald Confidence Interval		Hypothesis Test		
			Lower	Upper	Wald Chi-Square	df	Sig.
Threshold [BCS_ordinal=1.00]	-20.866	3.2423	-27.221	-14.511	41.416	1	.000
[BCS_ordinal=2.00]	-18.229	3.0233	-24.155	-12.304	36.356	1	.000
[BCS_ordinal=3.00]	-16.049	2.7949	-21.527	-10.571	32.971	1	.000
F3	-.188	.0364	-.260	-.117	26.845	1	.000
F4	-.184	.0358	-.254	-.113	26.249	1	.000
F6	-.494	.0858	-.663	-.326	33.188	1	.000
F7	-.526	.1097	-.741	-.311	22.995	1	.000
(Scale)	1 ^a						

The classification results of the Ordinal regression for the training set and testing set are presented in Tables 23 and 24 respectively.

Table 23- Training set classification results by Ordinal regression of thin-medium and fat cows

Manual BCS category observed by expert	Model output category				Total
	1-2.5	2.5-3	3-3.5	3.5-5	
1-2.5	20	12	0	0	32
2.5-3	8	16	2	0	26
3-3.5	1	7	2	3	13
3.5-5	0	0	3	13	16
Total	29	35	7	16	87

Table 24- Testing set classification results by Ordinal regression of thin-medium and fat cows

Manual BCS category observed by expert	Model output category				Total
	1-2.5	2.5-3	3-3.5	3.5-5	
1-2.5	14	7	1	0	22
2.5-3	6	7	3	1	17
3-3.5	1	2	3	1	7
3.5-5	1	4	8	5	18
Total	22	20	15	7	64

The results of the linear regression model are better than the results achieved by the classification model for both the training and testing sets (in Table 20: 57 BCS were classified correctly while in Table 23 only 51 cows were classified correctly; Table 21: 34 BCS were classified correctly while in Table 24 only 29 cows were classified correctly). Moreover, it seems that there are more miss-classifications with distances of two classes: in Table 21 there are no fat cows (3.5-5) that are classified as thin (1-2.5) and only one fat cow is classified as 2.5-3 while in Table 24 one fat cow is classified as 1-2.5 and four fat cows were classified as 2.5-3.

Model repeatability

Table 25 shows the BCS and its standard deviation given by the model for five different images of each cow. It is possible to notice that the biggest deviation is 0.21- smaller than one digression in Ferguson scale (0.25). In Figure 32 Each cow represented in a different color. The estimates of covariance parameters were generated from a linear-mixed-model (Table 26) showing that the variance between cows (0.201) is more than 12 times bigger than the variance within cows (0.016). It is important to clarify that the repeatability of the process highly depends on correct selection of the images.

Table 25- BCS repeatability for each cow and its standard deviation

num	2984	3186	3071	2579	3117
1	2.29	3.22	3.65	2.67	2.57
2	2.63	3.12	3.66	2.46	2.54
3	2.85	3.11	3.66	2.67	2.85
4	2.74	3.11	3.66	2.77	2.62
5	2.64	3.12	3.65	2.8	2.54
Std	0.21	0.05	0.01	0.13	0.13

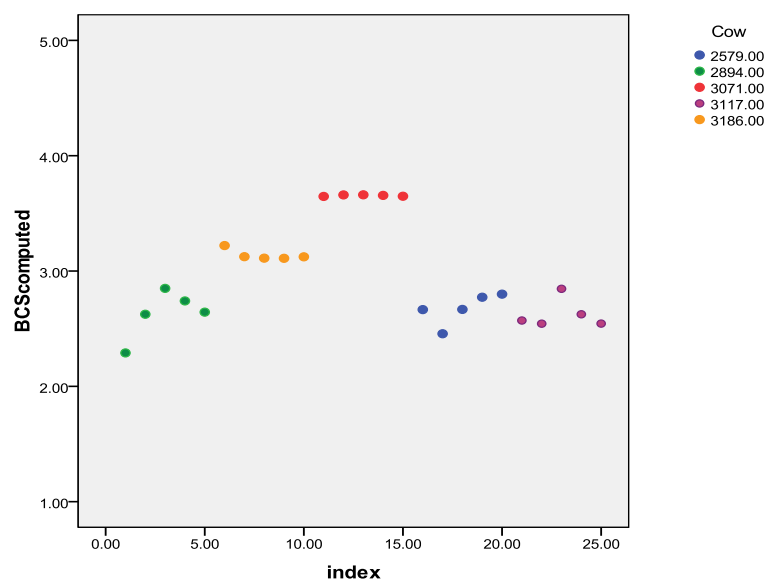


Figure 32- The BCS computed for 5 different images of 5 cows taken in the same day

Table 26- Variance within cows and between cows

Estimates of Covariance Parameters^a

Parameter	Estimate	Std. Error
Residual	.016214	.005127
Cow Variance	.201183	.144555

a. Dependent Variable: BCS.

Sensitivity analyses

5.1.1 Influence of the training data set size:

Table 27 shows the Pearson correlation of the calibration and validation results with the BCS taken manually, and the variables combining the model. All models, as the original model (1) were modified by backward elimination. In general, all models results with minor changes in the model performance and variables combining the model (Table 27) implying that the original model is reliable. Results indicate that the usage of the first, the ninth and the tenth Fourier descriptors may cause over-fitting of the model, due to a major drawback of the validation results (models 2-4, 5, 7). The results especially indicate that the second descriptor, that was not included in model 1, may contribute to the model performance (model 6,9-11), implying that further collection of data and modifying a model from more observation may improve the model results. It is interesting to mention that unlike the rest of the coefficients of the Fourier descriptors, the coefficient of the second descriptor is positive, indicating that combining it to the model may improve the model performance on fat cows.

Table 27- Estimation of influence of training data size on the model modified

Num	Training size	Actual size	R^2 calibration	R^2 Validation	Variables in the model
1- Original data	57.6%	87	0.77	0.64	F3...F8
2	15%	27	0.81	0.43	F1,F2,F8,F7
3	15%	21	0.77	0.25	F1,F2,F6,F10
4	15%	21	0.85	0.49	F1,F7,F8,F9
5	50%	77	0.80	0.63	F2...F9
6	50%	69	0.75	0.73	F2...F7
7	50%	74	0.77	0.59	F2...F7,F9
8	80%	123	0.73	0.86	F2...F8
9	80%	126	0.75	0.74	F2...F8
10	80%	126	0.76	0.67	F2...F8
11	100%	151	0.75	-	F2...F8

5.1.2 Influence of the distribution of the training and testing sets

The training set and validation set were not identically distributed (Table 7); for instance, in the training set there are no cows below 2 (the testing set has two cows with values below 2) and on the other hand, there are five cows above 4.5 in the training set and none in the testing set. If identically distributed sets could have being monitored, perhaps a different model would have been derived. The random creation of identical distributed sets was applied three times- each time a new training and testing set were created.

Figure 33 shows an example of the new separation between the training set (on the left side) and the testing set (right side). Table 27 shows the results of the models derived by the three different datasets.

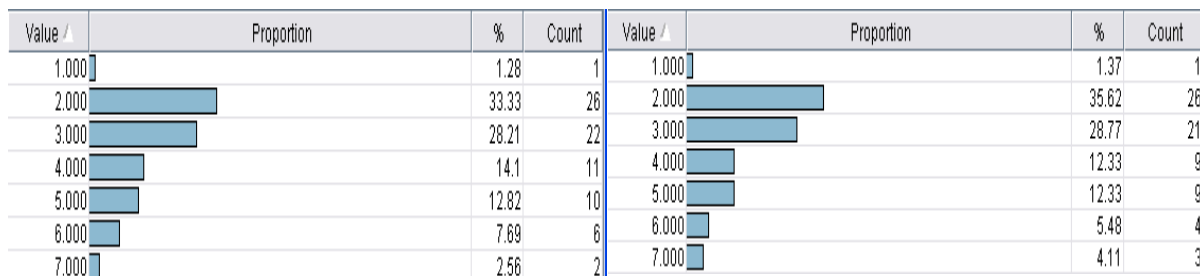


Figure 33- Randomly separation of equal distributed training (left side) and testing (right) sets

Table 27- Estimation of influence of training data size on the model modified.

Num	R ² calibration	R ² Validation	Variables in the model
1- Original data	0.77	0.64	F3...F8
2	0.78	0.68	F2..F8,F10
3	0.68	0.76	F1,F2,F4,F6,F7,F8
4	0.73	0.75	F2...F8

The different training sets did not produced models that are different in their essence. All variables coefficients are negative except F1 and F2. Similar to the conclusions related to the influence of size evaluation it is possible to see that F10 and F9 do not contribute to the model performance; on the other hand, again, it seems that F2 (which has positive coefficient) contributes to the model stability and performance (model 4 which show high results on both training and testing sets).

5.1.3 Influence of different resolutions and blurred images

Table 28 shows that the model is very sensitive to changes in the image resolutions. All Parried t-tests in Table 28 show significant difference from the original output. On the other hand, for resolutions that did not cause damage to the image (by changing dramatically the proportion of the image, set 2, 4, 5, 6) the Pearson correlation shows that a new calibration may be needed in order to obtain similar results as in the original images. Table 29 indicates that the model is not sensitive to blurring. Only for very intensive blur (set 4) the Parried t-test shows difference (Sig. 0.08) in the model outputs. Figure 34 shows an example of the blurring created by the “motion” filter; it is possible to see in the bottom right that for a very big filter (set 4) the image is damaged and the correlation with the original output drops to 0.39.

Table 28- Influence of different resolutions on model output

Set	Resolution	Resolution ratio	Parried t-test Sig.	Pearson Correlation
Original image	1632X2464	0.66		
1	1400X1800	0.77	0.00	0.67
2	1400X2100	0.66	0.00	0.78
3	1500X1000	1.5	0.00	0.26
4	1500X2000	0.75	0.00	0.84
5	1600X2200	0.72	0.00	0.94
6	1600X2000	0.8	0.00	0.87

Table 29- Influence of blurring on model output

Set	Filter size	Parried t-test Sig.	Pearson Correlation
1	1X20	.430	.980
2	1X40	.440	.970
3	1X80	.440	.870
4	1X160	.080	.390

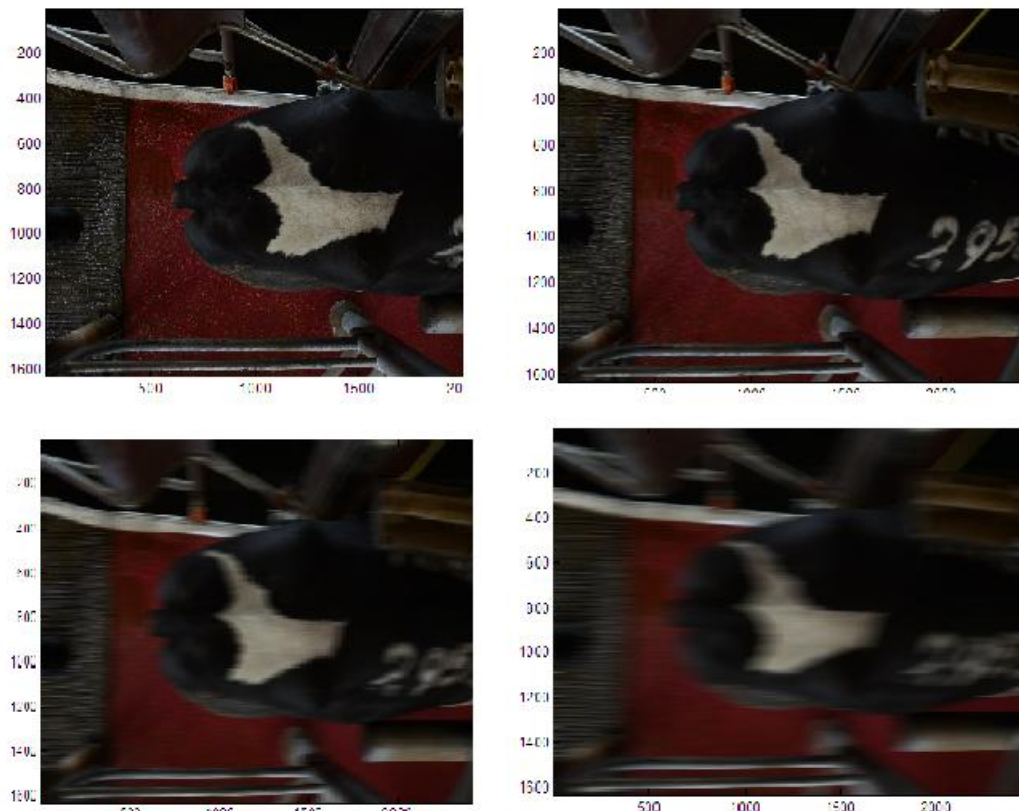


Figure 34- Blurring example with different filter sizes: on upper left- original image, upper right- 1X20, bottom left- 1X80, bottom right- 1X160.

6 Discussion, conclusions and future research

Three different models (based on anatomical points, PLS and FFT) were evaluated for automatic evaluation of the dairy cow's BCS using automatic segmentation and feature extraction computer vision methods. **The best model for describing BCS was based on Fourier descriptors of the one dimensional curve of the cow's contour.** The linear prediction model resulted in R^2 of 0.77 and 0.65 respectively for the training and testing databases. For both training and testing sets approximately 95% of the cows were classified correctly within a range of 0.75 and none of the cows were scored with an error rate bigger than 1. In addition, the model showed high ability to distinguish between thin, medium and fat cows. These results indicate the feasibility of using the model as a management tool for monitoring the status of a group of cows by emphasizing trends and changes in their body condition. For example, by applying the model to a herd, if 30% of the cows have moved between classes during a certain period this can indicate a health problem, influence of dietary change, etc.

Comparing results with state-of-the-art models: Prediction results are presented in the literature using different performance measures (average error rate (Azzaro et al., 2011), R^2 (Halacmi et al., 2008), classification (Bewley et al., 2008). There is no common method to evaluate performance.

The **average error rate** tested by Azzaro et al., (2011) for the state-of-the-art BCS prediction models obtained 0.98 average error for the parabolic model designed by Halachmi et al., 2008, 0.32 average error for the angles computed from 23 anatomical points model designed by Bewley et al., 2008 and 0.31 for the PCA model (of 23 anatomical points, suggested by Azzaro et al., 2011). The model developed in this thesis which is based on the FFT transform obtained an average error rate of 0.34 on the testing set implying that the proposed model is as good as state-of-the-art models. However, it is advent since it does not require manual labeling of points in the cow image. It is important to clarify that the average error rates stated in the different studies were tested on different data sets which may limit the comparison results.

Halachmi et al., 2009 measured the parabolic model performance by R^2 . The model developed in this thesis showed weaker results under this measure (0.77 vs. 0.89).

However, the parabolic model (Halachmi et al., 2009) was conducted with a thermal camera which allows better extraction of the entire body of the cow (including the hook area). However, it is a more expensive device.

Bewley et al., 2008 showed that the model based on the angles of 23 anatomical points classified correctly 100% of the scores within 0.5 range and 93% within range of 0.25. In the method presented in this thesis around half of the observations were miss-classified within the range of 0.25 (42% and 58 % in the training and testing set respectively) 82% were classified correctly within 0.5 (in testing set- 74%). Potential reasons for the weaker results are: (1) in addition to the tail head Bewley et al. (2008) used the hook area which was impossible to extract automatically under our research conditions. (2) Bewley et al. (2008) applied his methods manually which could improve the contour points as compared to our automatic procedures.

Image processing: The color of the background can change in different barns which may lead to a different color transformation, but the essence of the process will be the same. Hence, implementation of such a tool must include installing a best-fit background and its calibration, a common procedure in computer vision applications.

Contour extraction: The cow contour was extracted by selecting the highest 1500 points followed by interpolation to 1000 points (Chapter 4.2.1). Since the camera was not always located at the same position (distance and angle) 1500 points were selected as the number of points that are sufficient for describing the entire tail head area in any case. In order to eliminate the variance between images taken at different days the 1500 points were interpolated to 1000 points. It is important to clarify that the Fourier transform calculation is influenced by the size of the vector transformed. This implies that, selecting a different vector size will cause changes in the Fourier descriptors values. Hence, changes in vector size will require new model calibration.

Feature selection: The best feature proposed for BCS prediction was the vector of Fourier descriptors of the cow curve. The FFT is a well known method used in many image processing applications. The main advantage of FFT over the PLS method is that it is not influenced by the location of the peaks and valleys in the contour, it allows clear and easy reduction of the problem dimension by describing the data with only 1% of the descriptors. In addition, the FFT is less sensitive to noise -it allows smoothing of the curve by low pass filter and by placing the noise in the high frequencies.

Classification model: The classification tables in chapter 5.4 (performance analysis) show high ability of the model to distinguish between fat-medium and thin cows. The classification results of the ordinal regression which aims to predict the class of BCS and not its specific value showed weaker performance (Table 23-24). A potential reason may be the fact that for each class the model modifies a suitable equation. In our case, the eighty seven observations were probably not enough for avoiding over fitting of the model to the training set- causing the many errors in the testing set (Table 24). It is necessary to collect larger datasets in order to imply a reliable classification model.

Manual BCS: The manual BCS was provided by only one expert- its natural error and subjectivity may limit the model's statistical results. It is important to validate the model outputs with the manual score of a group of experts.

Future research: Further research is still necessary for fully automating the process. An automated decision system to determine the suitable color transform regarding the specific imaging conditions (e.g., natural color of background, lighting) must be developed. Furthermore, it is still required to automate the frame selection procedure: while capturing the image stream, the majority of the images are not suitable for processing due to many reasons such as cow out of frame or bad orientation of the tail. A classification model for classifying between suitable images and bad images should be developed using the features extracted out from the shape segmented. In robotic farms we expect that the percentage of images that are not suitable for processing will be reduced dramatically due to the fact that the images will be taken while the cow is standing instead of while it is walking. When implementing the system in the milking parlor and since the cow enters the parlor around three times a day, it is more than reasonable to assume that the system will be able to capture at least one suitable image a day, making this system practical for dairy farm usage.

It is important to **develop a standard procedure for evaluating performance** in order to compare different models with the same methods and performance measures.

Future work should also investigate the possibility of applying **fuzzy logic for the classification**. The definition of the border of a 'fat' cow is not clear cut: a cow of value 3.8 is very fat, but cows with values of 2.9 and 3.1 are both medium-fat cows, however, in the current method they will be assigned to different classes (fat and

medium) although they have close values. This is even more problematic due to the fact that the manual classification is also prone to errors and can cause misclassification. Fuzzy logic is well fit for problems in which borders between classes are artificially defined and vague and hence we expect that it can significantly improve performance.

7 References

1. Azzaro, G., Caccamo, M., Ferguson J.D, Battiato S., Farinella M., Guarnera C., Puglisi G., Petrigiliero R., Licitra G. (2011). Objective estimation of body condition score by modeling. *Journal of Dairy Science*, 94: 2126-2137.
2. Bar-Shalom, A. 2008. Method and system for monitoring physiological conditions of suitability of animal feed for ruminant animals. *United-States patent no:7,350,481, B2*.
3. Bewley, J.M., A.M. Peacock, O. Lewis, R.E. Boyce, D.J. Roberts, M.P. Coffey, S.J. Kenyon, and M.M. Schutz. (2008). Potential for estimation of body condition scores in dairy cattle from digital images. *Journal of Dairy Science* 91: 3439-3453.
4. Bin Shao, Hongwei Xin. 2008. A real-time computer vision assessment and control of thermal comfort for group-housed pigs. *Computers and Electronics in Agriculture* 6 : 15–21.
5. Boissarda, P., Martinb, V., Moisanb, S. 2008. A cognitive vision approach to early pest detection in greenhouse crops. *Computers and Electronics in Agriculture* 6 : 81–93
6. Blasco, J., Aleixosb, N. Cuberoa, S. Gomez-Sanchosa, J., Molto, E. 2009. Automatic sorting of satsuma (Citrus unshiu) segments using computer vision and morphological features. *Computers and Electronics in Agriculture* 6 : 1–8
7. Blasco J., Cubero S., Gmez-Sanches J., Mira P., Molto E. 2009. Development of a machine for the automatic sorting of pomegranate (Punica granatum) arils based on computer vision. *Journal of Food Engineering* 90: 27–34.
8. Canny, J., A computational approach to Edge detection. *IEEE Transactions on Pattern Analysis and Machine Intelligence*. 8 : 679-698
9. Catté, F., Lions, P., Morel, J., Coll, T. 1992. Image Selective Smoothing and Edge Detection by Nonlinear Diffusion. *Society for Industrial and Applied Mathematics* 29:182-183.
10. Chen Y. R., Chao K., Kim S. M. 2002. Machine vision technology for agricultural applications. *Computers and Electronics in Agriculture* 36: 173-191
11. Cherri, A.K., Karim, +M. A.,. 2006. Optical symbolic substitution: edge detection using Prewitt, Sobel, and Roberts operators. *Applied optics ISSN* 28:4444:4648.

12. Coffey, M. P., T. B. Motram, and N. McFarlane. 2003. A feasibility study on the automatic recording of condition score in dairy cows. *British Association Animal Science*: 131
13. Collins LM. Non-intrusive tracking of commercial broiler chickens in situ at different stocking densities. 2008. *Applied Animal Behavior Science* 112:94-105.
14. DeShazer, J.A., Moran, P., Onyango, C.M., Randall, J.M. and Schofield, C.P., 1990. Imaging systems to improve stockmanship in pig production. *Journal of Agricultural Engineering Research* 287: 296
15. Dawkins M.S, Lee H.J, Waitt C.D, Roberts S.J. 2009. Optical flow patterns in broiler chicken flocks as automated measures of behaviour and gait. *Applied Animal Behavior Science*; 119 (3-4):203-209.
16. Domecq, J.J., A.L. Skidmore, J.W. Lloyd, and J. B. Kaneene. 1997. Relationship between body condition scores and milk yield in a large dairy herd of high yielding Holstein cows. *Journal of Dairy Science*. 80: 101-112.
17. Earle, D. F. 1976. A guide to scoring dairy cow condition. *Journal of Agriculture (Victoria)* 74:228.
18. Ferguson, J. D., Galigan, D.T., Thomsen, N. 1994. Principal descriptors of body condition score in Holstein cows. *Journal of Dairy Science*. 77:2695 – 2703.
19. Ferguson, J. D., G. Azzaro, and G. Licitra. 2006. Body condition assessment using digital images. *Journal of Dairy Science*. 89:3833–3841
20. Flochini, A. J. (1980). Milk sensor for machine removal. Retrieved on October 12, 2009, from www.freepatentsonline.com.
21. Garnsworthy, P.C. 1988. The effect of energy reserves at calving on performance of dairy cows. In: Garnsworthy P.C., ed. *Nutrition and lactation in the dairy cow*: 157.
22. Gearhart, M.A., C.R. Curtis, H.N. Erb, R.D. Smith, C.J. Sniffen, L.E. Chase, and M.D. Copper. 1990. Relationship of changes in condition score to cow health in Holsteins. *Journal of Dairy Science*. 73:3132-3140.
23. Gillund, P., Reksen O., Grohn Y.T., Karlberg K. 2001. Body condition related to ketosis and reproductive performance in Norwegian dairy cows. *Journal of Dairy Science* 84:1390-1396.

24. Hady P,J , Domecq J. J., Kaneene J. B. 1994. Frequency and precision of body condition scoring in dairy cattle. *Journal of Dairy Science* 77: 6.
25. Halachmi I, Polak P., Roberts D., Klopčič M. 2008. Cow body shape and automation of scoring BCS. *Journal of Dairy Science* 91:4444–4451
26. Halachmi I, Polak P., Roberts D., Klopčič M., Bewley J.M. 2009. Thermally sensed, automatic, cow body condition scoring. *ECPLF 2009. The Netherlands. Paper number 2949: 193-201.*
27. Hogeveen, H., Ouweltjes, W., De Koning, C.J., Stelwagen, K. 2001 Milking interval, milk production and milk flow-rate in an automatic milking system. *Livestock Production Science* 72: 157–167.
28. Igathinathane, C., Pordesimo, L.O., Batchelor, W.D. 2009. Major orthogonal dimensions measurement of food grains by machine vision using ImageJ. *Food Research International* 42 :76–84
29. Wu J., Tillett R., McFarlane N, Xiangyang J.,J. Siebert P. Schofield P. 2004. Extracting the three-dimensional shape of live pigs using stereo photogrammetry. *Computers and Electronics in Agriculture* 44: 203–222.
30. Kawamura, S., Kawasaki, M., Nakatsuji, H., Natsuga, M. 2007. Near-infrared spectroscopic sensing system for online monitoring of milk quality during milking. *Sensing and Instrumentation for Food Quality and Safety* . 1:37–43
31. Keren, E. N., Olson B. E. 2007. Applying thermal imaging software to cattle grazing winter range. *Journal of Thermal Biology*. 32:204– 211.
32. Koenen, E.P.C., Veerkamp R. F. 1998. Genetic covariance functions for live weight, condition score, and dry-matter intake measured at different lactation stages of Holstein Friesian heifers. *Livestock Production Science*. 57:67-77.
33. Kunttu, I. Lepistö L. 2007. Shape-based retrieval of industrial surface defects using angular radius Fourier descriptor. *Images processing, IET* 1: 231–236.
34. Laykin S., Alchanatis V., Edan Y. 2002. Image processing algorithms for tomato classifications. *American society of agricultural and biological engineering* 45: 851–858.
35. Laykin S., Alchanatis V., Edan Y., Weisman Z. 2008. Image processing algorithms for table olives classification. *International Conference on Agricultural Engineering 2008: OP-2090*

36. Lee K., Choi W., Noh S., Kang S., Son J., Kim G. 2008. Nondestructive determination of soluble solid contents for watermelon using optical characters. *International Conference on Agricultural Engineering: OP-950*.
37. Lowman, B. G., N. A. Scott, and S. H. Somerville. 1976. Condition scoring of cattle. *Bull. No.6. East Scotland Coll. Agric., Anim. Prod., Advisory Dev. Dep.*
38. Maatje, K., Loeffler, S. H., & Engel, B. 1997. Predicting optimal time of insemination in cows that show visual signs of estrus by estimating onset of estrus with pedometer. *Journal of Dairy Science*. 80: 1098-1105.
39. Maltz, E. & Antler A. 2007. A practical way to detect approaching calving of the dairy cow by a behavior sensor. *International Conference in Precision Livestock Farming '07*, 141-146
40. Markusfeld, O., Nahari, N., Adler. H. 1988. Traits associates with the "fat cow syndrome" in dairy cattle. A combined clinical, epidemiological and biochemical study of a multifactorial disease syndrome. *Israel Journal of Veterinary Medicine* 44:111.
41. McFarlane N.J.B. Schofield C.P. 1995. Segmentation and tracking of piglets in images. *Machine Vision and Applications* 8:187-193
42. Mizrach A., Flitsanov U., Maltz E., Spahr S. L., Novakofski J. E., Murphy M. R.. 1999. Ultrasonic assessment of body condition changes of the dairy cow during lactation. *American society of agricultural and biological engineering* .42:805–812.
43. Morris S.T., Kenyon P.R., Burnham D.L. 2002. Body condition score and beef cow productivity. *Massey University Riverside Farm Open Day 16 July 2002*.
44. Nääs I.A, Carvalho V.C, Moura D.J, Mollo M.N. 2006. Animal behaviour analysis: signal and image processing approach. *Michigan: International Commission of Agricultural Engineering*; 313-325
45. Nielen M., Deluyker H., Schukken Y.H. Brand A. Electrical conductivity of milk: measurement, modifiers, and meta analysis of Mastitis detection performance. *Journal of Dairy Science* 75 : 606-614 .
46. Noordam J., van de Broek W., Buydens L., 2005. Detection and classification of latent defects and diseases on raw French fries with multispectral imaging. *Journal of the Science of Food and Agriculture* 85:2249-2259.
47. Otsu, N. 1979. A Threshold Selection Method from Gray-Level Histograms. *IEEE Transactions on Systems, Man, and Cybernetics*. 9: 62-66.

48. Ozkaya S., Bozkurt, Y. 2008. The relationship of parameters of body measures and body weight by using digital image analysis in pre-slaughter cattle. *Arch. Tierz., Dummerstorf* 51 :120-128.
49. Pastell M., Takko H., Gro H., Hautala M., Poikalainen V., Praks J., Veerma I., Kujala M., Ahokas J. 2005. Assessing cows welfare: weighing the cow in a milking robot . *Biosystems Engineering* 93: 81–87
50. Pedron O., Chell F., Senatore E., Baroi D., Rizzi R. 1993. Effect of body condition score at calving on performance, some blood parameters, and milk fatty acid composition in dairy cows. *Journal of Dairy Science*. 76: 2528-2535.
51. Pendell D.L, Brester G. W., Dhuyvetter K.C, Tonsor G.T. 2010 . Animal identification and tracing in the United States. *American Journal of Agriculture* 92:927-940
52. Peiper U.M, Edan Y., Devir S., Barak M., Maltz E., 1993. Automatic weighing of dairy cows. *Journal of Agricultural Engineering Research*. 56: 13-24.
53. Pompe, J. C. A. M., De Graaf V. J., Semplonius R., Meuleman J..2005. Automatic body condition scoring of dairy cows: Extracting contour lines. 5 *Eur. Conf. Precision Agric. 2nd Eur. Conf. Precision Live st. Farming.JTI/Swedish Institute of Agricultural and Environmental Engineering: 243 - 245.*
54. Poursaberia, A., Bahra, C., Pluka, A., Van Nuffelb, A., Berckmansa, D. 2010. Real-time automatic lameness detection based on back posture extraction in dairy cattle: Shape analysis of cow with image processing techniques . *Computers and Electronics in Agriculture* 74 : 110–119
55. Rajkondawar, P.G.U., Tasch, A.M., Lefcourt, B., Erez, R. M., Dyer, M.A., Varner, S. .2002. A system for identifying lameness in dairy cattle. *ASAE Journal of Applied Engineering in Agriculture* 18: 87-96.
56. Ram, T. 2009. Digital chemo-optic system for optimizing predictions of best harvesting date and of olive oil quality. MSc. thesis, Ben-Gurion University of the Negev, Beer Sheva, Israel.
57. Roche, J.R., Friggens, N.C., Kay, J.K., Fisher, M.W., Stafford, K.J., Berry, D.P. .2009. invited review: Body condition score and its association with dairy cow productivity, health, and welfare. *Journal of Dairy Science* 92: 5769 – 5801

58. Rodenburg, J. 2000. Body Condition Scoring of Dairy Cattle. *Retrieved on October 24, 2010, from www.omafra.gov.on.ca.*
59. Ruegg, P.L., Milton R.L. 1995. Body condition scores of Holstein cows on Prince Edward Island, Canada: Relationships with yield, reproductive performance, and disease. *Journal of Dairy Science* 78:552-564.
60. Schofield, C. P., Marchant, J. A., White, R. P., Brandle, N., Wilson, M. 1999. Monitoring pig growth using a prototype imaging system. *Journal of Agricultural Engineering Research* 72 : 205 – 210.
61. Schröder, U. J., and R. Staufenbiel.(2006). Invited review: Methods to determine body fat reserves in the dairy cow with special regard to ultrasonographic measurement of backfat thickness. *Journal of Dairy Science* 89:1–14.
62. Senger, P. L. (1994). The Estrus Detection Problem: New Concepts, Technologies, and Possibilities. *Journal of Dairy Science* 77: 2745-2753.
63. Song, X., Leroya, T., Vrankena, E., Maertensb, W., Sonckb, B., Berckmansa, D. 2008. Automatic detection of lameness in dairy cattle—Vision-based trackway analysis in cow's locomotion. *Computers and Electronics in Agriculture* 6 :39–44
64. Sonka, M. Hlavac V., Boyle R., Image Processing ,Analysis and Machine Vision, 3rd Ed, Brooks/Cole Publishing Co., 2007
65. Stone, M. 1974. Cross-validatory choice and assessment of statistical predictions. *Journal of the Royal Statistical Society* 36: 111-147.
66. Szeliski, R. Computer Vision:Algorithms and Applications. *Springer, Berlin, Germany, 1st edition, 2011.*
67. Syriyasathaporn, W., M. Nielen, S.J. Dieleman, A. Brand, E.N. Noordhuizen-Stassen, Schukken Y.H. 1998. A cox proportional-hazards model with time-dependent covariates to evaluate the relationship between body-condition score and the risks of first insemination and pregnancy in a high producing dairy herd. *Preventive Veterinary Medicine.* 37:159-172.
68. Tsenkova R., Atanassova S., Itoh K., Ozaki Y., Toyoda K. 2000. Near infrared spectroscopy for biomonitoring: cow milk composition measurement in a spectral region from 1,100 to 2,400 nanometers. *Journal of Animal Science,* 78: 515-522.

69. Van der Stuyft, E., Schofield, C.P., Randall, J.M., Wambacq P., Goedseels, V. 1991. Development and application of computer vision systems for use in livestock production. *Computers and Electronics in Agriculture*, 6: 243-265
70. Vazquez-Fernandez, E., Dacal-Nieto A., Martin F., Formella A., Torres-Guijarro, S., Gonzalez-Jorge H. 2009 A computer vision system for visual grape grading in wine cellars. *7th International Conference on Computer Vision Systems, ICVS 2009 Liège, Belgium, October 13-15. Lecture Notes in Computer Science* 5815.
71. Waltner, S.S., McNamara J.P., Hillers J.K.. 1993. Relationships of body condition score to production variables in high producing Holstein cows *Journal of Dairy Science*. 76:3410-3419.
72. Wildman, E.E., G.M. Jones, P.E. Wagner, and R.L. Bowman. 1982. A dairy cow body condition scoring system and its relationship to selected production characteristics. *Journal of Dairy Science*. 65:495-501.
73. White, R. P., Schofield, C. P., Green, D. M., Parsons, D. J. and Whittemore, C. T. 2004. The effectiveness of a Visual Image Analysis (VIA) system for monitoring the performance of growing/finishing pigs. *Animal Science* 78:409-418.
74. Zahn, T. Roskies R.Z. 1972. Fourier descriptors for plane closed curves, *IEEE Transactions on Computers* 21: 269–281.
75. Zhang, D.S. Lu G. 2003. A comparative study of curvature scale space and Fourier descriptors, *Journal of Visual Communication and Image Representation* 14 :41–60.
76. Zion, B., Alachantis, V., Ostrovsky, V., Barki, A., Karplus, I. 2006. Real-time underwater sorting of edible fish species. *Computers and Electronics in Agriculture* 56: 34–45.
77. Zheng, C., Sun, D. W., Zheng, L. 2006. Recent developments and applications of image features for food quality evaluation and inspection e a review. *Trends in Food Science & Technology* 17: 642-655.

8 Appendices

Appendix A. Data acquisition software

Camera control pro 2. Software by Nikon:

http://imaging.nikon.com/lineup/software/control_pro2/

Appendix B. Cow digital images

All training images are stored in CD in: Appendices\training images.

All testing images are stored in CD in: Appendices\testing images.

Images that were not selected for modeling are stored in CD in: Appendices\images not selected.

Example of selected cow image:



Appendix C. manual BCS

Training set

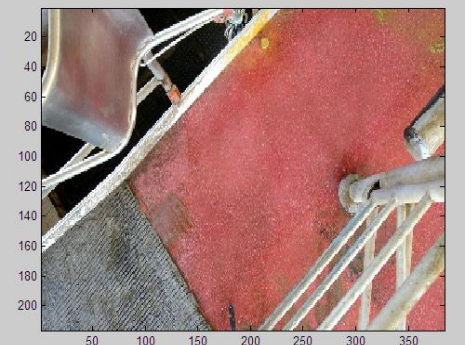
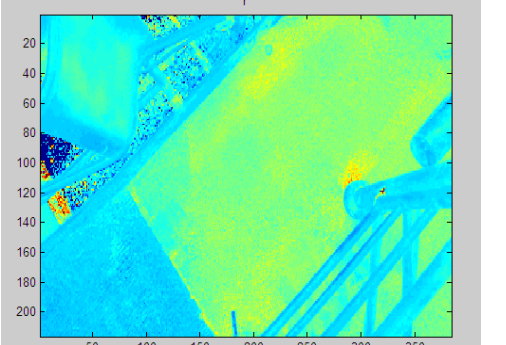
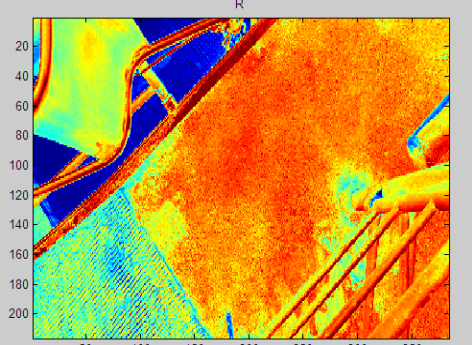
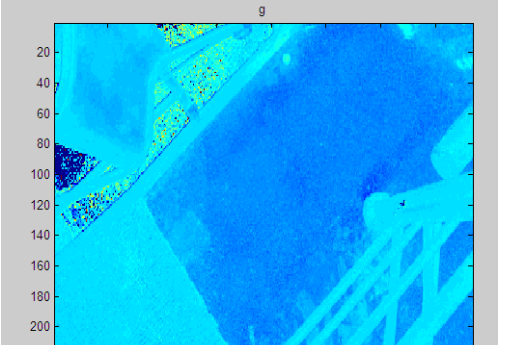
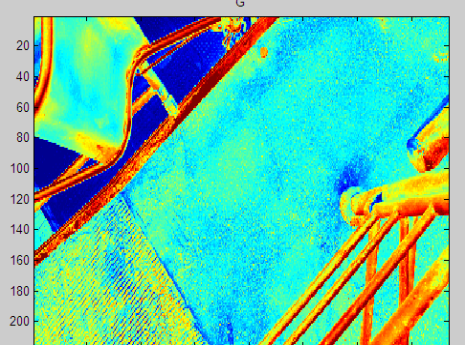
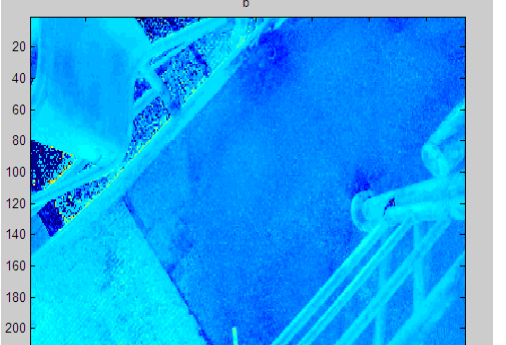
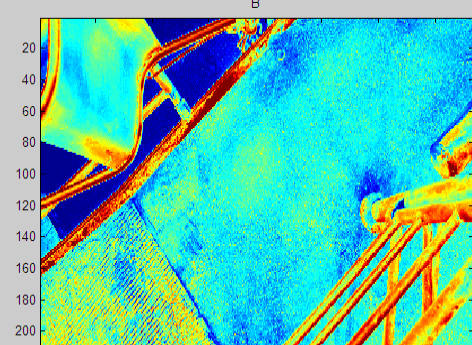
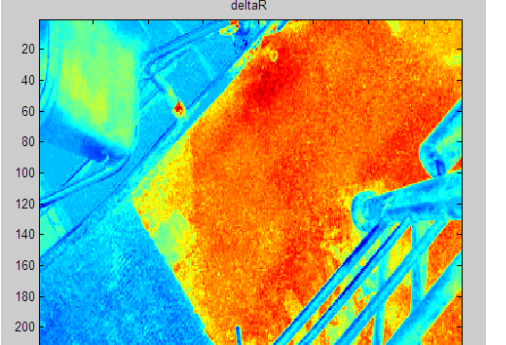
Training Set			Training Set			Training Set		
Num	COW	BCS	Num	COW	BCS	Num	COW	BCS
1	2646	4.4	32	3116	2.8	63	3212	2.3
2	2646	4.4	33	3116	2.8	64	2992	2.4
3	2703	2.25	34	3126	3.6	65	3070	2
4	2739	4.6	35	3128	3.9	66	3088	2.1
5	2791	3.4	36	3130	2.6	67	3091	2.2
6	2791	3.4	37	3130	2.6	68	3096	2.5
7	2815	2.3	38	3132	3.2	69	3122	2.7
8	2853	2.3	39	3138	2.5	70	3146	2.4
9	2853	2.3	40	3201	3	71	3157	2.3
10	2856	2.2	41	3211	2.5	72	3163	2.2
11	2902	2.5	42	2978	2.7	73	3193	3
12	2906	2.3	43	2970	2.3	74	3195	2.3
13	2906	2.3	44	3036	2.3	75	3196	2.8
14	2945	4.8	45	3058	3.3	76	3201	3.4
15	2985	2.5	46	3077	2.4	77	3212	2.3
16	2995	4.6	47	3077	2.4	78	3195	2.7
17	2995	4.6	48	3100	2.3	79	2974	3.4
18	2995	4.6	49	3122	2.7	80	3058	3.3
19	2996	2.7	50	3139	4.1	81	3058	3.3
20	3006	3	51	3146	2.4	82	3101	2.6
21	3006	3	52	3151	2.2	83	3096	2.5
22	3021	2.65	53	3158	2.1	84	3071	4.2
23	3021	2.65	54	3160	2.5	85	3071	4.2
24	3054	3.7	55	3183	2.3	86	3071	4.2
25	3061	2.65	56	3185	2.3	87	3122	2.7
26	3064	2.1	57	3185	2.3			
27	3074	3.6	58	3190	3.7			
28	3077	2.6	59	3200	2.5			
29	3096	2.4	60	3200	2.5			
30	3101	2.4	61	3203	2.4			
31	3116	2.8	62	3206	3.2			

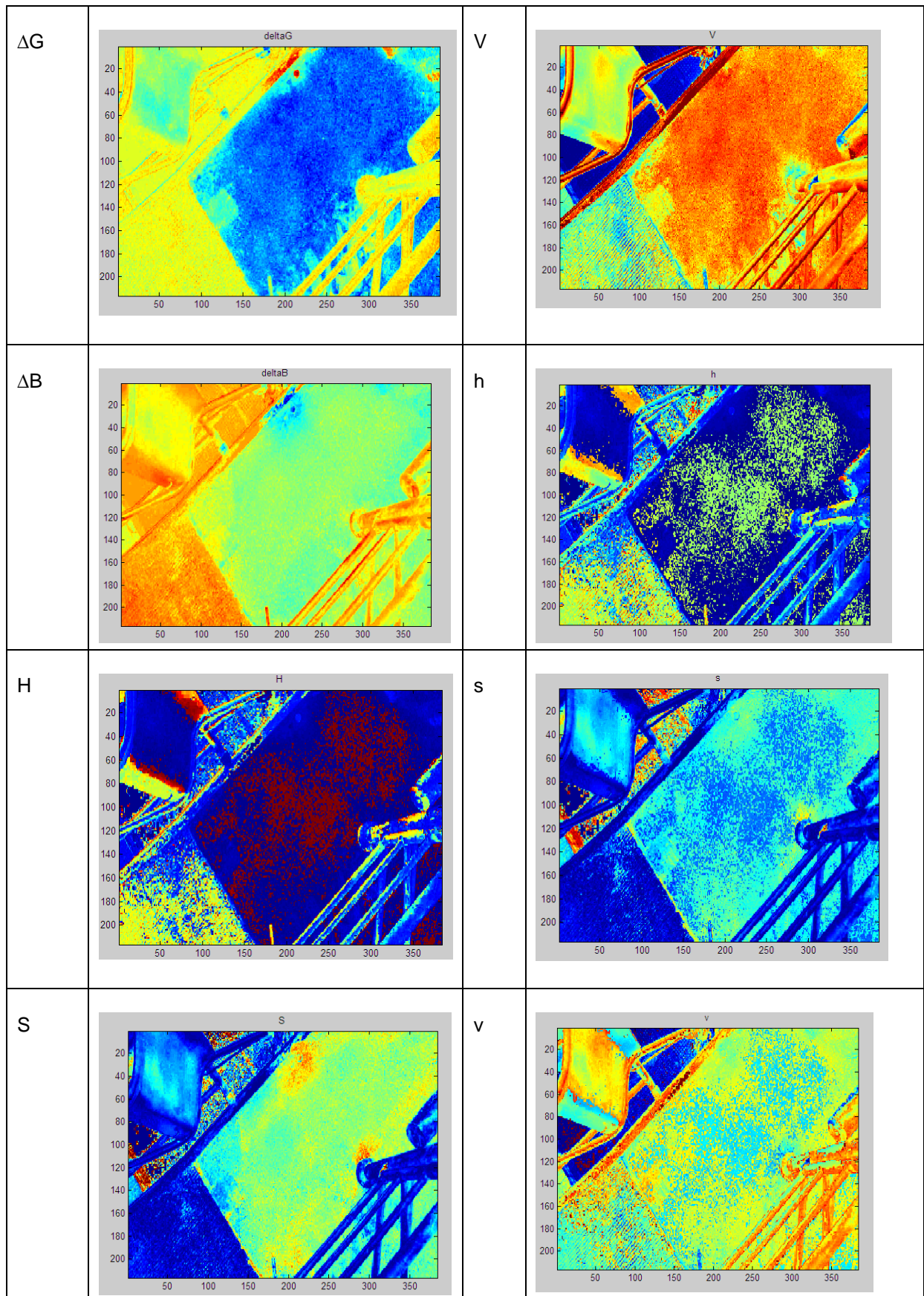
Testing set

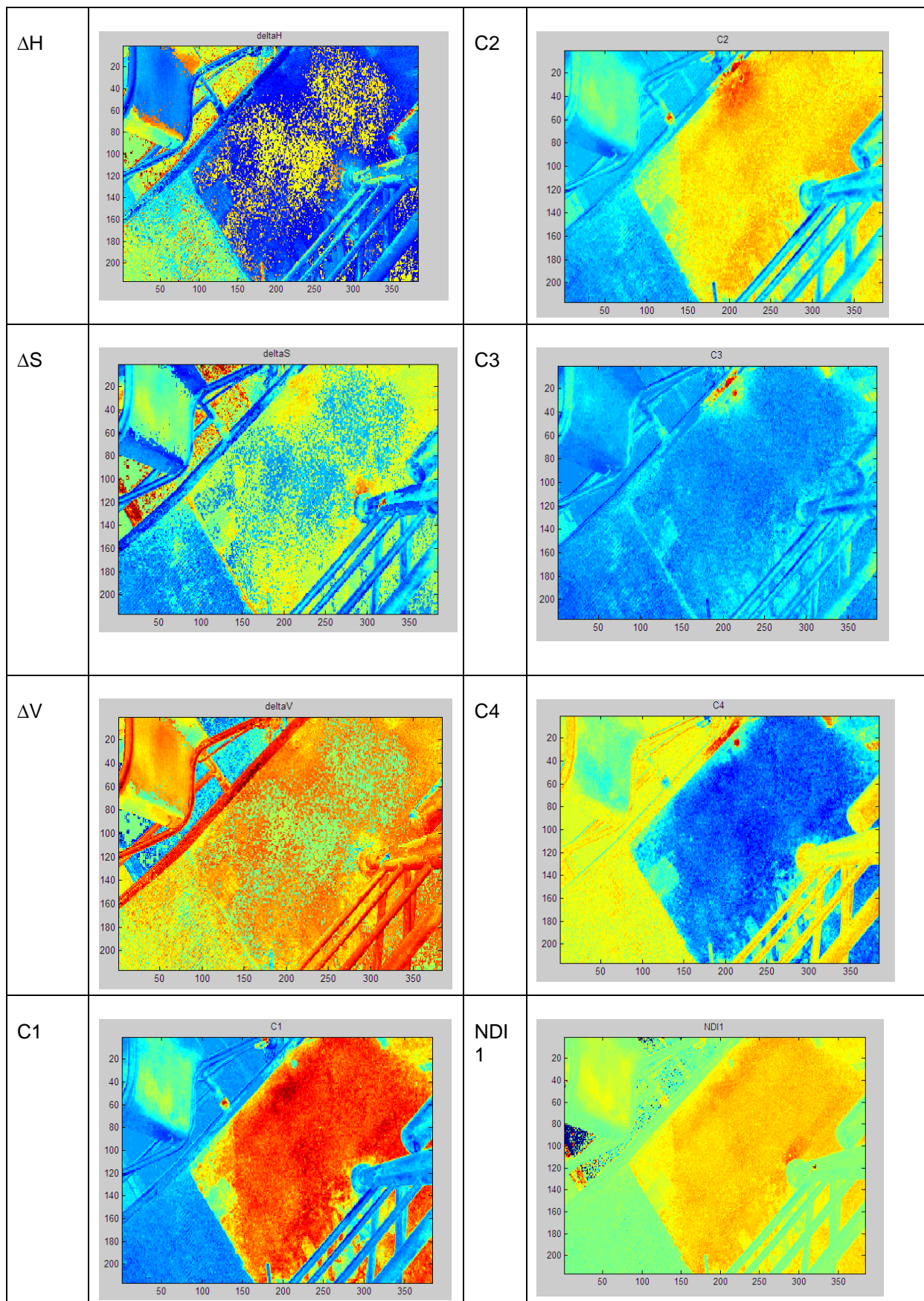
Testing set			Testing set		
Num	Cow	BCS	Num	Cow	BCS
1	2894	2.6	33	3028	2.6
2	2894	2.6	34	3037	3.2
3	2894	2.6	35	3071	4.2
4	2894	2.6	36	3071	4.2
5	2894	2.6	37	3071	4.2
6	2917	2.8	38	3071	4.2
7	2921	3.3	39	3122	2.8
8	2936	2.3	40	3124	3.1
9	3096	2.4	41	3139	3.5
10	3096	2.4	42	3139	3.5
11	3139	3.5	43	3146	2.5
12	3139	3.5	44	3146	2.5
13	3146	2.5	45	3149	2.4
14	3151	2.2	46	3154	2.1
15	3158	2.3	47	3163	2.3
16	3162	3	48	3167	3.5
17	3162	3	49	3171	2.3
18	3185	2.3	50	3206	2.5
19	3187	2.6	51	3212	2.2
20	3195	2.4	52	2858	2.1
21	3195	2.4	53	2858	2.1
22	3205	2.7	54	3154	2.1
23	3206	2.5	55	3167	3.5
24	3207	1.9	56	3167	3.5
25	3207	1.9	57	3167	3.5
26	3218	2	58	3186	3.9
27	2858	2.1	59	3186	3.9
28	2879	2.5	60	3186	3.9
29	2917	2.8	61	3186	3.9
30	2921	3.3	62	3186	3.9
31	2921	3.3	63	3186	3.9
32	2983	2.1	64	3218	2

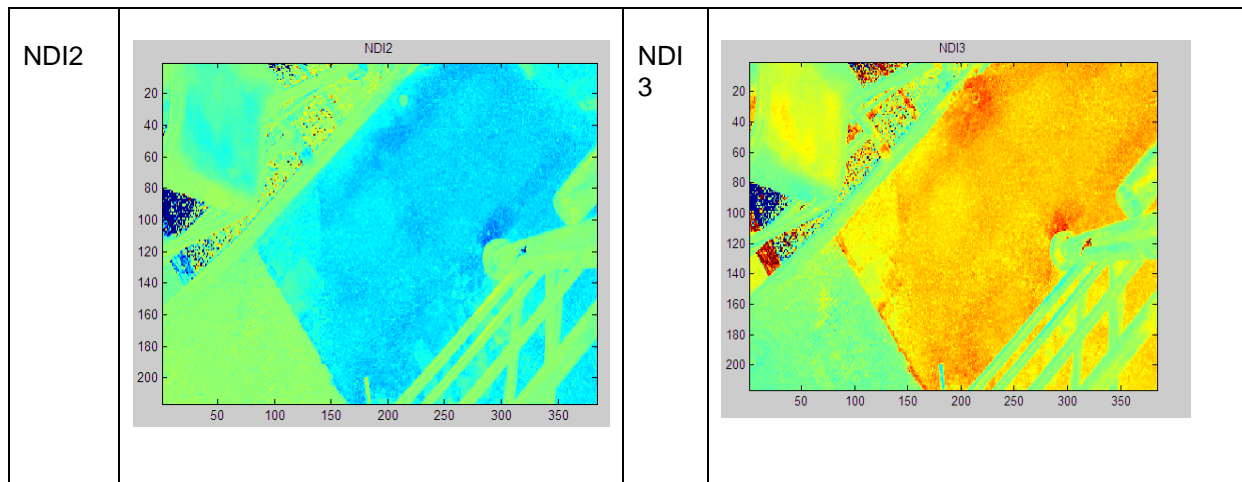
Appendix D. Color masks:

Images

<p>Backg round</p>		<p>r</p>	
<p>R</p>		<p>g</p>	
<p>G</p>		<p>b</p>	
<p>B</p>		<p>ΔR</p>	







Appendix E. Color masks effective statistics results:

Univariate analysis of variance

Tests of Between-Subjects Effects

Dependent Variable: Effectivness

Source	Type III Sum of Squares	df	Mean Square	F	Sig.
Corrected Model	3.811 ^a	17	.224	240.161	.000
Intercept	680.844	1	680.844	729393.783	.000
ColorMask	3.811	17	.224	240.161	.000
Error	1.042	1116	.001		
Total	685.696	1134			
Corrected Total	4.853	1133			

a. R Squared = .785 (Adjusted R Squared = .782)

LSD test- for color masks effectiveness

(I) ColorMask	(J) ColorMask	Mean Difference (I-J)	Std. Error	Sig.	95% Confidence Interval	
					Lower Bound	Upper Bound
19	1	.1601 [*]	.00544	.000	.1495	.1708
	2	.0841 [*]	.00544	.000	.0734	.0947
	3	.0850 [*]	.00544	.000	.0744	.0957
	4	.0231 [*]	.00544	.000	.0124	.0338
	5	.0602 [*]	.00544	.000	.0495	.0709
	6	.0996 [*]	.00544	.000	.0889	.1103
	7	.0427 [*]	.00544	.000	.0320	.0534
	8	.0182 [*]	.00544	.001	.0076	.0289
	9	.1339 [*]	.00544	.000	.1232	.1445
	11	.0284 [*]	.00544	.000	.0177	.0390
	12	.1623 [*]	.00544	.000	.1517	.1730
	20	.0922 [*]	.00544	.000	.0815	.1029
	21	.2050 [*]	.00544	.000	.1944	.2157
	22	.0182 [*]	.00544	.001	.0076	.0289
	23	.0210 [*]	.00544	.000	.0103	.0317
	24	.0212 [*]	.00544	.000	.0105	.0319
	25	.0603 [*]	.00544	.000	.0496	.0709

Appendix F. anatomical points results:

Backward Regression- anatomical point's features (model 1):

Model Summary

Model	R	R Square	Adjusted R Square	Std. Error of the Estimate
1	.816 ^a	.667	.592	.45454
2	.816 ^b	.666	.599	.45110
3	.816 ^c	.666	.604	.44797
4	.815 ^d	.665	.609	.44529
5	.814 ^e	.663	.613	.44304
6	.814 ^f	.662	.618	.44025
7	.813 ^g	.660	.621	.43840
8	.811 ^h	.657	.623	.43702
9	.810 ⁱ	.655	.626	.43521
10	.804 ^j	.647	.622	.43758

Model coefficients

10	(Constant)	-1.053	.658		-1.599	.114
	X2	-4.302	2.179	-.148	-1.974	.052
	Y3	1.855	.846	.339	2.192	.032
	Y4	4.680	1.957	.391	2.392	.019
	Angle2	.016	.005	.492	2.920	.005
	Angle4	.025	.005	.913	4.977	.000

Goodness of Fit^b

	Value	df	Value/df
Deviance	14.882	73	.204
Scaled Deviance	78.000	73	
Pearson Chi-Square	14.882	73	.204
Scaled Pearson Chi-Square	78.000	73	
Log Likelihood ^a	-46.072		
Akaike's Information Criterion (AIC)	104.143		
Finite Sample Corrected AIC (AICC)	105.326		
Bayesian Information Criterion (BIC)	118.283		
Consistent AIC (CAIC)	124.283		

Dependent Variable: BCS

Model: (Intercept), X2, Y3, Angle2, Angle4

Forward\ Stepwise Regression- anatomical points features (model 2):

Model Summary

Model	R	R Square	Adjusted R Square	Std. Error of the Estimate
1	.750 ^a	.562	.556	.47424

a. Predictors: (Constant), Angle3

Coefficients^a

Model	Unstandardized Coefficients		Standardized Coefficients	t	Sig.
	B	Std. Error	Beta		
1 (Constant)	.918	.201		4.568	.000
Angle3	.024	.002	.750	9.877	.000

a. Dependent Variable: BCS

Goodness of Fit^b

	Value	df	Value/df
Deviance	17.093	76	.225
Scaled Deviance	78.000	76	
Pearson Chi-Square	17.093	76	.225
Scaled Pearson Chi-Square	78.000	76	
Log Likelihood ^a	-51.474		
Akaike's Information Criterion (AIC)	108.947		
Finite Sample Corrected AIC (AICC)	109.272		
Bayesian Information Criterion (BIC)	116.017		
Consistent AIC (CAIC)	119.017		

Dependent Variable: BCS

Model: (Intercept), Angle3

a. The full log likelihood function is displayed and used in computing information criteria.

b. Information criteria are in small-is-better form.

Forward\ Stepwise\Backward Regression- anatomical points feature Average Angles and Distance (Model 3):

Model Summary

Model	R	R Square	Adjusted R Square	Std. Error of the Estimate
1	.730 ^a	.533	.527	.48961
2	.757 ^b	.573	.562	.47122
3	.788 ^c	.621	.606	.44713

Coefficients^a

Model		Unstandardized Coefficients		Standardized Coefficients	t	Sig.
		B	Std. Error	Beta		
1	(Constant)	1.220	.181		6.728	.000
	AvgAngleOut	.018	.002	.730	9.318	.000
2	(Constant)	.872	.218		3.994	.000
	AvgAngleOut	.014	.002	.564	5.745	.000
	AvgAngleIn	.008	.003	.260	2.654	.010
3	(Constant)	-.879	.610		-1.440	.154
	AvgAngleOut	.020	.003	.813	6.561	.000
	AvgAngleIn	.015	.004	.497	4.101	.000
	AvgY1_4	5.745	1.884	.492	3.049	.003

a. Dependent Variable: BCS

Goodness of Fit^b

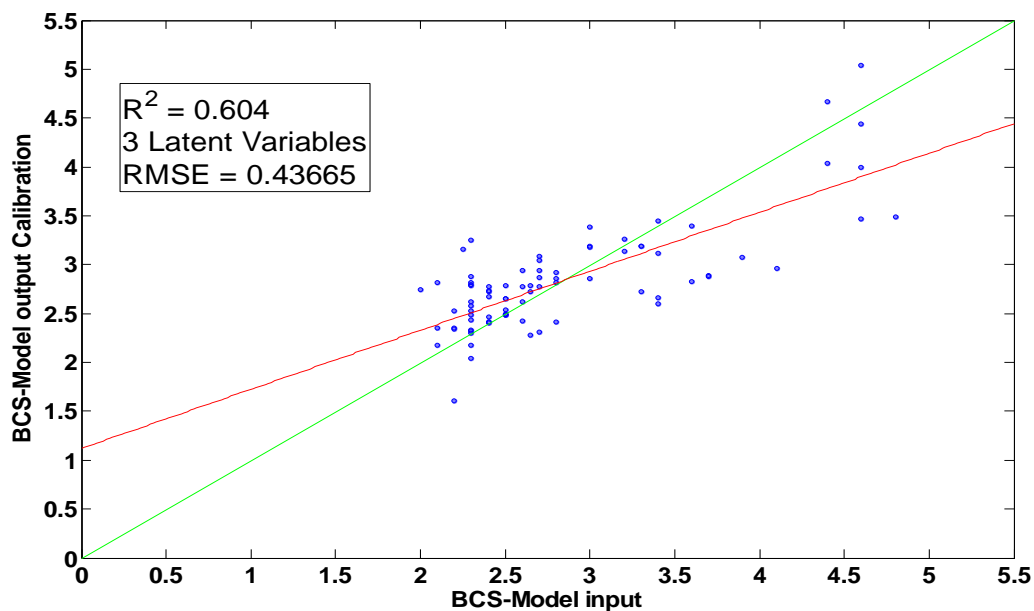
	Value	df	Value/df
Deviance	14.795	74	.200
Scaled Deviance	78.000	74	
Pearson Chi-Square	14.795	74	.200
Scaled Pearson Chi-Square	78.000	74	
Log Likelihood ^a	-45.842		
Akaike's Information Criterion (AIC)	101.683		
Finite Sample Corrected AIC (AICC)	102.517		
Bayesian Information Criterion (BIC)	113.467		
Consistent AIC (CAIC)	118.467		

Dependent Variable: BCS

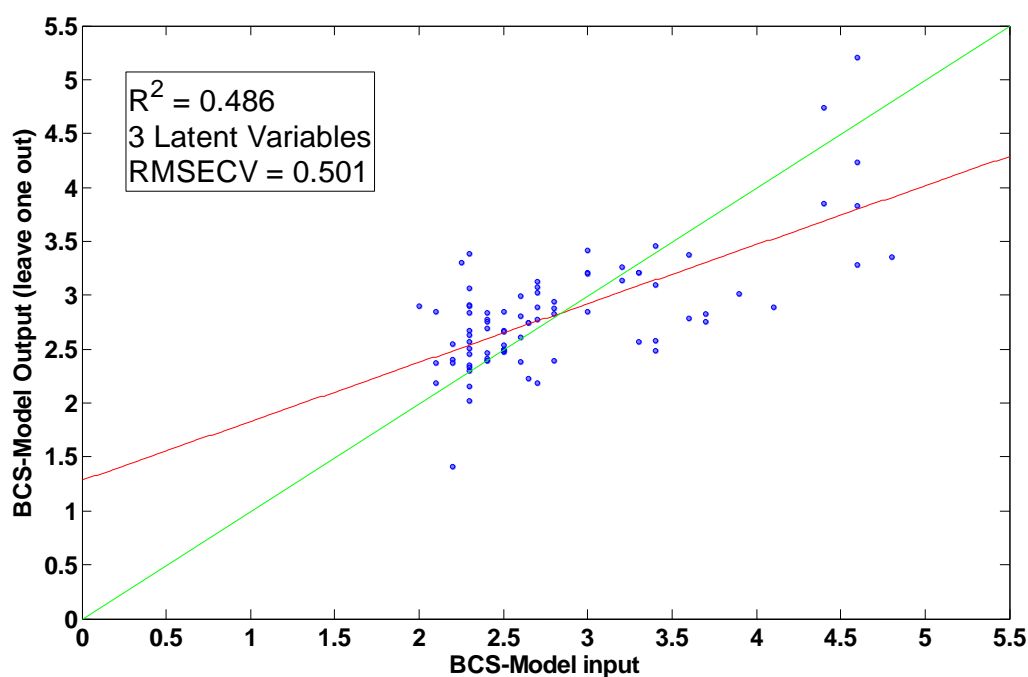
Model: (Intercept), AvgAngleIn, AvgAngleOut, AvgY1_4

Appendix G. PLS results:

The result of linear regression between 3 latent variables and the BCS measured by expert are shown on the calibration set and by using leave one out method (CV)



Correlation between the model output (calibration) and the manual BCS. Red line is the linear fitting between the scores observed manually by the expert (X axis), and the PLS model output (Y axis). The green line is the desired fitting



Correlation between the model output (Leave one out) and the manual BCS. Red line is the

linear fitting between the scores observed manually by the expert (X axis), and the PLS model output (Y axis). The grin line is the desired fitting

Appendix H. Fourier transform model results :

Model Summary^f

Model	R	R Square	Adjusted R Square	Std. Error of the Estimate
1	.887 ^a	.787	.759	.35840
2	.887 ^b	.787	.762	.35625
3	.886 ^c	.785	.763	.35544
4	.882 ^d	.778	.759	.35867
5	.878 ^e	.771	.754	.36243

Coefficients^a

Model		Unstandardized Coefficients		Standardized Coefficients	t	Sig.
		B	Std. Error	Beta		
5	(Constant)	6.405	.257		24.950	.000
	F3	-.027	.004	-.477	-5.997	.000
	F4	-.024	.005	-.278	-4.656	.000
	F5	-.011	.005	-.168	-2.061	.043
	F6	-.081	.013	-.520	-6.261	.000
	F7	-.087	.013	-.462	-6.518	.000
	F8	-.072	.020	-.215	-3.571	.001

Goodness of Fit^b

	Value	df	Value/df
Deviance	10.508	80	.131
Scaled Deviance	87.000	80	
Pearson Chi-Square	10.508	80	.131
Scaled Pearson Chi-Square	87.000	80	
Log Likelihood ^a	-31.500		
Akaike's Information Criterion (AIC)	79.000		
Finite Sample Corrected AIC (AICC)	80.846		
Bayesian Information Criterion (BIC)	98.727		
Consistent AIC (CAIC)	106.727		

Dependent Variable: BCS

Model: (Intercept), F3, F4, F5, F6, F7, F8

a. The full log likelihood function is displayed and used in computing information criteria.

b. Information criteria are in small-is-better form.

Forward \ Stepwise Regression:

Model Summary^a

Model	R	R Square	Adjusted R Square	Std. Error of the Estimate
1	.591 ^a	.349	.342	.59261
2	.708 ^b	.502	.490	.52168
3	.794 ^c	.630	.617	.45207
4	.852 ^d	.726	.713	.39133
5	.868 ^e	.754	.739	.37326
6	.876 ^f	.768	.751	.36462

Coefficients

6	(Constant)	3.654	1.599		2.286	.025
	F6	-.083	.013	-.529	-6.165	.000
	F8	-.074	.020	-.222	-3.660	.000
	F1	.005	.003	.246	1.798	.076
	F7	-.081	.013	-.431	-6.155	.000
	F4	-.022	.006	-.246	-3.739	.000
	F3	-.018	.008	-.326	-2.210	.030

Goodness of Fit^b

	Value	df	Value/df
Deviance	10.636	80	.133
Scaled Deviance	87.000	80	
Pearson Chi-Square	10.636	80	.133
Scaled Pearson Chi-Square	87.000	80	
Log Likelihood ^a	-32.025		
Akaike's Information Criterion (AIC)	80.051		
Finite Sample Corrected AIC (AICC)	81.897		
Bayesian Information Criterion (BIC)	99.778		
Consistent AIC (CAIC)	107.778		

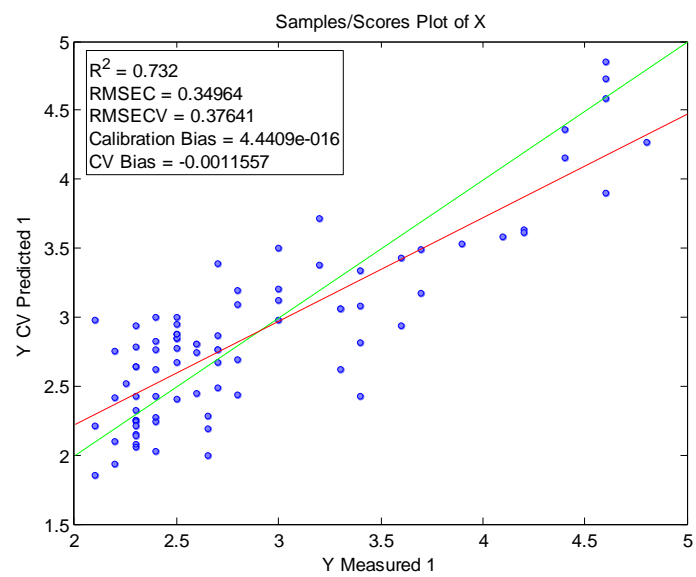
Dependent Variable: BCS

Model: (Intercept), F3, F4, F6, F7, F8, F1

a. The full log likelihood function is displayed and used in computing information criteria.

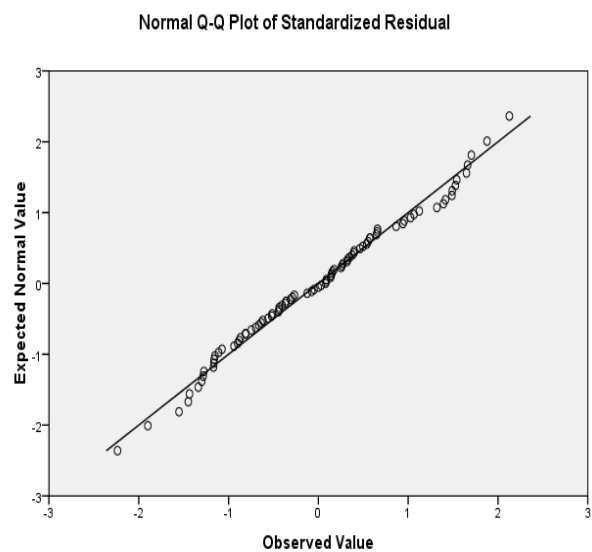
b. Information criteria are in small-is-better form.

Leave-one-out results of Model 2:

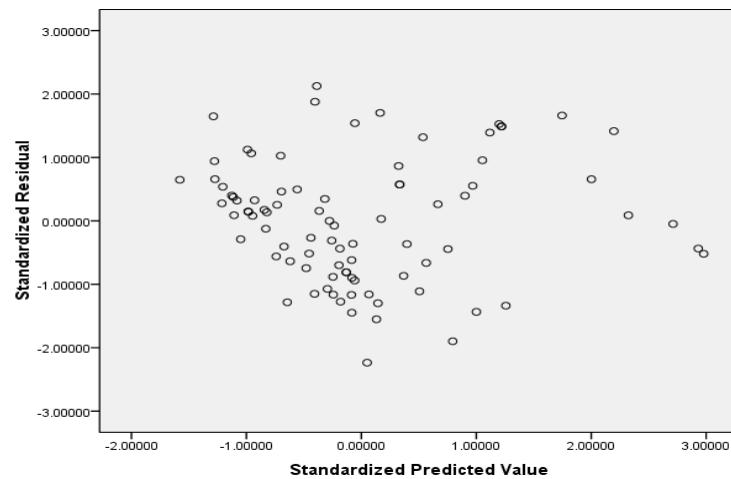


Linear Regression assumption testing (model 1):

Normal distribution of residuals:



Independence of residuals:



Appendix I. Combining anatomical points features and Fourier descriptors

Anatomical points features (average height, angle in and out) are excluded out of the linear regression model using Forward\ stepwise or backward methods:

Excluded Variables Forward\ Stepwise methods

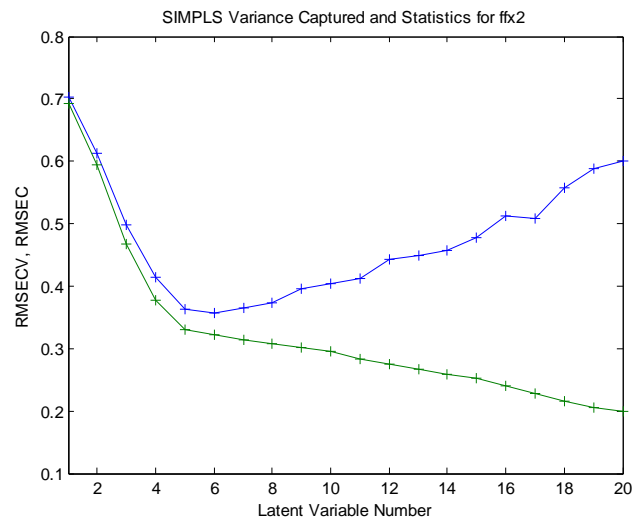
Model		Beta In	t	Sig.	Partial Correlation	Collinearity Statistics
						Tolerance
6	F2	.147 ^f	1.650	.103	.193	.335
	F5	-.052 ^f	-.286	.776	-.034	.082
	F9	-.076 ^f	-1.323	.190	-.156	.821
	F10	-.044 ^f	-.736	.464	-.088	.769
	AvgAngIn	.005 ^f	.097	.923	.012	.946
	AvgAngOut	.066 ^f	1.224	.225	.145	.924
	AvgHeight	-.053 ^f	-.988	.327	-.117	.950

Excluded Variables Backward method

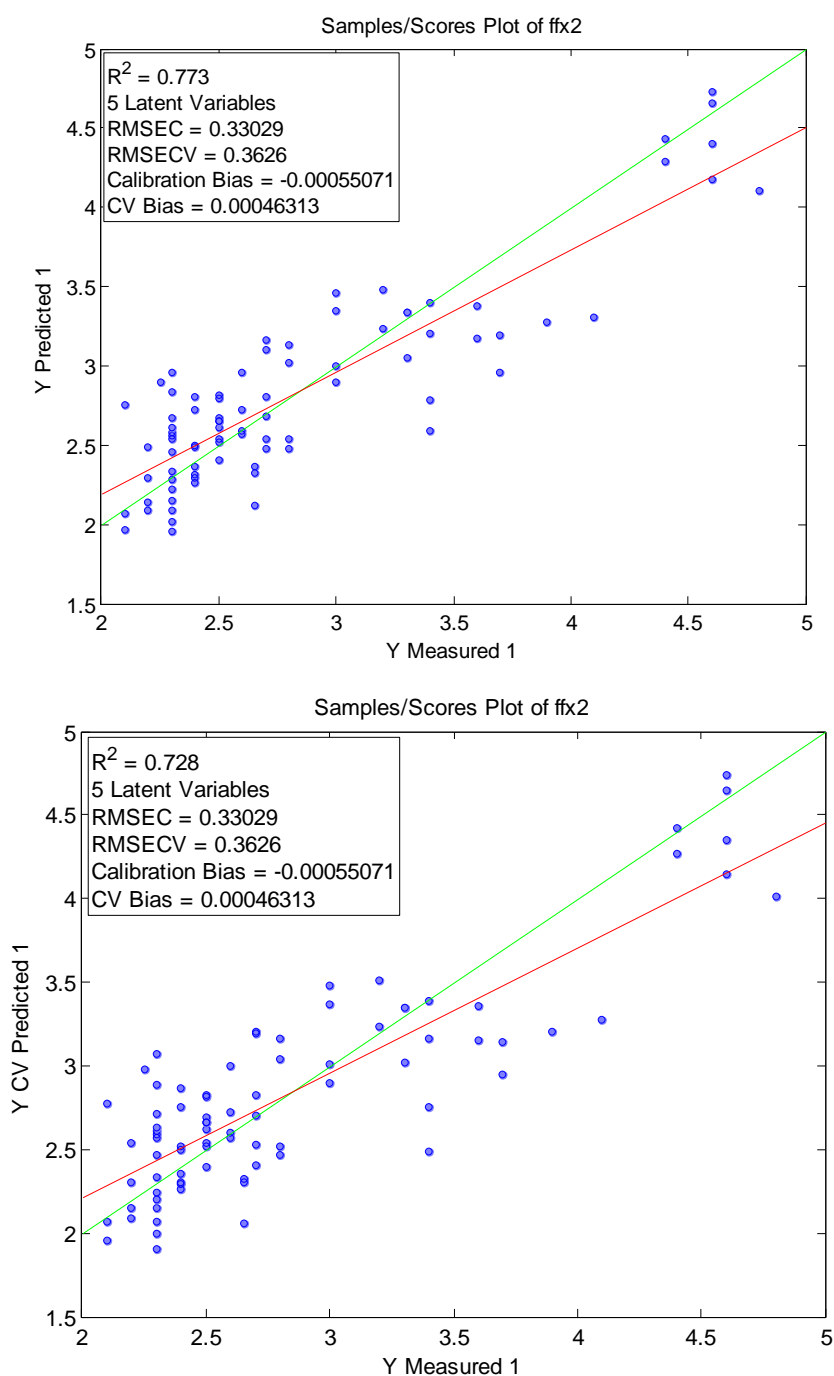
	Model	Beta In	t	Sig.	Partial Correlation	Collinearity Statistics
						Tolerance
8	F5	-.052 ^g	-.286	.776	-.034	.082
	AvgAngOut	.066 ^g	1.224	.225	.145	.924
	F10	-.044 ^g	-.736	.464	-.088	.769
	F9	-.076 ^g	-1.323	.190	-.156	.821
	AvgAngIn	.005 ^g	.097	.923	.012	.946
	AvgHight	-.053 ^g	-.988	.327	-.117	.950
	F2	.147 ^g	1.650	.103	.193	.335

Appendix J. Modeling by contour features using PLS and Fourier transform

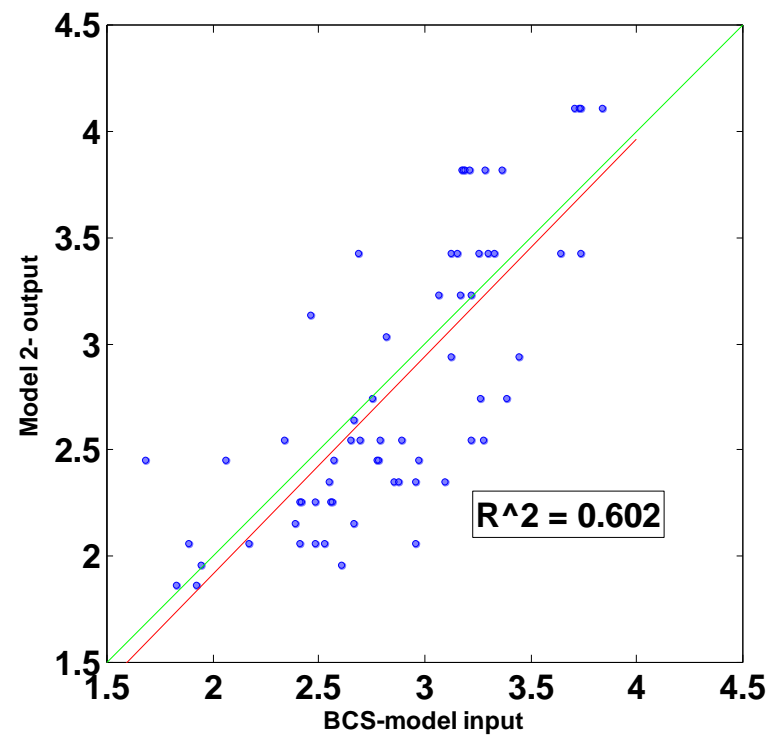
Number of latent variables for selection: It is possible to see that RMSE reach to minimum for 5 variables.



Results of PLS on Fourier transform –Leave one out and calibration set :



Appendix K. Model 2 performance on testing set:



Appendix L. Model classing performance:

Classify by ranges of 0.25-training set

		Binnes Predicted												Total
		2-2.25	2.25-2.5	2.5-2.75	2.75-3	3-3.25	3.25-3.5	3.5-3.75	3.75-4	4-4.25	4.25-4.5	4.5- 4.75	4.75-5	
Blms Observed	2-2.25	Count	4	2	1	1	0	0	0	0	0	0	0	8
		% within BCSBinn	50.0%	25.0%	12.5%	12.5%	.0%	.0%	.0%	.0%	.0%	.0%	.0%	100.0%
		% within PreBin	28.6%	15.4%	6.7%	5.6%	.0%	.0%	.0%	.0%	.0%	.0%	.0%	9.2%
		% of Total	4.6%	2.3%	1.1%	1.1%	.0%	.0%	.0%	.0%	.0%	.0%	.0%	9.2%
	2.25-2.5	Count	8	7	5	4	0	0	0	0	0	0	0	24
		% within BCSBinn	33.3%	29.2%	20.8%	16.7%	.0%	.0%	.0%	.0%	.0%	.0%	.0%	100.0%
		% within PreBin	57.1%	53.8%	33.3%	22.2%	.0%	.0%	.0%	.0%	.0%	.0%	.0%	27.6%
		% of Total	9.2%	8.0%	5.7%	4.6%	.0%	.0%	.0%	.0%	.0%	.0%	.0%	27.6%
	2.5-2.75	Count	2	3	6	10	0	1	0	0	0	0	0	22
		% within BCSBinn	9.1%	13.6%	27.3%	45.5%	.0%	4.5%	.0%	.0%	.0%	.0%	.0%	100.0%
		% within PreBin	14.3%	23.1%	40.0%	55.6%	.0%	20.0%	.0%	.0%	.0%	.0%	.0%	25.3%
		% of Total	2.3%	3.4%	6.9%	11.5%	.0%	1.1%	.0%	.0%	.0%	.0%	.0%	25.3%
	2.75-3	Count	0	1	1	0	2	0	0	0	0	0	0	4
		% within BCSBinn	.0%	25.0%	25.0%	.0%	50.0%	.0%	.0%	.0%	.0%	.0%	.0%	100.0%
		% within PreBin	.0%	7.7%	6.7%	.0%	25.0%	.0%	.0%	.0%	.0%	.0%	.0%	4.6%
		% of Total	.0%	1.1%	1.1%	.0%	2.3%	.0%	.0%	.0%	.0%	.0%	.0%	4.6%
	3-3.25	Count	0	0	0	1	2	1	2	0	0	0	0	6
		% within BCSBinn	.0%	.0%	.0%	16.7%	33.3%	16.7%	33.3%	.0%	.0%	.0%	.0%	100.0%
		% within PreBin	.0%	.0%	.0%	5.6%	25.0%	20.0%	28.6%	.0%	.0%	.0%	.0%	6.9%
		% of Total	.0%	.0%	.0%	1.1%	2.3%	1.1%	2.3%	.0%	.0%	.0%	.0%	6.9%
	3.25-3.5	Count	0	0	2	1	3	1	0	0	0	0	0	7
		% within BCSBinn	.0%	.0%	28.6%	14.3%	42.9%	14.3%	.0%	.0%	.0%	.0%	.0%	100.0%
		% within PreBin	.0%	.0%	13.3%	5.6%	37.5%	20.0%	.0%	.0%	.0%	.0%	.0%	8.0%
		% of Total	.0%	.0%	2.3%	1.1%	3.4%	1.1%	.0%	.0%	.0%	.0%	.0%	8.0%
	3.5-3.75	Count	0	0	0	1	1	2	0	0	0	0	0	4
		% within BCSBinn	.0%	.0%	.0%	25.0%	25.0%	50.0%	.0%	.0%	.0%	.0%	.0%	100.0%
		% within PreBin	.0%	.0%	.0%	5.6%	12.5%	40.0%	.0%	.0%	.0%	.0%	.0%	4.6%
		% of Total	.0%	.0%	.0%	1.1%	1.1%	2.3%	.0%	.0%	.0%	.0%	.0%	4.6%
	3.75-4	Count	0	0	0	0	0	1	0	0	0	0	0	1
		% within BCSBinn	.0%	.0%	.0%	.0%	.0%	100.0%	.0%	.0%	.0%	.0%	.0%	100.0%
		% within PreBin	.0%	.0%	.0%	.0%	.0%	14.3%	.0%	.0%	.0%	.0%	.0%	1.1%
		% of Total	.0%	.0%	.0%	.0%	.0%	1.1%	.0%	.0%	.0%	.0%	.0%	1.1%
	4-4.25	Count	0	0	0	0	0	4	0	0	0	0	0	4
		% within BCSBinn	.0%	.0%	.0%	.0%	.0%	100.0%	.0%	.0%	.0%	.0%	.0%	100.0%
		% within PreBin	.0%	.0%	.0%	.0%	.0%	57.1%	.0%	.0%	.0%	.0%	.0%	4.6%
		% of Total	.0%	.0%	.0%	.0%	.0%	4.6%	.0%	.0%	.0%	.0%	.0%	4.6%
	4.25-4.5	Count	0	0	0	0	0	0	0	1	1	0	0	2
		% within BCSBinn	.0%	.0%	.0%	.0%	.0%	.0%	.0%	50.0%	50.0%	.0%	.0%	100.0%
		% within PreBin	.0%	.0%	.0%	.0%	.0%	.0%	.0%	100.0%	50.0%	.0%	.0%	2.3%
		% of Total	.0%	.0%	.0%	.0%	.0%	.0%	.0%	1.1%	1.1%	.0%	.0%	2.3%
	4.5-4.75	Count	0	0	0	0	0	0	1	0	0	1	2	4
		% within BCSBinn	.0%	.0%	.0%	.0%	.0%	.0%	25.0%	.0%	.0%	25.0%	50.0%	100.0%
		% within PreBin	.0%	.0%	.0%	.0%	.0%	.0%	100.0%	.0%	.0%	100.0%	100.0%	4.6%
		% of Total	.0%	.0%	.0%	.0%	.0%	.0%	1.1%	.0%	.0%	1.1%	2.3%	4.6%
	4.75-5	Count	0	0	0	0	0	0	0	0	1	0	0	1
		% within BCSBinn	.0%	.0%	.0%	.0%	.0%	.0%	.0%	.0%	100.0%	.0%	.0%	100.0%
		% within PreBin	.0%	.0%	.0%	.0%	.0%	.0%	.0%	.0%	50.0%	.0%	.0%	1.1%
		% of Total	.0%	.0%	.0%	.0%	.0%	.0%	.0%	.0%	1.1%	.0%	.0%	1.1%

Classify by ranges of 0. 5- Training set

			Predicted Binnes						Total
			2-2.5	2.5-3	3-3.5	3.5-4	4-4.5	4.5-5	
Bins Observed	2-2.5	Count	21	11	0	0	0	0	32
		% within bcsBinn	65.6%	34.4%	.0%	.0%	.0%	.0%	100.0%
		% within preBinn	77.8%	33.3%	.0%	.0%	.0%	.0%	36.8%
		% of Total	24.1%	12.6%	.0%	.0%	.0%	.0%	36.8%
	2.5-3	Count	6	17	3	0	0	0	26
		% within bcsBinn	23.1%	65.4%	11.5%	.0%	.0%	.0%	100.0%
		% within preBinn	22.2%	51.5%	23.1%	.0%	.0%	.0%	29.9%
		% of Total	6.9%	19.5%	3.4%	.0%	.0%	.0%	29.9%
	3-3.5	Count	0	4	7	2	0	0	13
		% within bcsBinn	.0%	30.8%	53.8%	15.4%	.0%	.0%	100.0%
		% within preBinn	.0%	12.1%	53.8%	25.0%	.0%	.0%	14.9%
		% of Total	.0%	4.6%	8.0%	2.3%	.0%	.0%	14.9%
	3.5-4	Count	0	1	3	1	0	0	5
		% within bcsBinn	.0%	20.0%	60.0%	20.0%	.0%	.0%	100.0%
		% within preBinn	.0%	3.0%	23.1%	12.5%	.0%	.0%	5.7%
		% of Total	.0%	1.1%	3.4%	1.1%	.0%	.0%	5.7%
	4-4.5	Count	0	0	0	4	2	0	6
		% within bcsBinn	.0%	.0%	.0%	66.7%	33.3%	.0%	100.0%
		% within preBinn	.0%	.0%	.0%	50.0%	66.7%	.0%	6.9%
		% of Total	.0%	.0%	.0%	4.6%	2.3%	.0%	6.9%
	4.5-5	Count	0	0	0	1	1	3	5
		% within bcsBinn	.0%	.0%	.0%	20.0%	20.0%	60.0%	100.0%
		% within preBinn	.0%	.0%	.0%	12.5%	33.3%	100.0%	5.7%
		% of Total	.0%	.0%	.0%	1.1%	1.1%	3.4%	5.7%

Classify by ranges of 0. 25- Testing set

BCSBin * PredicteddBin Crosstabulation											
			PredicteddBin						3.75-4	4-4.25	Total
			2-2.25	2.25-2.5	2.5-2.75	2.75-3	3-3.25	3.25-3.5			
Bin Observe	2-2.25	Count	5	4	2	1	0	0	0	0	12
		% within BCSBin	41.7%	33.3%	16.7%	8.3%	.0%	.0%	.0%	.0%	100.0%
		% within PredicteddBin	71.4%	36.4%	15.4%	12.5%	.0%	.0%	.0%	.0%	18.8%
		% of Total	7.8%	6.3%	3.1%	1.6%	.0%	.0%	.0%	.0%	18.8%
	2.25-2.5	Count	0	5	2	3	0	0	0	0	10
		% within BCSBin	.0%	50.0%	20.0%	30.0%	.0%	.0%	.0%	.0%	100.0%
		% within PredicteddBin	.0%	45.5%	15.4%	37.5%	.0%	.0%	.0%	.0%	15.6%
		% of Total	.0%	7.8%	3.1%	4.7%	.0%	.0%	.0%	.0%	15.6%
	2.5-2.75	Count	2	1	7	2	2	0	0	0	14
		% within BCSBin	14.3%	7.1%	50.0%	14.3%	14.3%	.0%	.0%	.0%	100.0%
		% within PredicteddBin	28.6%	9.1%	53.8%	25.0%	12.5%	.0%	.0%	.0%	21.9%
		% of Total	3.1%	1.6%	10.9%	3.1%	3.1%	.0%	.0%	.0%	21.9%
	2.75-3	Count	0	0	1	0	1	1	0	0	3
		% within BCSBin	.0%	.0%	33.3%	.0%	33.3%	33.3%	.0%	.0%	100.0%
		% within PredicteddBin	.0%	.0%	7.7%	.0%	6.3%	33.3%	.0%	.0%	4.7%
		% of Total	.0%	.0%	1.6%	.0%	1.6%	1.6%	.0%	.0%	4.7%
	3-3.25	Count	0	1	1	0	1	1	0	0	4
		% within BCSBin	.0%	25.0%	25.0%	.0%	25.0%	25.0%	.0%	.0%	100.0%
		% within PredicteddBin	.0%	9.1%	7.7%	.0%	6.3%	33.3%	.0%	.0%	6.3%
		% of Total	.0%	1.6%	1.6%	.0%	1.6%	1.6%	.0%	.0%	6.3%
	3.25-3.5	Count	0	0	0	1	2	0	0	0	3
		% within BCSBin	.0%	.0%	.0%	33.3%	66.7%	.0%	.0%	.0%	100.0%
		% within PredicteddBin	.0%	.0%	.0%	12.5%	12.5%	.0%	.0%	.0%	4.7%
		% of Total	.0%	.0%	.0%	1.6%	3.1%	.0%	.0%	.0%	4.7%
	3.5-3.75	Count	0	0	0	1	5	0	2	0	8
		% within BCSBin	.0%	.0%	.0%	12.5%	62.5%	.0%	25.0%	.0%	100.0%
		% within PredicteddBin	.0%	.0%	.0%	12.5%	31.3%	.0%	33.3%	.0%	12.5%
		% of Total	.0%	.0%	.0%	1.6%	7.8%	.0%	3.1%	.0%	12.5%
	3.75-4	Count	0	0	0	0	5	1	0	0	6
		% within BCSBin	.0%	.0%	.0%	.0%	83.3%	16.7%	.0%	.0%	100.0%
		% within PredicteddBin	.0%	.0%	.0%	.0%	31.3%	33.3%	.0%	.0%	9.4%
		% of Total	.0%	.0%	.0%	.0%	7.8%	1.6%	.0%	.0%	9.4%
	4-4.25	Count	0	0	0	0	0	0	4	0	4
		% within BCSBin	.0%	.0%	.0%	.0%	.0%	.0%	100.0%	.0%	100.0%
		% within PredicteddBin	.0%	.0%	.0%	.0%	.0%	.0%	66.7%	.0%	6.3%
		% of Total	.0%	.0%	.0%	.0%	.0%	.0%	6.3%	.0%	6.3%

Classify by ranges of 0. 5- Testing set

Manual BCS category observed by expert		Model output category						Total
		1.5-2	2-2.5	2.5-3	3-3.5	3.5-4	4-4.5	
1.5-2	Count	1	1	0	0	0	0	2
	% within BCS category	50.0%	50.0%	.0%	.0%	.0%	.0%	100.0%
	% within Model output category	25.0%	7.1%	.0%	.0%	.0%	.0%	3.1%
	% of Total	1.6%	1.6%	.0%	.0%	.0%	.0%	3.1%
2-2.5	Count	2	10	8	0	0	0	20
	% within BCS category	10.0%	50.0%	40.0%	.0%	.0%	.0%	100.0%
	% within Model output category	50.0%	71.4%	38.1%	.0%	.0%	.0%	31.3%
	% of Total	3.1%	15.6%	12.5%	.0%	.0%	.0%	31.3%
2.5-3	Count	1	2	10	4	0	0	17
	% within BCS category	5.9%	11.8%	58.8%	23.5%	.0%	.0%	100.0%
	% within Model output category	25.0%	14.3%	47.6%	21.1%	.0%	.0%	26.6%
	% of Total	1.6%	3.1%	15.6%	6.3%	.0%	.0%	26.6%
3-3.5	Count	0	1	2	4	0	0	7
	% within BCS category	.0%	14.3%	28.6%	57.1%	.0%	.0%	100.0%
	% within Model output category	.0%	7.1%	9.5%	21.1%	.0%	.0%	10.9%
	% of Total	.0%	1.6%	3.1%	6.3%	.0%	.0%	10.9%
3.5-4	Count	0	0	1	11	2	0	14
	% within BCS category	.0%	.0%	7.1%	78.6%	14.3%	.0%	100.0%
	% within Model output category	.0%	.0%	4.8%	57.9%	33.3%	.0%	21.9%
	% of Total	.0%	.0%	1.6%	17.2%	3.1%		21.9%
4-4.5	Count	0	0	0	0	4	0	4
	% within BCS category	.0%	.0%	.0%	.0%	100.0%	.0%	100.0%
	% within Model output category	.0%	.0%	.0%	.0%	66.7%	.0%	6.3%
	% of Total	.0%	.0%	.0%	.0%	6.3%	.0%	6.3%

Appendix M. Matlab code

BCS computation with FFT:

```

%% TotalProcess9.m
% This function take a cow image and proper background image and return the
% BCS by:
%1. create binary object of the cow 2. extract the cow contour, normeliaz
and
% sacle the contour 3. tkae the 1000 distance from center and transform to
% Fourier 4. compute the BCS from the 2-8 Fourier descriptors.

%% clean binary files and create output subdirectory
clear all; close all; clc;
if ~isdir('Binary'), mkdir('Binary'); disp('Binary sub-directory was
created'); end;
listOfBinaryJpegs = dir('Binary*.jpg');
if 0<length(listOfBinaryJpegs), for k = 1:size(listOfBinaryJpegs),
delete(listOfBinaryJpegs(k).name); end; end; % k=2
% loading the image and Background image
Background=imread('Background.jpg');
listOfJpegs = dir('*.jpg');
R_back=Background(:,:,1);
G_back=Background(:,:,2);
B_back=Background(:,:,3);
C1_back1 = double(R_back-G_back); % transform Background to R-G space
Cmatb=mat2gray(C1_back1);
Cmatb = imadjust(Cmatb);
level = graythresh(Cmatb);
C1_back=im2bw(Cmatb,0.95*level); % treshold background image to
binary
C1_back=abs(C1_back-1);
se_back = strel('disk',7);
C1_back=imopen(C1_back,se_back); % cleaning small objects from binary
image
clear se_back R_back C1_back1 Cmatb level G_back B_back k Background
listOfBinaryJpegs ;
% % Runnig on cows images
for k = 2:size(listOfJpegs) % k=2
% 1. creation of binary object
listOfJpegs(k).im = imread(listOfJpegs(k).name) ;
Image_name=listOfJpegs(k).name; % taking the cow number
Cow=str2num(Image_name(5:8));
Image=(listOfJpegs(k).im);
imwrite(Image,[cd,'\Binary\RGB ',Image_name], 'jpg'); %%% < -----
% Transform to R-G space
R=Image(:,:,1);
G=Image(:,:,2);
B=Image(:,:,3);
C1 = double(R-G) ;
C1G=mat2gray(C1); % transform to gray
C1G = imadjust(C1G);
level2= graythresh(C1G); % computing threshold
C1S=im2bw(C1G,0.8*level2); % Treshold to binary
C1S=abs(C1S-1);
C1Seg=imsubtract(C1S,C1_back); % Subtracing Background image
C1_BW=bwlabel(C1Seg); % labeling the objects
imwrite(C1_BW,[cd,'\Binary\BW ',Image_name], 'jpg'); %%% < -----
clear R G B C1 C1Seg Image C1G level2 C1S ;

% Choosing the biggest object in image
C1_Label=(regionprops(C1_BW));

```

```

C1_Label_N=max([C1_Label.Area]);
C1_Label_ind=find([C1_Label.Area]==C1_Label_N);
C1_segment=zeros(size(C1_BW));
C1_segment=(C1_BW==C1_Label_ind);
clear C1_Label C1_Label_N C1_Label_ind C1_BW ;
    %% noise removal Opening- closing holes and opening %%%%%%%%%%
se2 = strel('disk',10);
OpenIm = imerode(C1_segment,se2);
se = strel('disk',12);      % closing holes
closeIm = imdilate(OpenIm,se);
%figure(3); imagesc(closeIm) ; title(Image_name);
    se2 = strel('disk',7); % opening noise
OpenIm = imerode(closeIm,se2);
%closing holes inside the object
[B OpenIm]=bwboundaries(OpenIm);
OpenIm(OpenIm>=1)=1;
imwrite(OpenIm,[cd,'\Binary\Disk ',Image_name],'jpg');   %%% < -----
clear B se se2 C1_segment closeIm ;
    %% rotating the object by the object orientation
Im_props=(regionprops(OpenIm));
Im_theta=(regionprops(OpenIm,'Orientation'));
Im_rotated=imrotate(OpenIm,-(Im_theta.Orientation)); % this line
doesnot seem to work          imshow(Im_rotated) imagesc(Im_rotated)
Pix=(regionprops(Im_rotated,'PixelList'));
    xj=Pix.PixelList(:,1);
    yj=Pix.PixelList(:,2);
    [Xmin I]=min(xj);
    cutIm=Im_rotated;
    Bound=(regionprops(Im_rotated,'BoundingBox'));
    Xlength=Bound.BoundingBox(3);
    cutIm(:,Xmin+ceil(Xlength/3):end)=0;

IM=imrotate(cutIm,-90);      % Rotate to 90 degrees figure; imshow(IM)
imwrite(IM,[cd,'\Binary\Rotated ',Image_name],'jpg');   %%% < -----
clear Im_props Im_theta Im_rotated OpenIm cutIm Pix
    %% choosing again the biggest object
ImBeforeCutting=bwlabel(IM);
ImBeforeCuttingProps=(regionprops(ImBeforeCutting));
ImBeforeCuttingProps_N=max([ImBeforeCuttingProps.Area]);

ImBeforeCuttingProps_ind=find([ImBeforeCuttingProps.Area]==ImBeforeCuttingP
rops_N);
IM2=zeros(size(ImBeforeCutting));
IM2=(ImBeforeCutting==ImBeforeCuttingProps_ind);
[B IM3]=bwboundaries(IM2);
IM3(IM3>=1)=1;      % imshow(IM3)
imwrite(IM3,[cd,'\Binary\IM3 ',Image_name],'jpg');   %%% < -----
clear IM ImBeforeCutting ImBeforeCuttingProps ImBeforeCuttingProps_N
ImBeforeCuttingProps_ind IM2 B;
% end of creation of binary object

%% 2. extracting the cow contour
figure;
Contour=imcontour(IM3,1)';
close;
Contour(1,:)=[]; % delete first line
Contour(:,2)=max(Contour(:,2))-Contour(:,2);
Contour=Contour(find(0<Contour(:,1)),:); % delete every y = zero
Contour=Contour(find(0<Contour(:,2)),:); % delete every x = zero
figure; plot(Contour(:,1),Contour(:,2),'.'); set(gca,'YDir','reverse');
title(sprintf('Cow %s ',Image_name));

```

```

    saveas(gcf, sprintf('Contour line 106; Cow %s; .jpg',Image_name));
    movefile( sprintf('Contour line 106; Cow %s;
.jpg',Image_name), 'Binary');
    close;
    clear IM3;
    %% sorting the points
    numOfpoints=min(1500,length(Contour(:,2))); % taking 1500 points or the
highest possible
    [Y Y_index]=sort(Contour(:,2),'descend');
    Contour2=Contour(sort(Y_index(1:numOfpoints)),:); % taking 1500 points
or the highest possible
    clear numOfpoints Y Y_index Contour ;
    figure; plot(Contour2(:,1),Contour2(:,2),'.');
set(gca,'YDir','reverse'); title(Image_name);
    saveas(gcf, sprintf('1500 points; Cow %s; .jpg',Image_name));
    movefile( sprintf('1500 points; Cow %s; .jpg',Image_name), 'Binary');
    close;

    %% taking 1000 only points near or far from the tail and Interpolation:
    numOfpoints2=1000;
    length1=length(Contour2(:,1));
    newXJ=interp1(1:length1, Contour2(:,1),1:length1/numOfpoints2:length1);
% Interpolation: 1000 points near the tail
    newYJ=interp1(1:length1, Contour2(:,2),1:length1/numOfpoints2:length1);
    clear numOfpoints2 length1 Contour2;
    %figure; plot(newXJ,newYJ, '.');
    %% scaling the contour from 0 to 1
    XXj= (newXJ-min(newXJ)) / (max(newXJ)-min(newXJ)) ;
    YYj= (newYJ-min(newYJ)) / (max(newYJ)-min(newYJ)) ;
    clear newYJ newXJ n c
    figure;
    plot(XXj,YYj, '.'); set(gca,'YDir','reverse'); title(Image_name);
    saveas(gcf, sprintf('0 to 1 1000; Cow %s; .jpg',Image_name));
    movefile( sprintf('0 to 1 1000; Cow %s; .jpg',Image_name), 'Binary');
    close;

    %% center points
    CenterX=0.5;
    CenterY=0.5;

    %% extracting distances from center by euclidean distances
    Distances=sqrt((YYj-CenterY).^2+(XXj-CenterX).^2);
    clear YYj XXj;
    %figure; plot(Distances, '.'); plot(Distances)

    %% 3. transform to Fourierer
    ffx=0; ffx2=0;
    windowsize=5; % smoothing the sign with low-pass filter
    DistancesFilt=filter(ones(1,windowsize)/windowsize,1,Distances');
    ffx=abs(fft(DistancesFilt));
    ffx=ffx';
    ffx2=ffx(1:10);

    %% 4. compute BCS from the 2-8 Fourier descriptors

    BCS=6.405-0.027.*ffx2(3)-0.024.*ffx2(4)-0.011.*ffx2(5)-0.081.*ffx2(6)-
0.087.*ffx2(7)-0.072.*ffx2(8);
    BCSV(k-1,1)=BCS;
    BCSV(k-1,2)=Cow;
% fprintf(1, '\n Cow %s ; \t BCS = %2.1f\n',Image_name,BCS);

```

```

figure; plot(Distances, '.');
title(sprintf('Distances; Cow %s; BCS = %2.1f', Image_name, BCS));
saveas(gcf, sprintf('Distances; Cow %s; BCS = %2.1f.jpg', Image_name, BCS));
movefile(sprintf('Distances; Cow %s; BCS = %2.1f.jpg', Image_name, BCS), 'Binary');
close;

%input(' press enter: ');

end % end of cows
save('BCSV')

```

Code for extracting anatomical point's angles and distances- in CD\Matlab codes.

Appendix N. SPSS syntax

All data for statistics exams are stored in CD\Excel files.

The SPSS syntax for the backward regression of first ten Fourier descriptors:

```

DATASET ACTIVATE DataSet0.
REGRESSION
  /MISSING LISTWISE
  /STATISTICS COEFF OUTS R ANOVA
  /CRITERIA=PIN(.05) POUT(.10)
  /NOORIGIN
  /DEPENDENT BCS
  /METHOD=BACKWARD F1 F2 F3 F4 F5 F6 F7 F8 F9 F10.

```

The SPSS syntax for the Ordinal regression of first ten Fourier descriptors:

```

DATASET ACTIVATE DataSet1.
PLUM BCS_ordinal WITH F1 F2 F3 F4 F5 F6 F7 F8 F9 F10
  /CRITERIA=CIN(95) DELTA(0) LCONVERGE(0) MXITER(100) MXSTEP(5)
PCONVERGE(1.0E-6) SINGULAR(1.0E-8)
  /LINK=LOGIT
  /PRINT=FIT PARAMETER SUMMARY

```

תקציר

ציון מצב גופני (BCS) זהו ציון המעיד על רזרבות האנרגיה של הפרה החולבת בסולם של 1 עד 5, כאשר הדיוק הנפוץ בציון הינו בקפיצות של 0.25. למרות מספר ניסיונות להפוך תהליך זה לאוטומאטי, עד היום הדרוג נקבע בהערכת עובי שכבת השומן התת עורית כפי שמשוקללת ע"י המתבונן כמופע המבנה המורפולוגי של מספר אזורים מקובלים על פני גוף הפרה. זהו תהליך ממושך וסובייקטיבי. מטרתו של מחקר זה הינה לפתח מערכת אובייקטיבי ת המבוססת עיבוד תמונה לצורך הערכת ציון המצב הגופני של פרה חולבת, בכוונה להפכה למערכת אוטומטית בעתיד. מאה וחמישים תמונות של פרות שצולמו במבט על במצלמת ניקון DLSR בכניסה לבמת המחלוב במכון החליבה ברפת בית דגן קיבלו ציונים על די מומחה בשיטה המקובלת וחולקו לסט אימון, לצורך בניית המודל וסט בחינה. תהליך עיבוד התמונה עד לקבלת קו המתאר של גב הפרה ואזור עצם הזנב בוצע באופן אוטומאטי בעזרת תכנת Matlab וכלל שלושה שלבים. בשלב ראשון, בודדה הפרה (האובייקט) מהרקע של התמונה בעזרת קביעת ערוץ צבע וערך סף מתאימים והחסרה של תמונת רקע מתאימה. השלב שני, הכיל פעולות מורפולוגיות על האובייקט הכוללות ניקוי רעשים (הסרת אובייקטים משניים) וסיבוב התמונה לאוריינטציה קבועה של תשעים מעלות. השלב השלישי והאחרון הינו חילוץ קו המתאר מן האובייקט. קו זה, מתאר את העקום של הגב האחורי ואזור עצם הזנב. כל קו עבר תהליך של החלקה להסרת רעשים, אינטרפולציה למספר זהה של נקודות ונרמול לטווח ערכים קבוע על מנת להפחית את ההשפעות של גודל וכיוון האובייקט בתמונה המקורית. חיזוי ציון המצב הגופני מקו המתאר של אזור עצם הזנב נבחן על ידי שתי שיטות. שיטה ראשונה, כללה זיהוי אוטומאטי של 5 נקודות מינימום ומקסימום על קו המתאר. עשרה מרחקים אנכיים ואופקיים וחמש הזוויות הנוצרות בין נקודות אלו נלקחו בתור מאפיינים מסבירים במודל רגרסיה ליניארי. ת. בשיטה שנייה הפכה ההסתכלות על קו המתאר של עצם הזנב לווקטור מרחקים ממרכז הכובד של האובייקט, ולאחר מכן הועבר ווקטור זה למרחב התדר על ידי התמרת פורייה. מווקטור מקדמי הפורייה של קו המתאר נלקחו עשרת מקדמי הפורייה הראשונים בתור משתנים מסבירים במודל הרגרסיה הליניארי. ת. התוצאות הטובות ביותר התקבלו על ידי שימוש במקדמי פורייה כאשר המשתנים שנכנסו בסופו של דבר למודל הם שבעת המקדמים מהקדם השלישי ועד השמיני. מדד הקורלציה בין תוצאות המודל לציון שניתן על ידי המומחה עמד על 0.77 על סט האימון ו 0.64 על סט הבחינה דבר המעיד על יציבות המודל ויכולת סבירה לחזות את ציון המצב הגופני של פרת החלב באופן אוטומאטי וללא כל התערבות ידנית.

אוניברסיטת בן-גוריון בנגב הפקולטה למדעי ההנדסה המחלקה להנדסת תעשייה וניהול

זיהוי מצב גופני אוטומאטי של פרת החלב

חיבור זה מהווה חלק מהדרישות לקבלת תואר מגיסטר בהנדסה

מאת : עמוס ברקוביץ

מנחים : פרופ' יעל אידן

ד"ר אילן הלחמי

OCTOBER 2012

חשוון תשע"ג